



NTT Remote Observing from Italy

A. BALESTRA, P. SANTIN, G. SEDMAK, *Astronomical Observatory of Trieste, Italy*
M. COMIN, G. RAFFI, A. WALLANDER, ESO

1. Introduction

Remote observing (RO) from ESO-Garching is by now a well-established service provided for the user community by ESO. So far it has been concerned with instruments located either at the CAT or at the 2.2-m telescope at La Silla, operated from Garching since 1987. The advantages of this observing mode include reduced travel times, the possibility to accommodate shorter and regular long-term monitoring observing programmes, the possibility for students to participate in the observation and the facilities (people, library and computers) normally available in a European astronomical institute [1].

In order to create a new remote observing environment for the EMMI and SUSI instruments on the NTT telescope, a collaboration with the Astronomical Observatory of Trieste, Italy, was started in 1989. The Trieste Observatory has a long experience in the field of Unix-based workstations and on distributed environments.

The project was based on the philosophy of a multi-telescope, multi-instrument system addressed by many users in parallel in a flexible scheduling environment compatible with the automatic execution of complex observing programmes.

The main goals of the collaboration were:

- The study, design and implementation of a portable kit, including hardware and software for remote observations with the ESO NTT from a European astronomical institute.
- The definition of the hardware ar-

chitecture for the RO computer network and communication system.

- The implementation of a "second" generation of RO software, based on Unix and workstations hardware. An important part of this was the extension of the real-time database of the NTT to a geographically distributed



Figure 1: Astronomers and visitors in the Trieste remote observing room – waiting during a long NTT exposure.

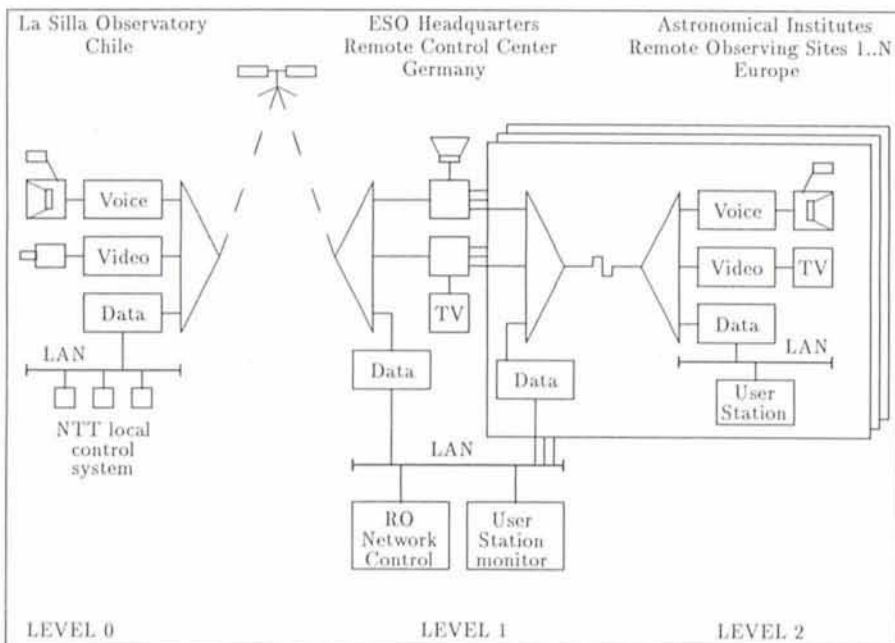


Figure 2: Block diagram of communication system.

telescope/instrument parameters' database (XPool).

- The availability of the same software and features for remote observing both at the first level site (ESO-Garching) and at a second level site (user's institute).

While the complete development of the project took three years, the first milestone was reached with the development and test of the remote observing system of first level in Garching. This system is now in the final test phase and the operation team is being trained. It is foreseen to offer routine remote observing from ESO-Garching on the NTT with EMMI/SUSI starting in April 1993.

Meanwhile, the relevant hardware had been procured and several tests took place, while arrangements were made for the installation of the 64 kbps link from Garching to Trieste.

The final milestone was reached when the second level remote observing run took place, from the 9th to the 11th of June 1992, at the Astronomical Observatory of Trieste, Italy, during three nights allocated for remote observation with the NTT telescope. The present article reports on the results of this run, which proved that the chosen concept and implementation were not just working but already quite reliable at the present stage. The system was in fact used for about 30 hours for real astronomical observations by a team of eight astronomers.

The aim of this project was not simply to build a remote observing environment for the NTT, but right from the beginning it was conceived by ESO to serve as a

pilot project for the VLT. In particular new computer technologies, software (user interface, on-line databases) and operational procedures should be tested, which are of importance for the VLT control system in general and not only for remote observations.

It is foreseen to repeat the second level remote observing run from other institutes in Europe, porting to them the set-up, which has been produced as a result of the ESO-AOT collaboration and leasing jointly a link to Garching.

2. System Architecture

2.1 First Level Remote Observing

ESO-Garching is permanently linked to La Silla via a 64 kbps leased satellite link [2]. During remote observing the bandwidth is subdivided, using time division multiplexing, into three parallel channels. A voice channel implements a point-to-point voice link between the night assistant at the NTT and the remote observer at ESO-Garching. A video image channel allows the remote observer to select one video source (e.g. field acquisition, slit viewer) for transfer in slow-scan-television mode. Due to the fact that video images obtained by the acquisition cameras are normally very simple, consisting of only a few sources on a black background, the compression algorithm works very well. Using a bandwidth of 12 kbps the normal frame repetition rate is one frame every 3 seconds. This makes it possible to use the video image system as feedback for interactive control, e.g. offsetting the telescope, even when the video

image system is using only one fifth of the available bandwidth. Thirdly, a data channel connects the local area networks of ESO-Garching and La Silla via routers. A dedicated local area network (LAN) has been created at ESO-Garching for remote observing. This network uses a separate interface on the router, while all other nodes connected to the general LAN use another interface. Any disturbances on the general LAN are thereby isolated from the remote observing network.

A dedicated room at ESO-Garching has been allocated as the NTT remote control room. It houses the remote control station and care has been taken to create an ergonomic installation. The remote control computer is a Unix workstation supported by two additional X terminals. Normally one of these X stations is allocated to telescope control, one to instrument control and one to quick look and image processing using MIDAS. A large video monitor displaying video images is installed above the X terminals. At both ends of the control station is a PC, which the user normally does not interact with very often. One is for video control and the other for receiving meteor data from the GOES satellite. Lastly a movable voice unit containing a microphone and a loudspeaker implements access to the voice system.

The NTT local control system is based on two main computers running the RTE-A operating system. In addition a Unix workstation is used for scientific data acquisition. The main characteristics of the software architecture are a decoupling of the control tasks from the user interface by means of a database and a command handler. The database and command handler, together with the TCP/IP protocol suit, provides the software bridge between the local and remote sites.

The remote control software architecture is discussed in detail in [3] and only a brief overview is given here. The distributed database (Xpool), implemented according to the client server model and using TCP sockets, allows remote read and write access. It is responsible for providing status information to the remote control computer and to allow definition of set-up parameters from the remote control computer. The command handler, implemented in a similar way, is responsible for routing commands, replies and asynchronous status and alarm messages between processes residing on different hosts. These two mechanisms allow a fully interactive remote control, providing the remote user with the same functionality available locally at La Silla.

Scientific data handling makes use of



Figure 3: The ESO-Garching remote control room.

standard network facilities, remote shell, ftp and the X protocol to transfer and/or display scientific data. It takes about one minute to display an image, independent of detector size, in a standard MIDAS display window using the X protocol. Actual transfer of the raw data takes between 3 and 7 minutes for a 1kx1k frame, depending on a user selectable compression algorithm.

The User Interface [6] based on the Pegasus package developed at CFHT, interfaces to these other packages. It runs on top of OSF/Motif and uses standard widgets for data presentation and user interactions. It is completely configurable in the sense that everything that appears on the screen and associated control actions are described in simple ASCII files.

2.2 Second Level Remote Observing

The second level hardware and software configuration has been developed with the aim of implementing a system able to manage remote observations on a multi-telescope, multi-instrument system from European astronomical institutes, and allowing the main control centre of ESO-Garching the full control of the remote operations [4]. The basic three-channel hardware configuration is also maintained for second level remote observing. Full compatibility with the first level and user-friendliness are, of course, provided. Since more than one instrument could be active in the general architecture, multiple secondary levels

are foreseen in the overall configuration in order to allow flexible scheduling. The possibility of managing remote observations from more secondary levels on more telescopes is therefore a natural extension of the system.

Since the data channel connects computers already operating, in most cases on networks, two bridges allow an easy way to connect the LAN of the first level with the LAN of the second one. A single Remote Control LAN, comprehensive of all the three levels, is thus obtained allowing an easier use of computing facilities. Future extension of this channel to multiple second levels is straightforward.

Voice and video channel, even if devoted to different uses, can be treated in the same way, since the original signals they have to manage are intrinsically analogous. This fact, on the other hand, added a few more problems to the channel management. The electrical and communication protocols of the serial lines (these channels are generally implemented according to X.21 or V.24 standards) define a point-to-point link instead of a distributed environment. Therefore, in the simplest configuration, voice and video channels directly connect zero level with the second level observing site. However, a direct connection between the zero and first level is required to allow communications between night assistants and the ESO-Garching control centre. In order to maintain a simple hardware configuration, a software solution (SUN talk) was

Tentative Time-table of Council Sessions and Committee Meetings

November 12-13	Scientific Technical Committee
November 16-17	Finance Committee
November 26-27	Observing Programmes Committee
December 1-2	Council
All meetings will take place in Garching.	

implemented. In the perspective of multiple second levels, a distribution board for serial lines has to be foreseen.

The link connecting first and second level sites should have a bandwidth of at least 64 kbps in order to completely manage all three channels. In a multiple-site configuration, while the first to second level lines will maintain this bandwidth, the main link between the zero level and the first one will obviously need a higher bandwidth, i.e. at least $N \times 64$ kbps where N is the number of secondary sites observing at the same time.

A 64 kbps digital ground-based link was leased jointly by ESO and OAT for this test for the duration of one month. Such a connection proved to be a novelty for the German and the Italian PTT companies. Some days at the beginning of the connection period were lost owing to tests on both sides. This kind of problem will hopefully disappear with the increasing integration of the European Community.

The control room at the secondary level site is a duplicate of the main control room at ESO-Garching in line with the resources of the institute. As a general rule, one workstation, two X-terminals and two PCs are required; if the need arises, a disk server for image storage could be used even if it is not essential. Specific equipment for voice and video channels (i.e. telephone set, monitor . . .) is also required.

The extension of the software for second level remote observing involved the implementation of a hierarchical structure. Each node must be defined as primary or secondary according to its level. The secondary node sends its requests (direct access or updating list) to the primary one. It is up to the primary node to route the request to the final target, i.e. the instrument or the telescope control computer. Thus, no direct access to zero level database is allowed from the secondary level. Even if this mechanism may induce some time delay in response, the resulting filter action obtained is very important for the con-

trol and monitoring actions of the ESO-Garching centre.

During remote observations, all the operations carried out by the second level site can be monitored by an operator in the ESO-Garching control room. Every updating action, from secondary to zero level and vice versa, is first performed by the primary level on its database. A monitoring process on the primary level control computer is thus able to check secondary level operations and, if necessary, also to filter out incorrect operations of the secondary node. The primary node can obviously perform its own operations toward zero level site, thus obtaining a complete control of the remote observing session.

All the software configuration is driven by few configuration files and environment variables, allowing the possibility of easily switching between various contexts, i.e. from simulation to reality.

3. The Final Test

The final test was carried out on the nights of 9, 10 and 11 of June [5]. The link created no specific problem, once German Bundespost and Italian SIP had solved theirs. The connection between the OAT LAN and the ESO LAN, with the creation of the extended remote observing LAN, was straightforward.

A telephone set was used as data channel terminal equipment. The only problem encountered with it was the "Donald Duck effect" on the voice due to the compression ratio of this channel. Some problems arose with the video channel due to the late and incorrect delivery of some boards on the part of the manufacturer. This channel started to work continuously as from the second night.

The OAT control room was configured in the following way. One workstation

HP-425 as control computer and as display for instrument UIF. Another workstation HP-375 was configured as X-terminal for telescope UIF display. A second HP-425 was used to run a remote MIDAS session on the SUN control workstation at La Silla. A Sylicon Graphics Indigo workstation was inserted in the network to use its disk space, through NFS, for image storage. One NCD X-terminal was used to run two "talk" sessions with the ESO-Garching control room and with La Silla through remote logins on two SUN in Garching and at La Silla. These last communication sessions were used in order to have a more complete interaction with the ESO-Garching control room and the La Silla night assistant due to the test nature of the nights. Two PCs were also used for the monitoring of the data channel and for the display of the Meteosat images.

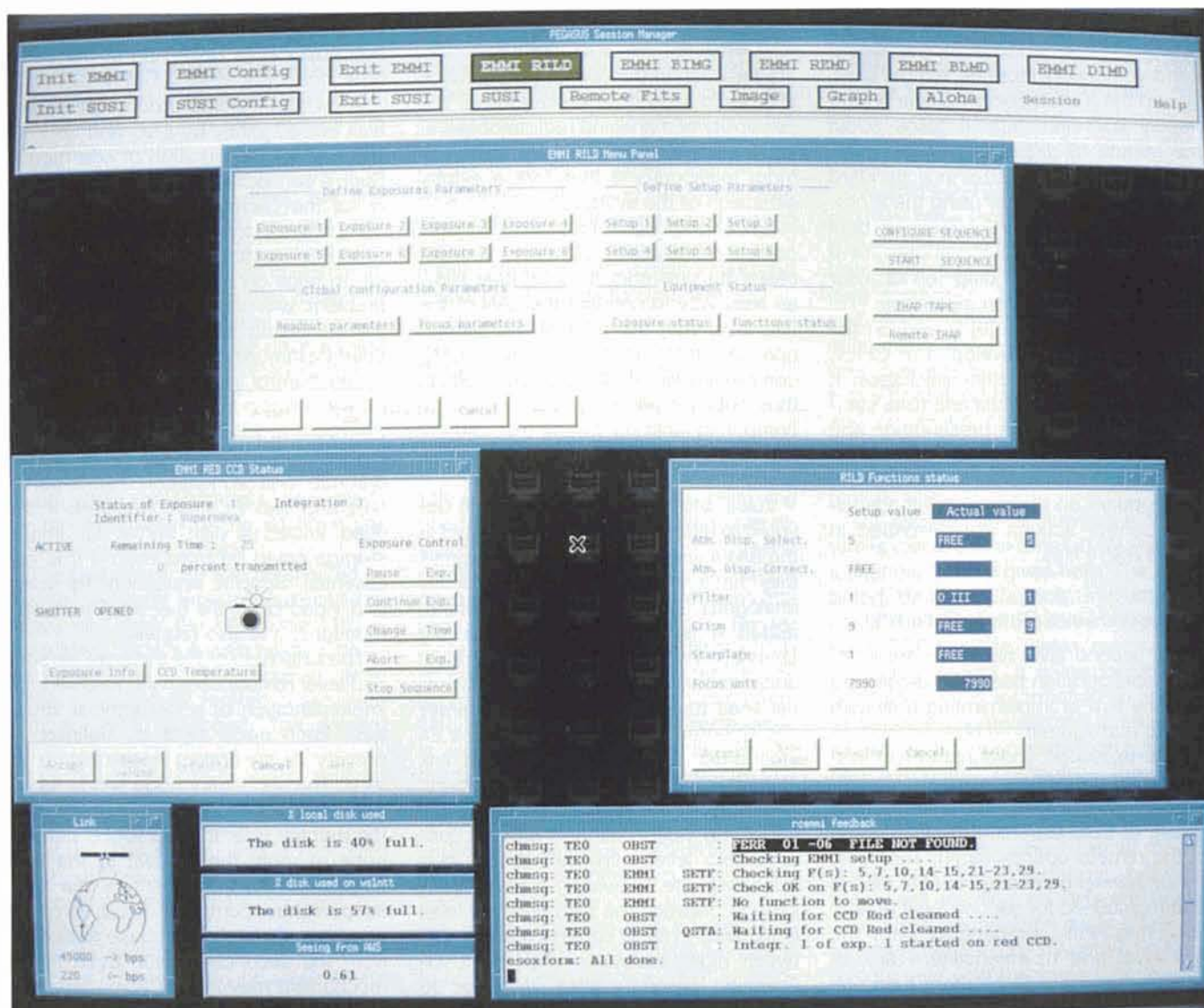


Figure 4: Example of the Pegasus User Interface for the control of the instrument (EMMI/SUSI) and of the telescope.

The software had to be ported from the remote control computer in ESO (an HP-720) to the OAT HP-425. No problem at all was encountered during this procedure. A porting of Xpool package on SUN and Sylicon Graphics was also put into effect, for test purposes, in the months preceding the final test.

On the first night ten hours were devoted to preliminary tests and to identify and fix some software bugs. From 4.00 UT astronomical observations could begin and continued until 11.00 UT. The second night started with some minutes of delay due to some minor software problems and lasted till 11.00 UT. The last night was entirely devoted to astronomical observations. On the whole, more than thirty hours were entirely devoted to astronomical observations. Eight OAT astronomers used this time to carry out various scientific observations. It should be stressed that while an observation was going on, the astronomers were able in remote MIDAS sessions to have a quick look at the previously acquired images in order to evaluate the validity of their data. Accordingly, if necessary, the transfer of the images from La Silla to Trieste could then be carried out.

4. Conclusions

This project was successful in proving the feasibility and reliability of second level remote observing already at this stage.

During the three nights of the final test over 30 hours were devoted to astronomical observations and, as can be inferred by the users' comments, the system proved to be very easy and flexible to operate, considering also that most of the observers had no experience in the use of EMMI.

In view of the success of the experiment it has been decided not to stop here but to proceed along two lines:

- To study and implement a special hardware/software system for on-line data compression technique, in order to reduce the quick-look time (at present of the order of minutes) and obtain an almost completely interactive environment.
- To identify other interested institutes in Europe to repeat a second level remote observing run from there, in order to test portability and reliability of the present set-up. This can also be useful to test operationally the feasibility of remote access during flexible scheduling, where more than one observing team can be active during the same night from different institutes.

The modalities are currently under definition. The candidate institute should have a network of Unix workstations,

and provide the possibility of dedicating part of the LAN to the remote observing tasks in addition to the astronomical interest in participating in such an experiment. The communication equipment could be provided by ESO for the purpose of a first test.

The joint procurement of the leased link to Garching is another condition to be fulfilled, and further preliminary daytime tests and remote test nights will be necessary.

As an independent parallel activity the first level remote observing system is now getting its final touch. The operation team is being trained and user guides are being produced. It is planned to start offering remote observing with EMMI/SUSI to the user community in April next year.

5. Acknowledgements

Many people have participated in the development of the described system. The NTT (local) control system was developed within the Electronics Department at ESO-Garching. Major contributions to the implementation of the remote control system were made by B. Gilli and J. Brynneel.

At the Astronomical Observatory of Trieste M. Pucillo was one of the designers of the second level hardware and software architecture and participated in the software development, and C. Vuerli implemented most of the software utilities. The help of P. Maruccci and R. Smareglia is also acknowledged. C. Corte gave his precious support during the set-up of the second level observing room.

J. Kerr of CFHT supported us in the initial use of the Pegasus user interface. G. Andreoni and the people from the La Silla operation group gave their support during installation and commissioning, and M. Pizzaro acted as the perfect night assistant during the three test nights.

The project has been financially supported, for the Italian side, by the Italian Council for the Astronomical Research C.R.A.

References

- [1] D. Baade, "Three Years' Experience with Routine Remote Observing at the European Southern Observatory", in Proceedings of Workshop on Remote Observing, Tucson, USA, April 1992.
- [2] A. Wallander, "New Communication Link between Garching and La Silla", in *The Messenger* No. 60, June 1990.
- [3] A. Wallander, "Remote Control of the ESO New Technology Telescope", in Proceedings of Workshop on Remote Observing, Tucson, USA, April 1992.
- [4] A. Balestra et al., "Remote Observing Activities at the Trieste Astronomical Observatory: The ESO/NTT Second Level Remote Observing and the Galileo Telescope Project", in Proceedings of Workshop on Remote Observing, Tucson, USA, April 1992.
- [5] A. Balestra et al., "The ESO/OAT Second Level Remote Observing Project. Final Test on ESO/NTT: 9-11 June 1992", Technical Report OAT Publication No. 1443, June 1992.
- [6] M. Comin, J. Kerr, "A Prototype for the VLT user Interface", in Proceedings of Conference on Progress in Telescope and Instrumentation Technology, ESO-Garching, April 1992.

A Fourth VLT Instrument Science Team

At its May, 1992 meeting the ESO Scientific and Technical Committee approved the two Ultraviolet-Visible Echelle Spectrographs (UVES1 and UVES2) for the Nasmyth foci of the second and third VLT telescopes. The ESO staff responsible for building these instruments is now proceeding with the design studies of this major facility which will do high-resolution spectroscopy (resolution-slit width product = 40,000) in the 300 to 1100 nm wavelength range. At the same time an Instrument Science Team has been formed for this facility. Its members are:

B. Gustafsson (Uppsala)
H. Hensberge (Brussels)
P. Molaro (Trieste)
P. Nissen (Aarhus)

The team will select its chairman at its first meeting on December 9. As is the case for the other VLT instruments (see *The Messenger* 68, page 8), the IST members and myself welcome your input on scientific matters relating to these instruments.

J. M. BECKERS, ESO

“Remote” Science with the NTT from Italy

PRELIMINARY SCIENTIFIC RESULTS

M. FRANCHINI, P. MOLARO, M. NONINO, F. PASIAN, M. RAMELLA, G. VLADILLO,
Osservatorio Astronomico, Trieste, Italy

M. CENTURION, *Instituto de Astrofísica de Canarias, Tenerife, Spain*

P. BONIFACIO, *Scuola Internazionale Superiore di Studi Avanzati, Trieste, Italy*

1. Introduction

We report here on the preliminary analysis of the observations carried out with the NTT telescope during the final test of the “Second Level Remote Observing Project” at the Astronomical Observatory of Trieste (OAT). The test took place during the nights of 9, 10 and 11 June 1992. Details on the “remote observing” project can be found in the article by Balestra et al. on page 1 of this issue of the *Messenger*.

A preliminary constraint to the planning of the observations was imposed by the people responsible for the test, who required frequent changes between different instrumental configurations, in order to better evaluate the response of the distributed system to a heavy load. Furthermore, tune-up and communication problems occurred at different times of the test nights requiring either a reshuffling of the scheduled observations or the loss of some calibrations and/or astronomical targets. In particular, several exposures which were planned during the dark time at the end of one night were postponed to grey time of the following night.

We believe however that, during the test nights, an acceptable compromise was reached between the technical requirements of the test itself and the wish of a full use of the nights for real astronomical work.

All the targets pointed were selected within research projects currently ongoing at the OAT. These projects are: T Tauri stars (MF), Lithium abundance (PM), high velocity clouds (GV, MC), Planetary Nebulae (FP, PB), Seyfert galaxies (MN, MR), distant clusters of galaxies (MN, MR), gravitational lenses (MN, MR). The following is a brief description of the research projects and an assessment of the quality of the data obtained.

2. The Observations

2.1 NaI D Variability in the T Tauri Star Sz 68

We have performed echelle spectroscopy of a T Tauri Star (Sz 68) with the NTT using the EMMI spectrograph in the REMD mode: grating #10, grism #5, decker 5 arcsec. The detector was a

CCD THX 31156 (ESO #18) with 1024×1024 square pixels, $19 \mu\text{m}$ in size. The instrument is described in Dekker et al. (1991). This detector has been used for all the observations described in this paper. With a slit of 1.2 arcsec, a resolution $R \sim 25,000$ is obtained; this can be verified from well-separated lines of a thorium comparison spectrum. Wavelength calibration was performed for each order by a polynomial, fitted to 12 lines at least; the r.m.s. of the residuals is about 0.5 km s^{-1} .

Figure 1 shows the spectrum of Sz 68 ($V=10.5$), in the region of the NaI D doublet. With an exposure of 1 hour, a S/N ratio of about 200 has been achieved. This object is a target of a more general research, concerning the basic observational parameters of T Tauri stars: projected rotational velocities and inclination angles, spectral types, luminosities, effective temperatures, element abundances, etc. In par-

ticular, Sz 68 belongs to a sample of T Tauri stars for which the velocity fields in the circumstellar environment are under investigation. Sz 68 has shown clear variability of the NaI D line profiles: multiple blue-shifted absorption components are present, with variable intensity and position. This might indicate the existence of a complex circumstellar structure, varying with time.

So, the spectrum in Figure 1 can be compared – taking into account the different instrumental resolution – with preceding observations, made in 1985 (Finkenzeller and Basri 1987), in 1989 (Franchini et al. 1992 a), and in 1991 (Franchini et al. 1992 b). While the actual configuration appears to be rather similar to the ones observed in 1991 and 1985 (with the blue-shifted component at about the same v_{rad}), the same cannot be said for 1989 (when the main blue-shifted component – relative to the star – was at more than -90 km s^{-1}). Clearly

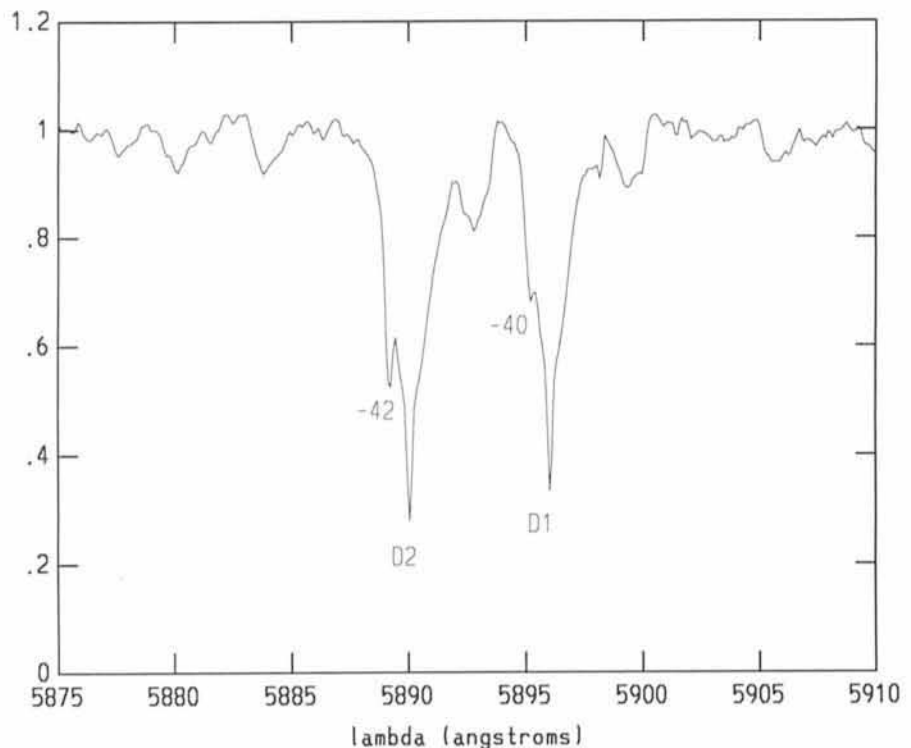


Figure 1: Normalized NaI D doublet of T Tauri star Sz 68. Radial velocities (in km s^{-1}) of blue-shifted absorptions are relative to the interstellar component which is clearly recognizable in the stellar profiles.

the time intervals between these observations are too wide to allow a complete reconstruction of the evolution of a given absorption component. However, more detailed analysis of the present data, together with those of 1991, may provide a quantitative interpretation of this variability, in terms of mass ejection events and/or sudden changes in the physical properties of the circumstellar material.

2.2 Lithium in the Halo Dwarfs G 64-37 and G 275-4

The abundance of lithium in the Population II stars hotter than 5500 K shows a characteristic *plateau* around $\log N(\text{Li})=2.1\pm 0.1$ (where $\log N_{\text{H}}=12$), in striking contrast with that observed in the younger population where the abundances are scattered over three orders of magnitude. Although this is not fully understood, the most straightforward explanation remains the absence of any significant lithium depletion in halo dwarfs, and thus the atmospheric abundance reflects the pristine lithium abundance of the interstellar gas from which these old stars formed. It appears very probable that the lithium in the old halo dwarfs is primordial in origin. In fact the good agreement between the lithium abundance observed in the halo dwarfs and the theoretical predictions of the big-bang theory is very impressive. According to the theory, the lithium yields are particularly sensitive to nucleon density, and the knowledge of the precise amount of primordial lithium allows a determination of the η value ($\eta=n_{\nu}/n_{\text{b}}$), which is related to the critical mass Ω . The astronomical relevance of lithium has been recently discussed by Lemoine et al. (*The Messenger* No. 67, p. 40).

Lithium observations in the Population II stars are severely limited by the intrinsic faintness of the known halo dwarfs and by the relatively small equivalent widths of the lithium line. We used the EMMI spectrograph on the NTT to observe the halo dwarfs G 64-37 and G 275-4, taken from the sample of Ryan et al. (1991). The observations have been performed with the REMD EMMI mode using the 31.6 grooves/mm grating 10 and grism 3 as a cross disperser. S/N ratios of ≈ 180 and ≈ 100 are achieved for exposures of 3600 sec for G 64-37 ($V=11.1$ mag) and of 3800 sec for G 275-4 ($V=12.2$ mag), respectively. The resolving power measured from the thorium lines is of $\approx 26,000$.

Interest in these two objects stems specifically from their particularly low metal abundances. The abundances of G 64-37 and G 275-4 are of $[\text{Fe}/\text{H}]=-3.38$ and -3.70 , respectively. So

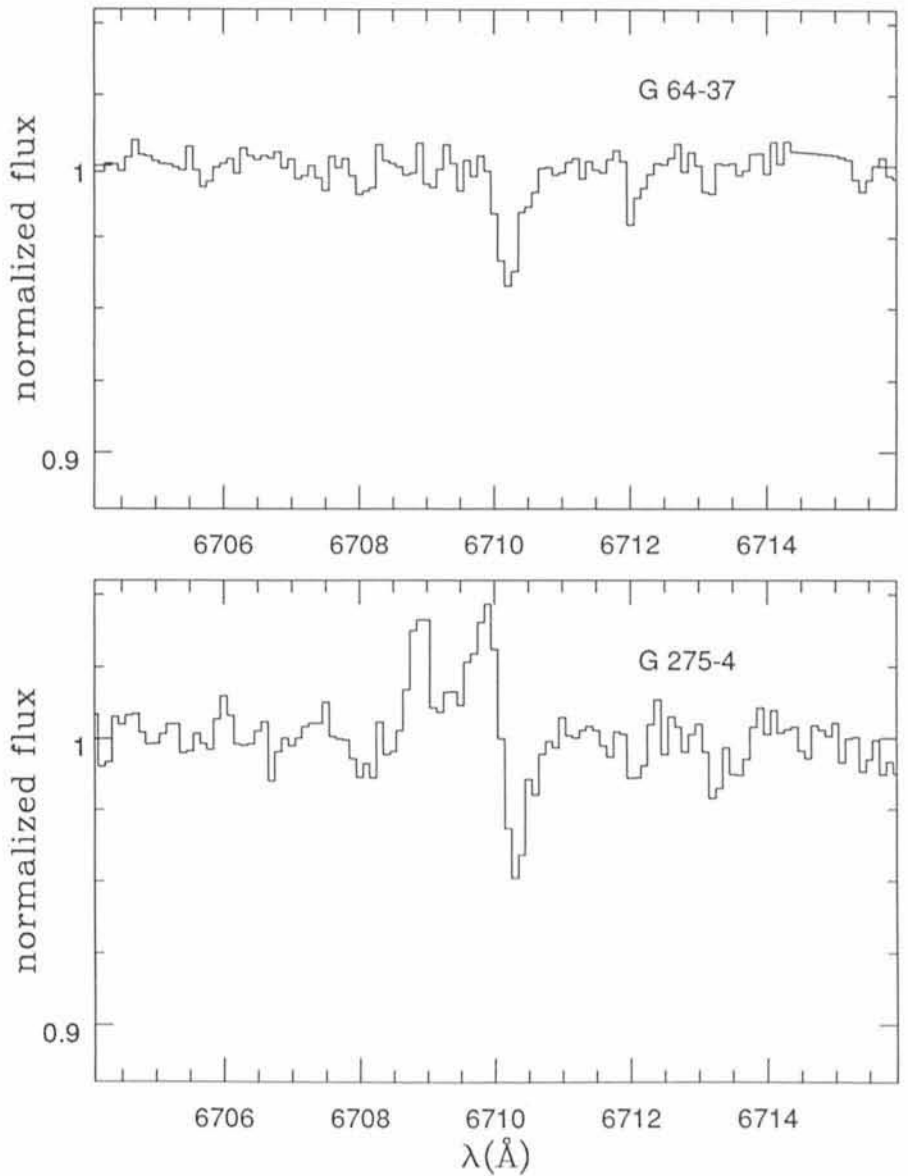


Figure 2: The Li I spectral region for G 64-37 (top panel) and G 275-4 (bottom panel). The spectra are not corrected for the earth motion.

far there are only few objects studied for lithium with metallicity below $[\text{Fe}/\text{H}]<-3.0$. In particular, the lowest metallicity dwarf in which lithium has been detected is G 64-12 with $[\text{Fe}/\text{H}]=-3.5$, but the spectroscopic binary CS 228876-32, with metallicity $[\text{Fe}/\text{H}]=-4.2$, surprisingly does not show any lithium (Molaro 1991).

The regions around the Li I 6707 Å resonance line for both the stars are shown in Figure 2. It can be seen from the figure that the lithium features are clearly present in both halo dwarfs. The redshift of the absorptions corresponds to $V_{\text{hel}} = 114 \text{ km s}^{-1}$ for G 64-37 and $V_{\text{hel}} = 142 \text{ km s}^{-1}$ for G 275-4, in agreement with the displacement observed by the stellar Na I lines. Unfortunately, the blue wing of the line in G 275-4 is contaminated by an emission remnant of a previous observation, and the equivalent width could be slightly greater

than observed. However, the presence of the lithium line in G 275-4 by itself is of interest since it extends down to $[\text{Fe}/\text{H}]=-3.7$ the metallicity range in which lithium is observed. In the case of G 64-37 the equivalent width of the lithium line is of 17 mÅ. According to Ryan et al. G 64-37 has a T_{eff} of 6350 K and is one of the hottest dwarfs in the present sample of Population II stars. An accurate determination for the lithium abundance will be presented elsewhere, but a comparison with HD 84937 and G 64-12, which have similar T_{eff} and similar line strength, indicates that the lithium abundance for G 64-37 should be also at the *plateau* level.

2.3 Interstellar/Intergalactic Na I Absorptions at High Galactic Latitudes

Interstellar observations in the direction of distant sources at high galactic

latitudes are important to cast light on the high-velocity clouds (HVCs) phenomenon. HVCs were discovered at 21 cm, but are extremely difficult to detect in absorption in the optical (see e.g. Keenan et al. 1988). In the framework of the investigations on the interstellar/intergalactic medium carried on at the OAT, we observed the halo star PG 1303-114 ($V=14.0$) and the extragalactic object 2155-304 ($V=13.1$) in a search for NaI absorption lines. For both objects we used the EMMI spectrograph in the REMD echelle mode with the grating #10 and the grism #3. The resolution in the region of the NaI doublet was measured from the FWHM of several lines in a spectrum of the Thorium calibration lamp. We found $\Delta\lambda=0.23\text{\AA}$, corresponding to $\approx 12\text{ km s}^{-1}$.

PG 1303-114 belongs to a sample of halo sub-dwarfs (sdO and sdB) for which a determination of the distance was performed by Moehler et al. (1990). In the framework of a collaboration with the Sternwarte of Bonn we are currently analysing this sample of stars in order to study the gas distribution at large z distances. PG 1303-114 is one of the few stars of our sample which were observable from La Silla at the time of the present observations. In Figure 3 we show the portion of the EMMI spectrum of PG 1303-114 in the NaI region. The exposure time was one hour and the resulting signal-to-noise ratio $S/N = 50$ (1σ level). An interstellar absorption component close to rest velocity is visible at the red side of the NaI atmospheric emissions: this component is probably due to local gas in the galactic disk. No absorption components are detected at higher or lower radial velocities outside the 3σ level. The minimum detectable equivalent width is of about 14 m\AA , corresponding to an upper limit $N(\text{NaI}) < 7 \times 10^{10}\text{ atoms cm}^{-2}$. By adopting the interstellar NaI-HI correlation derived by Ferlet et al. (1985), this in turn implies $N(\text{HI}) < 10^{19}\text{ atoms cm}^{-2}$ in the direction of the star, which is located at about 1.5 kpc from the Sun at a galactic latitude $b=+51^\circ$. If the lack of high-velocity absorption components will be confirmed also in the other lines of sight of our sample, then the idea that high-velocity gas is generally located at $|z| > 1\text{ kpc}$ will receive a sound observational support.

The BL Lac 2155-304 was observed by Morton and Blades (1986) with the AAT in CaII and NaI at a resolution of 17 km s^{-1} and 24 km s^{-1} respectively. They found an absorption component at $V_{\text{LSR}} = -8\text{ km s}^{-1}$ in CaII, but only an upper limit of 83 m\AA in NaI. We decided therefore to re-observe this object in the red spectral range in order to search for NaI absorptions with a high-

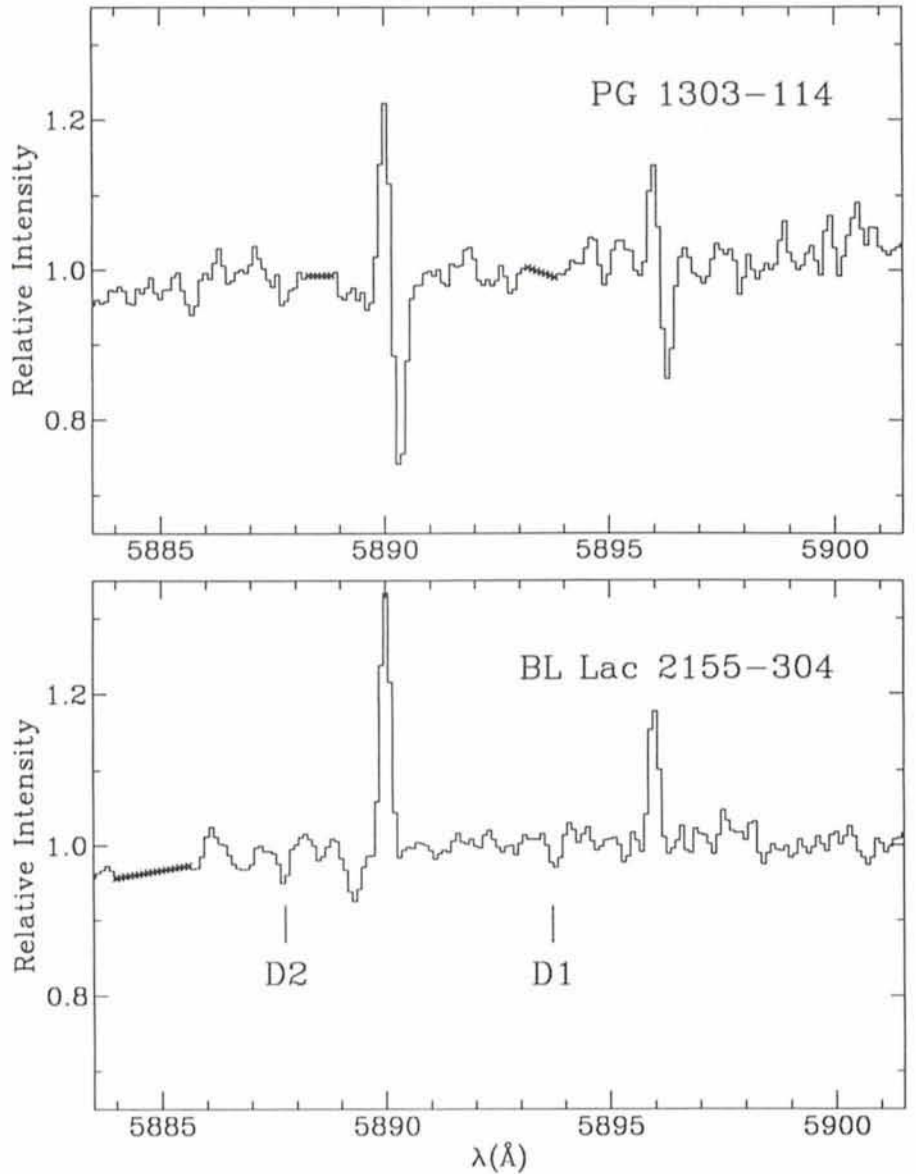


Figure 3: Interstellar NaI absorptions in the direction of the two high-latitude background sources PG 1303-114 and 2155-304. Emission lines at rest velocity are atmospheric. Telluric absorptions were removed by using the spectrum of the bright star HR 5625 as a template. Portions of the spectra cleaned up of cosmic events are marked with crosses.

er sensitivity and spectral resolution. In Figure 3 we show the NaI spectrum of 2155-304; the exposure time was one hour and the resulting $S/N=60$. A NaI absorption of $\approx 28\text{ m\AA}$ is clearly present at the blue side of the D2 atmospheric emission. The radial velocity of this feature, $V_{\text{LSR}} = -9\text{ km s}^{-1}$, is in very good agreement with that of the CaII component detected by Morton and Blades. The D1 absorption at the same velocity is visible as a weak feature close to the noise level. A preliminary estimate of the NaI column density in our spectrum, combined with the CaII column density estimated by Morton and Blades, gives $\text{NaI/CaII} = 0.15$. This low value of the NaI/CaII ratio is characteristic of high-velocity interstellar gas in our Galaxy. This suggests that the

$\approx -9\text{ km s}^{-1}$ component may be produced in high-velocity gas with a low projected velocity along the line of sight.

An exciting feature of the 2155-304 spectrum is the presence of a D1 and D2 absorption at $V_{\text{LSR}} = -90\text{ km s}^{-1}$, both marked in the lower panel of Figure 3. These absorptions are close to the detection limit, but the fact that the line of sight to 2155-304 ($l=18^\circ$, $b=-52^\circ$) falls in a region of the sky where HVCs with negative velocities are predominant (Wakker and van Woerden 1991) encourages us to believe that they are real.

The presence of the -90 km s^{-1} component, if confirmed by future observations, would provide an almost unique opportunity to study a HVC by means of absorption line spectroscopy.

2.4 Detection of PN Candidates in Two Galaxies of the Virgo Cluster

The use of PNe as standard candles has been described in a series of papers (e.g. Ciardullo et al. 1991 and the previous papers in the series), and has been applied to the determination of the distance of the Virgo Cluster (Jacoby et al. 1990) from data taken at the KPNO and CFHT telescopes. The method used by the above authors relies on images taken through a narrow band filter centred on $[OIII]\lambda 5007$, redshifted at the systemic velocity of the cluster being analysed, and images taken through and intermediate-band filter of FWHM $\approx 300 \text{ \AA}$. Jacoby et al. (1990) performed the detection by "blinking" the on-band and the off-band images and selecting as candidates those objects which were detected on the on-band images but not on the off-band ones.

Is it possible to carry out this kind of scientific investigation on the NTT? This question was raised in the framework of a collaboration including OAT scientists (FP, PB), a group at the Sternwarte München led by R.P. Kudritzky, and I.J. Danziger, P. Mazzali and L.B. Lucy at ESO. The "second-level" Remote Observations technological experiment carried out at OAT gave us a chance to test the feasibility of such observations.

Using the general philosophy of Jacoby et al. (1990), we tested the performance of the filters available on EMMI. Due to the lack of an intermediate-band filter in an emission-line-free region, similar to that used by the American investigators, we used filter #591 ($[OIII]$ redshifted at 6000 km/s bandwidth 61 \AA) and #606 (V) as off-band filters and filter #589 ($[OIII]$, bandwidth 56 \AA) as on-band filter. $H\alpha$ images would have been desirable to help the PNe-HII regions discrimination but could not be secured, in the limited observing time available.

For our test we selected two spiral galaxies in the Virgo Cluster: NGC4639 and NGC3627. These targets were selected since they have been the host galaxies of two recent and well-observed type Ia supernovae: 1990N (Leibundgut et al. 1991, Mazzali et al. 1992) and 1989B (Barbon et al. 1990), and thus present the opportunity to compare two different distance determination methods: the PNLF and the maximum brightness of SNe Ia. The images were taken in EMMI RILD mode; the detailed observation log is reported in Balestra et al. (1992). The Remote MIDAS facility allowed us to have an on-line quick look at the images, after acquisition. This was extremely useful both for identification purposes and to assess the image quality; on one occa-

sion this check led us to take a second exposure with a longer exposure time.

Some preliminary work has been done at a very early stage using images which were transferred from La Silla to OAT through the network link. Subsequent data reduction work, aimed at the detection of PNe candidates, was done off-line at OAT on an HP/Apollo 4000/425 workstation running MIDAS. The images were bias subtracted and divided by sky-flat-fields. On each of the calibrated images we ran an automated object finder (MIDAS invent context) and, for the time being, the identifications are then checked visually.

As can be seen from the two images of NGC4639 reproduced here (Fig. 4), there are many objects which are detected in $[OIII]$ but not in V; such objects are our PN candidates. The redshifted $[OIII]$ filter proved to be less effective than the V filter, probably because, due to the limited observing time and the fact that this filter is narrow, this image is not deeper than the on-band $[OIII]$ image. Before we can claim that our candidates are PNe we must worry about: (1) detection of spurious objects; (2) missing true PNe. There are substantially three types of objects which we can expect to detect in the $[OIII]\lambda 5007$ filter: HII regions, Novae and PNe. Novae are likely to contaminate the sample only marginally since we expect PNe to be much more numerous than Novae in outburst at any given time. Therefore, the only objects we really have to worry about are HII region galaxies. HII regions should appear to be extended and moreover their ratio of $[OIII]$ magnitude to V should be lower than that of PNe, since HII regions are usually of lower excitation than PNe.

The other concern is that a true PN may be detected also in V, since this filter includes $H\alpha$ and $[OIII]\lambda 5007$, although the contribution of the continuum from the central stars of PNe should be negligible with respect to the galaxy background. Anyhow, in this filter the contrast with the galaxy background is lower, which makes the detection more difficult. In order to avoid detecting PNe in the V images, one should keep the detection threshold rather high, yet low enough to detect safely all the HII regions.

The next step of this work, to be carried out in collaboration with the Sternwarte München and ESO groups, will be to discriminate PNe from HII regions in our candidate list and perform astrometry and photometry on the candidates. It is not clear whether the images we have will allow a satisfactory discrimination against HII regions, $H\alpha$ images may prove to be necessary in this respect; yet we believe the feasibility

of this project to be now well established.

2.5 Distant Clusters: EMSS Source 2137.3-2353

The target of our observations belongs to a list of 'distant' ($z > 0.2$) clusters of the Southern Sky, identified as X-ray sources with the Einstein Medium Sensitivity Survey (Gioia et al. 1990, Stocke et al. 1991) and lacking good optical images. The list has been compiled in collaboration with astronomers of several Italian Institutes. The purpose of obtaining images for the clusters in the list is to create a good statistical sample with well-determined optical and X-ray properties. This sample is necessary in order to analyse the evolution of the relation between the galaxies of the cluster galaxies and the ICM from local to distant clusters. That the local relation between galaxies and gas should change in the redshift range $0.2 \leq z \leq 0.6$, is suggested by several evidences (e.g. Garilli et al. 1992, Fabricant et al. 1991, Henry et al. 1992, Nesci et al. 1991). In particular there seems to be a trend for clusters of given richness to be less X-ray bright and richer of blue galaxies as the redshift increases. This trend is predicted by some current cosmological models (e.g. Evrard 1990).

Among the objects of the list we have observed the source 2137.3-3553 ($z=0.313$, $F_x=21.78 \cdot 10^{-13} \text{ erg cm}^{-2} \text{ sec}^{-1}$) since it was observable at a small zenithal angle. We have taken VRI images with EMMI in the RILD configuration and the only CCD available during the test, the Thompson 1024×1024 CCD (ESO #18). The scale on the CCD is .44 arcsec/pixel and the field is 56.3 arcmin². The seeing during our observations was ≈ 1 arcsec.

The total exposure time in each of the three colours V, R and I is of 45 minutes, 20 minutes and 30 minutes respectively.

After the bias subtraction and the flat-field correction, a preliminary photometry in the V band shows that we have reached $V = 23$. As soon as all the frames will be properly co-added, we will separate galaxies from stars and use a colour-colour diagram to identify background/foreground objects. The final result we expect from our observations is the measurement of the main properties of the distribution of galaxies in the cluster, such as the richness and the content and space distribution of 'blue' galaxies.

2.6 Candidate Einstein Ring PKS 1830-211 2

PKS 1830-211 is a flat-spectrum source which shows two lobes in the

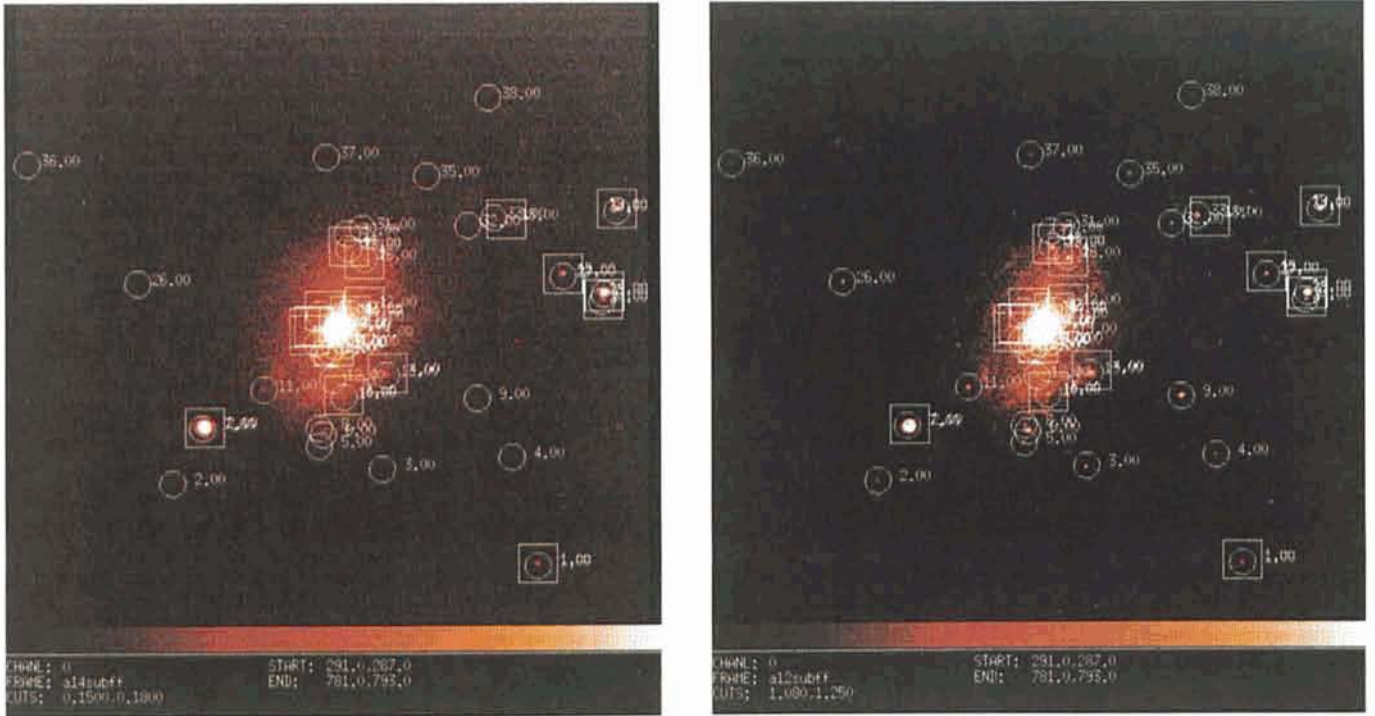


Figure 4: Two images of NGC 4639 taken with EMMI in RILD mode. On the left-hand side the image taken through the V filter, on the right-hand side the image taken through the $[OIII]\lambda 5007$ filter. Circles surround the positions of objects detected in the $[OIII]$ image, while squares surround the positions of objects detected in the V image. The objects which are detected in the $[OIII]$ image, but not in the V image, are PN candidates. The low cut has been kept lower in the V image to stress the absence of detectable objects.

radio (VLA and VLBI observations; Rao and Subrahmanyan 1988, Subrahmanyan et al. 1990, Jauncey et al. 1991). The separation of the two radio lobes is 1 arcsec. The shape and spectra of the radio ‘lobes’ (NE and SW) suggest that PKS 1830-211 is a strong Einstein Ring (Rao and Subrahmanyan 1988, Subrahmanyan et al. 1990, Jauncey et al. 1991). This kind of gravitational lenses are particularly interesting since they can be very powerful cosmological tools, allowing, in principle, the determination of the Hubble constant and the mass distribution of the lensing galaxies.

Optical observations of PKS 1830-211 have failed, so far, to reveal the counterparts of the two radio components (Subrahmanyan et al. 1990, Djorgovsky et al. 1992). Djorgovsky et al. (1992) have recently presented the whole set of data they used in search for optical counterparts of the candidate radio ring. The optical data include CCD images taken with the ESO 3.6-m (BVR bands) and ESO NTT (BRI bands) telescopes and with the Palomar 200-inch telescope (K and Gunn ‘i’ bands).

We had planned our remote observations with SUSI, which, however, was not available for the test run. We decided to use EMMI in the RILD configuration (see section 2.5). Our primary goal with EMMI was to reach a fair depth and obtain good magnitudes for the objects in the field of PKS 1830-211,

rather than identify and/or separate the possible optical components of the radio source. In fact, as far as angular resolution is concerned, our observations cannot compete with those of Djorgovsky et al. from the NTT with SUSI (0.13 arcsec/pixel) and a seeing of 0.75 arcsec. However, their night was not photometric and magnitudes were only roughly estimated.

We have taken 5 frames in the I band centred on the position of the radio source PKS 1830-211. Each frame has been exposed for 10 minutes. After the first three exposures we have offset the telescope 4" (or 10 pixels) eastward.

A preliminary analysis of the fields shows that the PSF has a FWHM slightly smaller than 1 arcsec and that we have reached $I = 18.5$ in each frame. Unfortunately, this is not faint enough for our purposes. The reason is that the brightness of the sky was too high at the time our observations took place: the moon was still up, even if very low.

2.7 Seyfert Galaxies

One of the most interesting questions in extragalactic astronomy is what triggers the activity in the nuclei of some galaxies (AGNs): e.g. Norman et al., Scoville et al. suggested a relationship between AGNs and starburst activity in the sense that the starbursts are the evolutionary precursor of AGNs; on the other hand (e.g. Daly) the energy re-

leased by an AGN could trigger star formation in the surrounding galaxy. This interrelation may reflect in peculiar morphologies and/or colours in regions surrounding the nucleus. With this problem in mind we started a programme to observe both in the infrared and optical bands galaxies hosting AGN. Pilot observations were conducted during this test: targets are selected from the CfA list (Huchra et al.), 5 galaxies were selected on the basis of observing time constraints and because we already have multi-aperture photometry in J, H, K infrared bands for these objects. Images were taken in V and R bands with exposure times ranging from 120 to 420 sec; the seeing was ≈ 1 arcsec; preliminary analysis shows that we reached at least 26 mag arc⁻² in shorter exposures.

Acknowledgements

The authors are grateful for the opportunity they were given to perform scientific observations on the NTT in the framework of the ESO/OAT technological project on “second-level” remote observing. They would like to thank in particular A. Balestra, C. Corte, P. Maruccci, P. Santin, R. Smareglia and C. Vuerli of OAT, and M. Comin and A. Wallander of ESO who, through their hard work, set up at OAT a temporary but absolutely functional and efficient clone of the ESO remote observing system. Special thanks to S. D’Odorico,

who gave some very important suggestions on NTT instrumental set-ups and observing procedures, and to the La Silla night assistant M. Pizzaro who played an essential role for the success of the observing run.

References

A. Balestra et al., 1992, *OAT Publ.* No. 1443.
 R. Barbon et al., 1990, *A&A* **237**, 79.
 Ciardullo et al., 1991, *Ap.J.* **383**, 487.
 R. Daly, 1990, *Ap.J.* **355**, 416.
 H. Dekker et al., 1991, ESO Operating Manual No. 14.
 S. Djorgovsky et al., 1992, preprint.
 A.E. Evrard, 1990, *Ap.J.* **363**, 349.

D. Fabricant et al., 1991, *Ap.J.* **381**, 33.
 R. Ferlet, A. Vidal-Madjar, C. Gry, 1985, *Ap.J.* **298**, 838.
 U. Finkenzeller, G. Basri, 1987, *Ap.J.* **318**, 823.
 M. Franchini et al., 1992a, *A&A* **256**, 525.
 M. Franchini et al., 1992b, in preparation.
 B. Garilli et al., 1992, *A.J.* in press.
 I. Gioia et al., 1990, *Ap.J.S.* **72**, 567.
 P. Henry et al., 1992, *Ap.J.* **356**, L35.
 J. Huchra, R. Burg, *Ap.J.* **1992**, 393, 90.
 Jacoby et al., 1990, *Ap.J.* **356**, 332.
 D. Jauncey et al., 1991, *Nature* **352**, 132.
 F.P. Keenan et al., 1988, *A&A* **192**, 295.
 B. Leibundgut et al., 1991, *Ap.J.* **371**, L23.
 M. Lemoine et al., 1992, *The Messenger* **67**, 40.

P.A. Mazzali et al., 1992, *A&A* in press.
 S. Moehler, U. Herber, K.S. de Boer, 1990, *A&A* **239**, 265.
 P. Molaro, 1991, *Mem. S.A.It.* **62**, 17.
 C.D. Morton, J.C. Blades, 1986, *M.N.R.A.S.* **220**, 927.
 R. Nesci et al., *A&A* **252**, 13.
 C. Norman, N. Scoville, 1988, *Ap.J.* **332**, 124.
 A.P. Rao, R. Subrahmanyam, 1988, *M.N.* **231**, 229.
 S.G. Ryan, J.E. Norris, M.S. Bessel, 1991, *A.J.* **102**, 303.
 N. Scoville, C. Norman, 1989, *Ap.J.* **332**, 163.
 J.T. Stocke et al., 1991, *Ap.J.S.* **76**, 813.
 R. Subrahmanyam et al., 1990, *M.N.* **246**, 263.
 B.P. Wakker, H. van Woerden, 1991, *A&A* **250**, 509.

The Giant Arc in EMSS2137-23

M. RAMELLA and M. NONINO, *Osservatorio Astronomico, Trieste, Italy*

During the three nights devoted to the test of the 'second level remote observing' we observed the cluster EMSS 2137-23 with NTT and EMMI. This cluster is a rather bright EMSS source and has a redshift $z = 0.32$. These characteristics make EMSS2137-23 a perfect candidate for the study of the relation between the gas and the galaxian components of a non-local cluster. We wanted to obtain photometry for the galaxies of the clusters in order to build a magnitude limited sample. Details of the observations are found in the article by Franchini et al. in this issue.

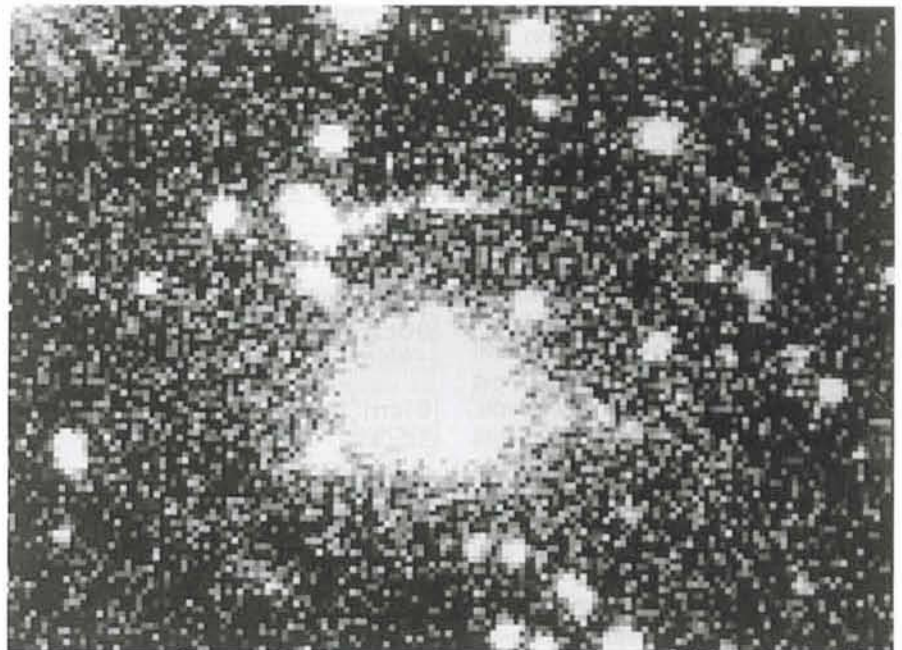
The choice of the cluster was very fortunate, since our images also revealed a giant gravitational arc and several arclets surrounding the cD galaxy of the cluster. However, after our observations had taken place we learned that this arc had already been discovered by Fort et al. in 1991, also with the NTT. (See also the article by G. Soucail in this issue of the *Messenger*.) Our images of the arc are of good quality (see the figure).

Because of our original project on this cluster we also have redshifts for about 50 galaxies in the field (the redshifts are available to us thanks to a collaboration with Dan Fabricant at the Center for Astrophysics). The fact that the arc is in a cluster for which we have such a complete set of optical and X-ray information makes the study of this arc particularly interesting for the determination of the mass distribution within the cluster and for the verification of the model of the lens. Before building the model, in collaboration with Emilio Falco (CfA), deeper images will be needed in order to confirm the several candidate arclets,

which set very important constraints on the model itself.

We moreover note that at least one substructure of the main arc is probably bright enough to be observed spectroscopically (the integrated magnitude of

the feature is $R = 21.5$ and its surface brightness is $\geq 5\%$ of the sky). The spectroscopy of the arc would reveal the nature of the lensed object, something that has been possible only in four cases so far.



This image shows the compact cluster of galaxies EMSS2137-23 and the 15 arcsec long "giant arc", just north of the centre of the cluster, as obtained in June 1992 with the ESO 3.5-m New Technology Telescope (NTT) and the ESO Multi-Mode Instrument (EMMI) during remote observations from the Trieste Astronomical Observatory. The frame is a combination of 5 exposures in V, R and I, with a total exposure time of 95 min. The seeing was ~ 1.0 arcsecond. 1 pixel = 0.44 arcsecond. The field measures 70×52 arcsec; north is up and east is to the left.

The Squeeze is on the La Silla Observatory

H. VAN DER LAAN, Director General, ESO

Visiting La Silla in early August, it struck me again how our observatory and its staff are squeezed between two developments in ESO, developments which by their nature tend to continue and which must be adjusted soon if we are to maintain a healthy working climate on La Silla. In a talk to all staff on the mountain I raised these and some other issues. The relevant developments are: (1) the increase in both quantity and technical complexity of the hard- and software in the domes, and (2) the slow but steady reduction of resources in favour of the VLT Observatory now under construction. Actually there is a third tendency which is laudable but makes matters more difficult still, namely the increasing ambition of our users community, manifest in increasing proposal pressure and more subtly in increased expectations if not demands of services to be provided by ESO/Chile staff.

The circumstances can be partly inferred from the two accompanying tables, which give the menus offered to visiting astronomers just five years apart. They are from the Announcements for Period 41 and Period 51 respectively, issued in August five years ago and this year. Close inspection of these two menus reveals how much a major observatory changes in just five years, over and above the addition of the NTT with all its sophistication and corresponding technical fragility. Nearly all detectors on the major telescopes have been renewed, thanks to industrial developments and a large effort by the Instrumentation Groups in Garching to stay on top of this evolution. The readiness maintenance for all these detectors on La Silla is no small task. The power and versatility of EFOSC on the 3.6-m have spawned the second EFOSC now on the 2.2-m telescope as well as EMMI on the NTT and DEFOSC, ready next year for the 1.54-m Danish telescope. EMMI is a veritable suite of instruments all rolled into one compact multi-mode device. Infrared capacities on La Silla have dramatically improved with the renovated IRSPEC on the NTT and the IRAC2 imager on the 2.2-m. Next year the 10-micron spectrophotometer TIMMI adds another infrared state-of-the-art capability to the 3.6-m.

For Periods 39 and 40 (1 April 1987 – 31 March 1988) there were 670 proposals while for Periods 49 and 50 (1 April 1992 – 31 March 1993) there were 880, with in addition two dozen Key Pro-

grammes running now. While I have re-distributed resources for La Silla somewhat over the several departments in the Observatory, the total manpower resources have actually decreased slightly in the last five years. Yet our teams there

have maintained a high service quality while coping with the greatly augmented quantity of telescope-instrument mode combinations. It is an impressive increase in productivity which is now approaching its limits.

3.6m	PF Triplet	Blue	Red	Direct photography	
	Infrared Photometer			Grism	
	Infrared Speckle			Photometric Wedge	
	IRSPEC			Bolometer	
	Cass B & C Spectrograph			In Sb Detector	
	Cass B & C Optopus			CCD (LR*)	
	Cass Echelle Spectrograph			CCD (coated GEC)	
	EFOSC			CCD (LR*)	
				CCD (HR*)	
				CCD (LR*)	
2.2m	Cass Direct Imagery			CCD (coated GEC)	
	Cass B & C Spectrograph			Bolometer	
	Polarimeter			In Sb Detector	
	Infrared Photometer				
1.5m	Cass B & C Spectrograph			Reticon	
	Echelec Spectrograph			CCD (coated GEC)	
	Coudé Spectrograph			CCD (LR*)	
1.4mCAT	CES Short Camera	Blue	Red	Camera I	Camera II
	CES Long Camera	Blue	Red	CCD (HR*)	
				Scanner	
				Reticon	
1m	Infrared Photometer			Bolometer	
	Single Channel Photometer			In Sb Detector	
50cm	Single Channel Photometer				
				PM RCA 31034	
90cm DUTCH	Single Channel Photometer			PM EMI 9789 QB	
	Walraven Photometer			PM EMI 9658	
61cm BOCHUM	Single Channel Photometer				
				CCD Camera	
1.5m DANISH	Direct Imagery			Photography	
	6 Ch Photometer				
50cm DANISH	uvby H β Photometer				
				LR - Low Resolution RCA 512-320 pixels 30-30 μ	
Schmidt GPO	With Prism			HR - High Resolution RCA 1024-640 pixels 15-15 μ	
	Without Prism				
SEST	3mm Receiver				

Table 1. Telescopes and Available Auxiliary Equipment (Period 41, 1 April-1 October 1988).

ESO Headquarter resources are now predominantly directed towards the design and construction of the VLT Observatory. Readers of the *Messenger* are well aware of the new observatory's scope and the multiplicity of its technological systems. They are unprecedented in the history of ground-based astronomy. They are also a daunting challenge for the whole of ESO and our partners, industrial and institutional. I have had no choice but to divert to the VLT all the resources that could in my view be possibly spared in the Science Division and on La Silla. We have now reached the stage where users have to be confronted with resource limits, where the present opportunities on La Silla will be curtailed for the sake of future opportunities on Paranal.

In the Scientific-Technical Committee a discussion is to take place on the options for containing the La Silla staff's workload. It is clear that quality and reliability cannot be compromised. Instead, the menu of what is offered in any one period must be simplified. Instrument changes, with the attendant alignment, stabilization and calibration tasks, are the prime source of technical workloads. I have asked the heads of the Technical Research Support and of the Astronomy Support Departments to prepare a paper for the November meeting of the STC. We astronomers are notoriously incapable of deciding what we do *not really* need; as a community we usually behave like the character in the popsong who asserts that "I want it all and I want it now". But ESO is

"caught between a rock and a hard place" and if we do not make choices then the compromises that are the worst choice of all will arise by default. And so the squeeze on La Silla will be diverted, to a squeeze on the STC and subsequently on Council, the next Executive and ultimately on ESO's users. All for the sake of the exciting prospects created on Cerro Paranal. I am sure they are worth it!

New ESO Scientific Preprints

(June – August 1992)

3.6m	Infrared Photometer	Bolometer	
	Prime Focus Direct Imaging	InSb Detector	
	EFOSC 1	CCD TH1K#19 Coated	
	MEFOS	CCD TEK#26	
	CASPEC	CCD TEK512#16	
	Link to CES (Specify camera under 1.4m CAT)		
3.5m NTT †	S _A) IRSPEC	CCD TEK1K#25	
	S _A) SUSI	CCD TH1K#18	
	S _B) EMMI Standard Configuration Red	CCD TEK1K#28	
	S _B) EMMI High Resolution Echelle Red		
S _B) EMMI Standard Configuration Blue			
2.2m	Direct Imaging	CCD RCA#8 H-Res	
	EFOSC 2	CCD TH1K#19 Coated	
	Infrared Photometer	Bolometer	
	IRAC 1	InSb Detector	
	IRAC 2		
PISCO			
1.52m	Cass. B&C Spectrograph	CCD FA2K# Coated	
	Echelec Spectrograph	CCD RCA#13 H-Res	
1.4m CAT *	CES : Short Camera (Blue) *	CCD FA#27 Coated	
	CES : Short Camera (Red) *	CCD RCA#9 H-Res	
	CES : Long Camera (Blue) *		
	CES : Long Camera (Red) *		
1m	Infrared Photometer	Bolometer	
	Single Channel Photometer	In Sb Detector	
50cm	Single Channel Photometer	P.M.T. RCA 31034	
		P.M.T. EMI 9789 QB	
		P.M.T. EMI 9658	
		P.M.T. HAM R943-02	
50cm Danish	uvby H β Photometer		
1.54m Danish	Direct Imaging	CCD TEK1K#	
90cm Dutch	Direct Imaging	CCD GEC#7 Coated	
Schmidt GPO	With prism	IIa-O	IIIa-F
	Without prism	IIIa-J	IV-N
SEST	0.8mm Receiver	Narrowband AOS	
	1.3mm Bolometer	Broadband AOS	
	1.3mm Receiver		
	3.0mm Receiver		

Notes: (*) The combination of these telescopes, instruments and detectors can be used remotely from the ESO Headquarters in Garching.
 (†) S_A/S_B Option available simultaneously.

Table 2. Available Telescopes and Auxiliary Equipment (Period 51, 1 April–1 October 1993).

844. P. Ruiz-Lapuente and L. B. Lucy: Nebular Spectra of Type Ia SNe as Probes for Extragalactic Distances, Reddening and Nucleosynthesis. *The Astrophysical Journal*.
845. M. A. Prieto, J. Walsh and Robert Fosbury: IPCS Observations of Extended Gas in Radio Galaxies. *Gemini*.
846. J. Einasto and M. Gramann: Transition Scale to a Homogeneous Universe. *Astronomy and Astrophysics*.
847. F. Murtagh, M. Sarazin and H.-M. Adorf: Statistical Prediction of Astronomical Seeing and of Telescope Thermal Environment. ESO Conference on "Progress in Telescope and Instrumentation Technologies".
848. G. A. Tammann: The Cosmic Expansion and Deviations from It. Crafoord-Symp. "Extragalactic Astronomy including Observations Cosmology".
849. L. Wang and E. J. Wampler: The Supernova SN 1987A: the Nebular Loops and "Napoleon's Hat". *Astronomy and Astrophysics*.
850. T. Richtler, E. K. Grebel, H. Domgörgen, M. Hilker and M. Kissler: The Globular Cluster System of NGC 1404. *Astronomy and Astrophysics*.
851. R. F. Peletier: The Stellar Content of Elliptical Galaxies: Optical and Infrared Colour Profiles of M 32 and NGC 205. *Astronomy and Astrophysics*.
852. R. Siebenmorgen, E. Krügel and J. S. Mathis: Radiative Transfer for Transiently Heated Particles. *Astronomy and Astrophysics*.
853. M. Della Valle and N. Panagia: Type Ia Supernovae in Late Type Galaxies: Reddening Correction, Scale Height and Absolute Maximum Magnitude. *The Astronomical Journal*.
854. L. Pasquini: The Ca II K Line in Solar Type Stars. *Astronomy and Astrophysics*.
855. Bo Reipurth and B. Pettersson: Star Formation in Bok Globules and Low-Mass Clouds. V. H α Emission Stars Near SA 101, CG 13 and CG 22. *Astronomy and Astrophysics*.

856. P. Dubath, G. Meylan and M. Mayor: Core Velocity Dispersions and Metallicities of Three Globular Clusters Belonging to the Fornax Dwarf Spheroidal Galaxy. *The Astrophysical Journal*.
857. R. P. Saglia et al.: Stellar Dynamical Evidence for Dark Halos in Elliptical Galaxies: The Case of NGC 4472, IC 4296 and NGC 7144. *The Astrophysical Journal*.
858. P. A. Mazzali et al.: Models for the Early Time Spectral Evolution of the 'Standard' Type Ia Supernova 1990N. *Astronomy and Astrophysics*.
859. S. Heathcote and Bo Reipurth: Kinematics and Evolution of the HH 34 Complex. *The Astronomical Journal*.
860. M.-H. Ulrich: Multiwavelength Observations of the Quasar Q1821+643 During the ROSAT All Sky Survey. *Astronomy and Astrophysics*.

PROFILE OF A KEY PROGRAMME:

CCD and Conventional Photometry of Components of Visual Binaries

E. OBLAK¹, A.N. ARGUE², P. BROSCHE³, J. CUYPERS⁴, J. DOMMANGET⁴, A. DUQUENNOY⁵, M. FROESCHLÉ⁶, M. GRENON⁵, J.L. HALBWACHS⁷, G. JASNIEWICZ⁷, P. LAMPENS⁴, E. MARTIN⁹, J.C. MERMILLIOD⁸, F. MIGNARD⁶, D. SINACHOPOULOS⁴, W. SEGGEWISS³, E. VAN DESSEL⁴

¹Observatoire de Besançon, France; ²Institute of Astronomy, Cambridge, United Kingdom; ³Observatorium Hoher List, Bonn, Germany; ⁴Royal Observatory of Belgium, Brussels, Belgium; ⁵Observatoire de Genève, Sauverny, Switzerland; ⁶Observatoire de la Côte d'Azur, Grasse, France; ⁷Observatoire de Strasbourg, France; ⁸Institut Astronomique de Lausanne, Sauverny, Switzerland; ⁹Instituto de Astrofísica de Canarias, Tenerife.

1. Introduction

The study of double stars, apart from long being recognized as a basic key to the understanding of star formation and evolution, actually deserves particular attention for many additional reasons:

(1) the ratio of known double to single stars is continuously upgraded and the rate of detection is steadily increasing, both from ground-based and space observations;

(2) space observations (Hipparcos, HST) significantly improve the quality and the importance of stellar samples. They permit to better take into account some of the former selection effects as they reveal a lot of new double stars, especially among the close visual pairs;

(3) the high-quality astrometric (and partly photometric) data that will be made available for a large number of double stars by the space results should be matched accordingly with accurate and homogeneous complementary astrophysical information such as colour indices and spectral types.

(4) Such accurate ground-based information for each of the components of close visual double stars (angular separations less than some ten arcseconds) is almost nonexistent on a large scale – e.g. the astrometric "Catalogue des Composantes d'Etoiles Doubles et Multiples" (CCDM; Dommanget, 1989) contains over 65,000 systems but fewer than 10% have accurate and reliable photometry –, but is recently made possible with the breakthrough of CCD de-

tectors in spectroscopic and photometric techniques.

The importance of studies of visual double stars lies not only in the traditional determination of stellar masses in orbital pairs – however fundamental these may be – but also in the determination of the characteristics and the frequency of double stars in different stellar populations and evolutionary stages. The distributions of the characteristics typical of double stars such as periods, eccentricities, mass ratios, relative ratios of double and multiple star systems are actually not sufficiently well known to provide valuable constraints on the different star formation scenarios.

In order to acquire this knowledge, the astrophysical information available from magnitudes, colours, spectral types and velocities is fundamentally needed. The usefulness of photometry of visual binaries is especially obvious in applications concerning, for example, luminosity calibrations, the mass-luminosity relationship, mass-ratio determination from differential magnitudes, age and evolution determination. But the type and the accuracy of the photometric information depend very strongly on the separation of the binary components:

– Wide visual double stars (with separations larger than 12") present no difficulty to conventional photoelectric photometry. Individual data are easily secured, even though a more careful

procedure (choice of sky, centring) than in the case of single stars may be desirable to obtain high-quality data.

– To the extreme other end of the range in separation, the interest for the very close binary systems (visually non-separable) arose during the last decade because of the physically interesting underlying mass transfer problem. In these cases, global photometry is performed.

– The technical difficulties of observing two images in close proximity to one another are especially pronounced in carrying out conventional photoelectric photometry for the remaining class of double stars with separations in the intermediate range. This class of objects has therefore largely been neglected in past photometric programmes. When available, global photometry in combination with visual or photographic estimates of the magnitude differences are not sufficiently precise to match the actual requirements and the accuracy achieved in other techniques.

With the introduction of CCD detectors on photometric telescopes, it now also appears feasible to obtain accurate photometric data for each of the components of close visual double stars with angular separations between 1 and 12".

2. The Scientific Justification

A comprehensive catalogue of physical pairs – from the very close to the

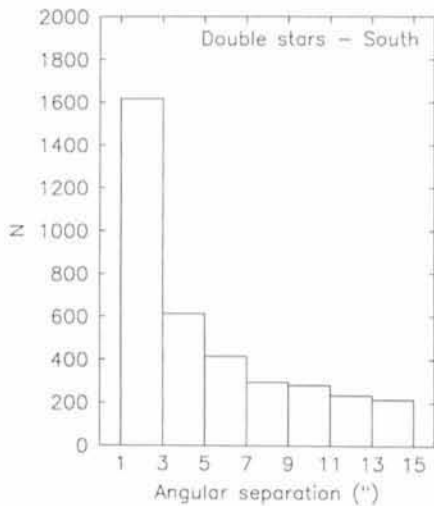


Figure 1: Distribution of the angular separations between the components of the double stars for the southern hemisphere ($\delta < +10^\circ$).

very wide ones – with a maximum number of astrometric, spectroscopic and photometric good-quality data would be a highly valuable astrophysical tool because it would contain several clues concerning the mode of star formation and consequently also the structure and the evolution of our galaxy.

The construction of such a basic sample of double stars is now within reach, thanks to the ground-based technological progress as well as to the huge preparational work and fine results from the Hipparcos space mission. On one side, its systematic all-sky survey has permitted the detection of a large number of new double stars, with separations small enough to partially fill the known “gap” between the spectroscopic and the visual double stars. On the other side, the mission will provide accurate parallaxes and proper motions for all the double stars included in the Hipparcos Input Catalogue (more than 10 %), allowing to precisely define the distance-limited samples but also to recognize more surely optical systems. Moreover, different groups have already addressed the spectroscopic aspect (ESO Key Programmes for radial velocities) of the Hipparcos stars, containing at least partially the basic sample we wish to investigate.

The aim of this group, collaborating in the frame of a European network of laboratories (Oblak et al., 1992), is to contribute to a systematic and unbiased photometric survey of the components of double and multiple stars.

The available photometric data, obtained at ground-based observatories or in space programmes, are mostly concerned with the global system. To obtain the relevant astrophysical information we need the individual photometric

data on all the components of a double or multiple system. A programme of systematic and homogeneous acquisition of precise colour indices for several thousands of components of double and multiple systems has been defined in both hemispheres, with the following priorities:

(1) to supplement the Hipparcos magnitudes by astrophysically significant colour indices providing the additional physical parameters such as temperature and gravity;

(2) to complete the photometric information for the components not included in the Input Catalogue. This is important since accurate micrometric data for the wider pairs may indicate whether or not the components are optical. Our principal scientific objective is to provide the missing photometric data needed to supplement the high quality and extensive astrometric and photometric data on known and newly detected double stars in order to be able to adequately study the mechanisms of formation and evolution of double and multiple star systems.

Such a less-biased survey is urgently needed to improve current theories on

formation, evolution and structure of the Galaxy. Indeed, ground-based and space observations reveal that at least half of the stars belong to double and multiple systems but current theories still cannot explain the formation of such a large number of systems.

3. The Observational Programme

The selection of the programme stars (Oblak and Lampens, 1992) was made amongst 11,434 double systems, 1960 triple systems, 536 quadruple systems and 237 multiple systems from Annex 1 of the Hipparcos Input Catalogue, containing objects to a distance of 500 pc (Turon et al., 1992).

In view of repeated photometric campaigns distributed over both hemispheres the observational programme consists of a northern (declination of the primary component > -10) and a southern sample ($\delta A \leq +10$). The overlapping zone in declination $-10 < \delta A \leq +10$ is only once observed according to feasibility.

Since both classical photometry and CCD are considered, the selection further included splitting according to

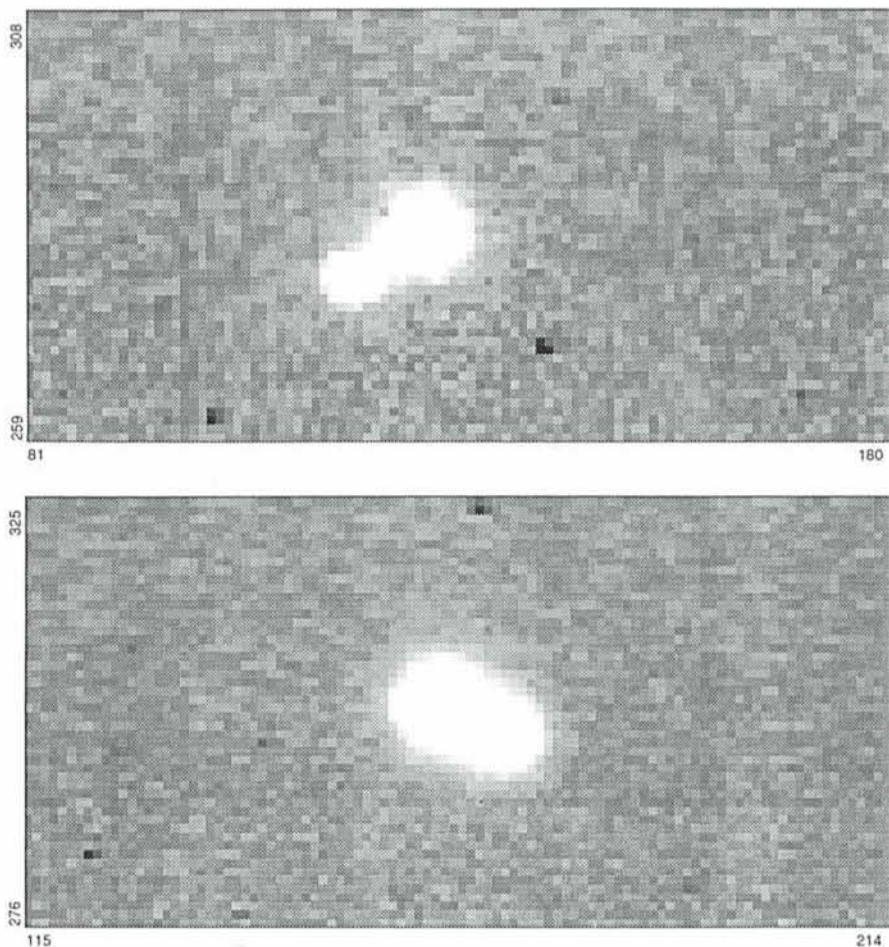


Figure 2: CCD frames for the stars HD 24445: $\varrho = 8''.2$, $V(A) = 8.3$, $V(B) = 10.6$, in the I filter and HD 87239: $\varrho = 6''.3$, $V(A) = 9.0$, $V(B) = 9.6$, in the V filter (OHP – seeing = 2", December 1991).

angular separation and differential magnitude. For separations larger than $12''$, individual magnitudes and colours are easily obtained from classical photometry on small telescopes. For separations smaller than $15''$, CCD photometry is more efficient and adequate as long as the difference in magnitude is smaller than three. Astrometric information is obtained as a by-product. The overlapping range in separation has been considered for calibration purposes between two very different techniques. A comparison with the "Catalogue Photométrique des Systèmes Doubles et Multiples" (CPSDM; Oblak, 1988) allowed to identify those systems lacking individual photometric information.

Observations have already started in various observatories located in both hemispheres: Calar Alto, Jungfraujoch, Observatoire de Haute-Provence and La Palma (Argue et al., 1992) for the northern part and La Silla for the southern part.

The ESO Key Programme has been introduced to obtain photometry (occasionally astrometry) in the Cousins VRI bands for those selected systems of the southern hemisphere lacking such precise information (Fig. 1). The observations are made with the CCD detector attached to the 90-cm Dutch telescope for the close visual pairs and on the 50-cm telescopes for the conventional VRI photometry for that part of the programme consisting of wide double and multiple stars.

4. Reduction of the Observations

While the conventional photometry will be reduced in a standard way, a preliminary reduction can only be done with the known packages for the photometric reduction of CCD frames. Crowded-field-photometry routines cannot be applied without modifications to most of the frames obtained, since no reference star images are available (Fig. 2). Therefore, individual profile fittings are necessary. Accurate profiles are needed to separate the closest pairs in the programme (Fig. 3).

In one of the techniques in use for the reductions, a row and a column projection is applied on each CCD frame and a Franz's profile is fitted on the data according to the least-square method supported by an expert system routine (Sinachopoulos, 1992). Other techniques are in use in Geneva and Cambridge (Irwin, 1985). A further one is still under development at Bonn. All these techniques will be compared and the most appropriate for the stellar images on the CCD frames will be accepted for the final data reduction.

Differential magnitudes and relative

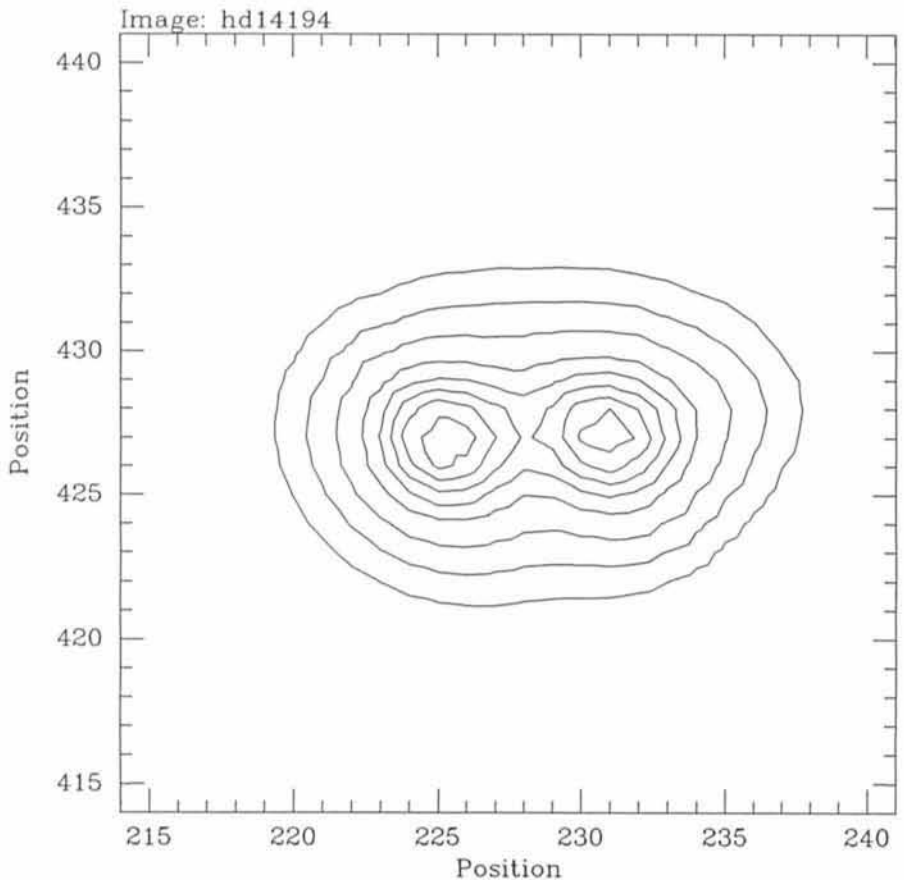


Figure 3: CCD image of the double star HD 14194 observed with the 90-cm Dutch telescope at ESO: date: 17/10/91; exposure time: 15s; mag A: 9.6; $dm = .1$, $\rho = 2''.1$, seeing = $1''.3$. The preliminary reduction gives: $dm = 0.054$, $\rho = 2''.15$.

positions will be obtained with high precision. Efforts are also made in writing and testing additional software for extraction of individual magnitudes and colour indices with an accuracy at the 1% level.

Standard star measurements allow to correct for extinction and to transform the magnitudes to the standard VRI system. Extinction coefficients derived from photometric observations at nearby telescopes will be used when available. Finally, all observations will be processed as homogeneously as possible with a well-defined adopted "standard" procedure.

5. Forthcoming Extensions

In order to have a less biased observational programme and to supplement in a useful way the photometric data, we intend to introduce the double stars not yet included in the Input Catalogue but listed in more recent double star catalogues (Cousteau (1992), Worley and Douglas (1984; or its new version)). By arrangement with ESA, we will also be able to include the new double stars with separations greater than one arc-second detected in the Hipparcos mission. This limit could eventually be de-

creased in the future, with the use of larger telescopes.

For a better evaluation of the multiplicity on our samples, the information of spectroscopic and speckle interferometric duplicity will be introduced as well. A double star photometric data base, to be integrated in the "Centre de Données Astronomiques de Strasbourg", will be established at the Observatory of Besançon.

We gratefully thank ESO for the allocation time to the Key Programme and are confident that accurate basic data for astrophysically well-defined samples of visual double stars will be within reach during the next few years.

References

- Argue, A.N., Bunclark, P.S., Irwin, M.J., Lampens, P., Sinachopoulos, D. and Wayman, P.A., 1992, *Mon. Not. R. Astr. Soc.*, in press.
- Cousteau, P., 1992, *Catalogue des Etoiles Doubles Cousteau*, available at Centre de Données Astronomiques de Strasbourg, Strasbourg.
- Dommanget, J., 1989, in: *Star Catalogues: A Centennial Tribute to A.N. Vyssotsky*, Eds. Philip and Uppgren, 77-82.
- Irwin, M.J., 1985, Automatic analysis of crowded fields, *Mon. Not. R. Astr. Soc.*, **214**, 575.

THE 3rd ESO/OHP SUMMER SCHOOL:

Provençal Summer, Hard Work and Warm Hospitality

M. VÉRON, OHP, France, and D. BAADE, ESO

Introduction

Counting the observatories that on the territories of the ESO member countries still operate several telescopes with up-to-date instrumentation, requires the fingers not even of one hand. Accordingly scarce are the opportunities for students to get practical observing experience before this experience is really needed. The scope of the ESO/OHP Summer Schools is to help alleviating this deficiency. For obvious practical reasons neither La Silla and certainly not Garching are suitable sites for this purpose.

One of the few remaining observatories in Europe is the Observatoire de Haute-Provence (OHP). It is named after one of the most attractive regions in the south of France. However, between July 15 and 25 the focus of the attention of 18 graduate students from nine different countries was not on tourism but on the OHP where the third ESO/OHP Summer School took place. Their aim was to partly fill in the observational void in the standard university curriculum.

Practical Work

The layout of the School followed the scheme that had proved useful already in 1988 and 1990 (cf. *The Messenger* No. 53, p. 11, and No. 61, p. 8). Seven tutors (Claude Chevalier, Denis Gillet, Sergio Ilovaisky, and Philippe Prugniel from the OHP, Alain Jorissen, Werner Zeilinger and D.B. from Garching) had designed six small observing programmes for as many groups of three students each. The preparation started already the first afternoon, only interrupted by a small reception and the subsequent dinner, because the first observations were to be done the following night.

Each group had one night at the 1.2-m telescope for direct imaging with a CCD camera. For the spectroscopic part, three groups worked at the 1.93-m

telescope with its Cassegrain spectrograph Carelec, and the other three used the high-resolution coude spectrograph Aurelie of the 1.5-m telescope. These two instruments, too, deploy a CCD as the detector.

The director of the OHP, Philippe Véron, had in his welcoming address emphasized the observatory's efforts in the previous weeks to save some good weather for the Summer School. These efforts proved, in fact, quite successful. Only one group had to depend on one of the spare nights for a second attempt to obtain a useful set of direct images. The amount of observations kept the students more than busy with the reduction

of their data, using either MIDAS or IHAP or both. The prediction by the organizers that during the School sleep would at best be optional was amply confirmed, especially in the night before the last day in the morning of which each group had to present its results to the other participants.

The diversity of scientific subjects was quite considerable: rotation curves of spiral galaxies and triaxiality of their bulges, a search for inhomogeneities in the internal extinction of a planetary nebula, the optical identification of ROSAT X-ray sources, photometry of an open star cluster in search for δ Scuti stars and the detection of the spectros-



Figure 1: In the break of Hans Dekker's talk, students, tutors, and organizers assembled in the shadow of a tree for a group photograph. First row (from left to right): Mathias Kunz, Hans Dekker, Nadine Rons, Jesús Gallego, Iordanka Borissova, Christian Surace, Simon Portegies-Zwart; sitting: Lutz Wisotzki; second row: Jean-Philippe Beaulieu, Sandro Bardelli, Helmut Jerjen, Salvatore Scuderi, Susanne Vogel, Mira Véron; third and fourth row: Dietrich Baade, Roland Reiss, Richard Dallier, Eugenio Carretta, Nancy Ageorges, Mikael Sahrling, Volker Ossenkopf, Werner Zeilinger, Alain Jorissen, Marc Ferrari, Karine Bocchialini.



Figure 2: Data reduction accounted for most of the work done by the students. (a) Sergio Ilovaisky shows Mathias Kunz, Karine Bocchialini, and Simon Portegies-Zwart (from left to right) how to sweep blemishes from a CCD image. (b) Tutor Philippe Prugniel and students Volker Ossenkopf and Jesús Gallego (from left to right) seem to have slightly different views of the ease of learning to use PLEINPOT.

copic signature of high-order nonradial pulsation in such stars, follow-up photometry of some recent supernovae, the rejection of an earlier suggestion of shocks in the atmosphere of a bright low-amplitude β Cephei star, a search for technetium in red giants and candidate-AGB stars, and a new determination of the velocity dispersion in an elliptical galaxy which now is in much better agreement with the general velocity dispersion-absolute magnitude calibration. However, the purpose of the School was not to give the students deep insights into these subjects. Rather, the topics had been chosen as an illustration of how an observing programme is to be carried out from its definition to the formulation of the results and the estimate of their significance. The aim was that after these exercises the students would be in a position to conceive and conduct observing programmes of their own.

Theoretical Reinforcement

In order to provide the students with a more systematic introduction to the tools they were using, a number of experts had been invited to give a one-and-a-half hour lecture (cf. box). Most speakers kindly agreed to stay for an extra day or two so that the students

had the opportunity to discuss subjects which were of particular interest to them in more depth. Ray Wilson also demonstrated at the 1.2-m telescope what can be deduced about a telescope's aberrations from an image of its pupil. At the same telescope Roland Reiss together with the students measured the readout noise and gain of the CCD camera and its controller.

Unfortunately, a sudden health problem prevented Pierre Léna from giving his lecture on high-resolution imaging. However, on a short notice this gap could be filled by the kind agreement of Jean-Paul Schneider of the Atmospheric Research Group and Michel Grenon of the Geneva Observatory to demonstrate the LIDAR experiment for the determination of the ozone contents of the upper atmosphere from the back-scattered light of a laser beam and the CORAVEL stellar radial velocity measuring engine, respectively.

Of course, competence in handling an instrument and reducing the data obtained with it can only be an intermediate goal for an astronomer. The interpretative power of cleverly designed observational experiments and a thoughtful analysis of their results was beautifully demonstrated by Gustav Tammann in a lively talk given in his typical, unmistakable style.

Relaxation

An important contributor to keeping the level of the intensity of the work as high as it actually was were a few social activities which were much enjoyed by everyone. On Sunday, July 19th, a full-day excursion was organized by Philippe Prugniel to the town of Gordes which is magnificently set on a steep hill and to the nearby 12th-century Abbey of Senanque and the museum village des Bories with its curious houses made of piled-up natural stone plates. The Gordian knot had to be cut only a few days later during the Petanque (Boule) tournament (also arranged by Philippe Prugniel) when the book keeping of the results of matches between many teams of ever changing compositions demanded the utmost of its organizers. However, there was unanimous agreement that a team formed by three ladies from the OHP hotel (Maison Jean Perrin) beat all other teams by their outstanding performance. This certainly is explained by all three team members being locals and thereby having grown up with this national pastime of the south of France. However, a more relevant inference is the level of quality which the participants enjoyed in the services provided by the kitchen.

Judging by the feedback provided by the students, all of them got something out of their stay at the OHP, although everyone differently according to personal background and interest. On behalf of the students, we cordially thank our numerous colleagues who in addition to their usual workload and in many different ways have made essential contributions to what appears to have been a successful summer school in the practice of astronomical observing techniques.

Lecturers	Subjects
H. Dekker (ESO):	Concept and Design of Optical Instruments
J.-M. Lecontel (Nice):	High-resolution Spectroscopy
S. Ortolani (Padova):	Crowded Field Photometry
R. Reiss (ESO):	Charge-coupled Devices
G. A. Tammann (Basel):	The Local Extragalactic and Cosmic Expansion Field
M. Véron (OHP), D. Baade (ESO):	Data Reduction Techniques
R. Wilson (ESO):	Modern Telescope Layout
L. Wisotzki (Hamburg):	Low-resolution and Slitless Spectroscopy

Visiting Astronomers

(October 1, 1992 – April 1, 1993)

Observing time has now been allocated for Period 50 (October 1, 1992 – April 1, 1993). As usual, the demand for telescope time was again much greater than the time actually available.

The following list gives the names of the visiting astronomers, by telescope and in chronological order. The complete list, with dates, equipment and programme titles, is available from ESO-Garching.

3.6-m Telescope

October 1992: De Graauw et al. (9-003-49K), Mazure/Rhee et al. (1-014/005-43K), Vettolani et al. (1-019-47K), Bergvall/Rönback/Melnick, Danziger et al. (6-003-45K).

November 1992: Danziger et al. (6-003-45K), Gouiffes/Ögelman/Augusteijn, Jüttner/Baschek/Stahl/Wolf, Wagner, Macchetto/Giavalisco/Sparks, Warren/Iovino/Shaver/Hewett, Mellier/Fort/Mathez/Soucil/Arnaud, Böhringer et al. (1-023-49K), Danziger/Bouchet/Gouiffes/Lucy/Fransson/Mazzali/Della Valle, Westerlund/Azzopardi/Breysacher.

December 1992: Westerlund/Azzopardi/Breysacher/Danziger/Bouchet/Gouiffes/Lucy/Fransson/Mazzali/Della Valle, Courvoisier/Bouchet/Blecha/Orr/Valtaoja, Petitjean/Carswell/Rauch, Wampler et al. (2-010-45K), Danziger/Bouchet/Gouiffes/Lucy/Fransson/Mazzali/Della Valle, Caulet/Käuffl/McCaughrean, Melnick/Gopal-Krishna/Altieri/Steppe, Testor/Schild/Lortet/Niemela.

January 1993: Lagage/Cabrit/Nordh/Olofsson/Pantin, Lagage/Pantin, Courvoisier/Bouchet/Blecha/Orr/Valtaoja, Danziger/Bouchet/Gouiffes/Lucy/Fransson/Mazzali/Della Valle, Turatto et al. (4-004-45K), Gouiffes/Ögelman/Augusteijn, Grenier/Gouiffes/Ögelman, Melnick/Gopal-Krishna/Altieri/Steppe, Danziger/Bouchet/Gouiffes/Lucy/Fransson/Mazzali/Della Valle, Turatto et al. (4-004-45K), Zweigle/Diesch/Kreysing/Grewing, Werner/Dreizler/Heber/Hunger/Rauch, Hensberge et al. (5-005-45K).

February 1993: Hensberge et al. (5-005-45K), Blaauw/Srinivasan-Sahu, Felenbok/Jablonka/Alloin/Arimoto/Bica/Balkowski/Cayatte/Kraan-Korteweg, Zamorani/Vettolani/Bardelli/Scaramella/Böhringer/Schwarz R./MacGillivray/Collins, Pettersson, Zamorani/Vettolani/Bardelli/Scaramella/Böhringer/Schwarz R./MacGillivray/Collins, Zaggia/Capaccioli/Piotto/Stiavelli.

March 1993: Zaggia/Capaccioli/Piotto/Stiavelli, Thomas, Beckers, Reimers et al. (2-009-45K), Danziger/Bouchet/Gouiffes/Lucy/Fransson/Mazzali/Della Valle, Danziger et al. (6-003-45K), Macchetto/Giavalisco/Sparks, Augusteijn/van Paradijs/van der Klis, di Serego Alghieri/Cimatti/Fosbury, Böhringer/Ebeling/Pierre/Voges/Schuecker/Seitter/Cruddace/Collins/MacGillivray, Gouiffes/Ögelman/Augusteijn.

3.5 m-NTT

October 1992: De Graauw et al. (9-003-49K), Capaccioli/Pellegrini/Piotto/Aparicio/Hansen, D'Odorico et al. (2-013-49K), Azzopardi/Breysacher/Lequeux, De Lapparent et al. (1-003-43K), Bergeron et al. (1-012-43K), Bender et al. (1-004-43K).

November 1992: Bender et al. (1-004-43K), Oliva/Moorwood/Origlia, Käuffl/Rosa/Viegas, Capaccioli/Pellegrini/Piotto/Aparicio/Hansen, Meylan/Azzopardi/Dubath/Lequeux, Storm/Della Valle, Miley et al. (2-001-43K), Lorenz H./Böhm/Capaccioli/Richter, Marano/Zamorani/Cimatti/Mignoli/Zitelli.

December 1992: Danziger/Bouchet/Gouiffes/Lucy/Fransson/Mazzali/Della Valle, Kudritzki/Lennon/Husfeld/Herrero/Gabler, Clausen/Storm/Tobin/Hilditch/Hill/Giménez, Spite F./Spite M./François/de Boer, Wampler et al. (2-010-45K), Paquet/Davies/Bender, Tolstoy/Griffiths/Miley, West/Hainaut/Marsden/Smette, Warren/Theuns, Möller/Warren, Reipurth.

January 1993: Grebel/Bomans/Bhatia/Mateo, Lagrange-Henri/Beust/Beuzit/Deleuil/Gry/Ferlet/Vidal-Madjar, Leitherer/Clampin/Nota/Origlia, Siebenmorgen/Peletier, Shearer/Redfern/Pedersen/Cullum, Wang/Wampler, Fort et al. (1-015-45K), Pakull/Motch.

February 1993: Paresce/Ferrari/Roberto/Clampin, Zeilinger/Möller/Stiavelli, Danziger/Matteucci/Zeilinger, Danziger/Bouchet/Gouiffes/Lucy/Fransson/Mazzali/Della Valle, Piotto/Capaccioli/Stiavelli/Zaggia, West/Hainaut/Marsden/Smette, Mirabel/Duc, Chincarini/Buzzoni/Molinari/Longhetti, Campusano/Clowes/Melnick.

March 1993: Pottasch S. R./Manchado/Garcia-Lario/Sahu K. C., Walsh/Meaburn/Gehring, Nussbaumer/Mürset/Schmid/Schmutz, D'Odorico et al. (2-013-49K), Peterson/D'Odorico/Tarengi/Yoshii/Silk, Tammann et al. (1-022-47K), Kudritzki/Roth/Mendez/Giardullo/Jacoby, Turatto et al. (4-004-45K), Surdej et al. (2-003-43K), Dubath/Meylan.

2.2-m Telescope

October 1992: Danziger/Carollo, Stiavelli/Zeilinger, Beuermann/Thomas H.-Ch./Fink/Reinsch/Pakull, Breysacher/Azzopardi/Lequeux/Meysonnier/Stasinska/Westerlund, Turatto et al. (4-004-45K), Bergvall/Rönback/Melnick, Bender et al. (1-004-43K), Appenzeller/Beckmann/Grieger/Kohl/van Elst/Wagner/Weghorn/Weigelt, Weigelt/Weghorn/Beckmann/Grieger/Kohl/van Elst.

November 1992: Weigelt/Weghorn/Beckmann/Grieger/Kohl/van Elst, Peletier/Valentijn/Moorwood/Freudling, De Boer et al. (3-003-43K), Hunt/Malkan/Rush/Spinoglio, Lamer/Staubert/Brunner, Miley et al. (2-001-43K), Böhringer et al. (1-023-49K), Turatto et al. (4-004-45K), Westerlund/Azzopardi/Breysacher, Barbieri et al. (2-007-43K).

December 1992: Barbieri et al. (2-007-43K).

January 1993: Zijlstra/Loup/Waters/Trams/Omont/de Jong, Nota/Origlia/Clampin/Leitherer, Andersen M. I./Jonch-Sørensen/Jørgensen, Block/Bertin/Moorwood/Rupprecht/Moneti/vd Bergh, Dennefeld/Boller/Meurs, Dennefeld/Boller/Meurs, Carollo/Danziger, Ferraro/Testa/Fusi Pecci/Origlia/Buonanno/Corsi, Wolf/Stahl/Szeifert/Mandel/Zickgraf/Sterken.

February 1993: Moorwood/Kotilainen/Forbes/Ward/Oliva, Gredel, Lorenzetti/Moneti/Spinoglio/Liseau, Beuermann/Schwope/Thomas H.-Ch., Dettmar/Klein/Dahlem, Tsvetanov/Fosbury/Tadhunter, Turatto et al. (4-004-45K).

March 1993: Courvoisier/Bouchet/Blecha/Orr/Valtaoja, van der Hucht/Williams/Yudiawati/Anggraeni/Bouchet/Prusti/Natta/Palla, Prusti/Henning/Whittet, Courvoisier/Bouchet/Blecha/Orr/Valtaoja, Surdej et al. (2-003-43K).

1.5-m Spectrographic Telescope

October 1992: Danziger et al. (6-003-45K), Ramella/Da Costa/Focardi/Geller/Nonino.

November 1992: Ramella/Da Costa/Focardi/Geller/Nonino, Baade/Kolb/Kudritzki/Simon, Gerbaldi et al. (5-004-43K), Peletier/Burkert, Horellou/Casoli/Dupraz, Longo/Busarello/Rifatto/Richter/Tenjes.

December 1992: Thè/de Winter/van den Ancker, Favata/Sciortino/Micela/Schachter/Elvis, De Ruiter/Lub, Kinkel, Testor/Schild, Bues/Karl/Pragal.

January 1993: Bues/Karl/Pragal, North/Glagolevskij, Seggewiss/Moffat/Turbide, Moffat/Leitherer/Drissen/Hubeny/Langer/Nota/Robert/St-Louis/Schmutz, Zweigle/Kreysing/Diesch/Grewing, Proust/Maurogordato/Cappi, Courvoisier/Bouchet/Blecha, Pasquini/Belloni/Schmitt.

February 1993: Pasquini/Belloni/Schmitt, Lorenz R./Drechsel/Mayer, Bianchini/Della Valle/Orio/Ögelmann/Bianchi, Zeilinger/Möller/Stiavelli, Spinoglio/Malkan/Rush, Christensen/Sommer-Larsen/Beers/Flynn.

March 1993: Courvoisier/Bouchet/Blecha, Gerbaldi et al. (5-004-43K), Pottasch S. R./Manchado/Garcia-Lario/Sahu K. C., Henning/Pfau/Braun, Reimers et al. (2-009-45K), Danziger et al. (6-003-45K), Krautter/Alcalá/Schmitt/Mundt/Wichmann/Zinnecker.

1.4-m CAT

October 1992: Randich/Gratton/Pallavicini/Pasquini, Ferlet/Hobbs/Wallerstein, Nissen/Lambert/Smith, Baade/Kolb/Kudritzki/Simon.

November 1992: Baade/Kolb/Kudritzki/Simon, Kürster/Hatzes/Cochran/Dennerl/Döbereiner, Barbuy / Jorissen / Rossi / Arnould, Barbuy / Medeiros / Lèbre, Maurice / Silvy, Strassmeier / Kürster / Rice / Wehlau, Poretti / Bossi / Mantegazza / Zerbi, Pallavicini / Haisch / Schmitt / Pasquini / Randich.

December 1992: Pallavicini/Haisch/Schmitt/Pasquini/Randich, Mathys/Landstreet / Lanz / Manfroid, Ferlet / Hobbs / Wallerstein, Lagrange-Henri/Beust/Deleuil/Ferlet/Gosset/Gry/Vidal-Madjar, Lagrange-Henri / Beust / Deleuil / Ferlet / Gosset / Gry / Vidal-Madjar, Kürster/Hatzes/Cochran/Dennerl/Döbereiner, Favata/Sciortino/Micela, Plets/Waters/Waelkens, Franco/Araujo Vieira.

January 1993: Mathys/Landstreet/Lanz/Manfroid, Lemoine / Ferlet / Vidal-Madjar / Emerich, Ferlet / Hobbs / Wallerstein, Lemoine / Ferlet / Vidal-Madjar / Emerich, Nussbaumer / Mürset / Schmid / Schmutz, Waelkens / Conlon / Dufton, Holweger / Stürenburg, Blauuw / Srinivasan-Sahu, Mathys/Landstreet/Lanz/Manfroid, Danks/Penprase/Caulet.

February 1993: Danks/Penprase/Caulet, Grenon / Barbuy, Plets / Waters / Waelkens, Vincent / Hackman / Hubrig / Piskunov / Saar / Tuominen / Ryabchikova, Nussbaumer / Mürset / Schmid / Schmutz, Reipurth/Lago/Calvet/Pedrosa, Gredel.

March 1993: Gredel, Kürster/Hatzes/Cochran/Dennerl/Döbereiner, Benvenuti/Porceddu, Jorissen/Mayor/North, North Monai/Vladilo/Molaro/Centurion, Vladilo/Centurion/Cassola, Mathys/Landstreet/Lanz/Manfroid.

1-m Photometric Telescope

October 1992: Randich/Gratton/Pallavicini/Pasquini, Manfroid/Vreux/Sterken, Silvotti / Bartolini / Guarnieri / Piccioni / Stanghellini, Barwig/Reimers/Mantel/Häfner.

November 1992: Barwig/Reimers/Mantel/Häfner, Jourdain de Muizon / d'Hendecourt/Puget, Gochemann/Höppner, Gochemann/Höppner, Bouvier / Cabrit / Fernandez / Martin / Matthews / Covino / Terranegra, Barbieri et al. (2-007-43K), Thé/de Winter/van den Ancker.

December 1992: Thé/de Winter/van den Ancker, Beust/Lagrange-Henri/Ferlet/Char/Deleuil / Vidal-Madjar / Foing / Gry, Liller / Alcaïno/Alvarado/Wenderoth.

January 1993: Courvoisier/Bouchet/Blecha, Pallavicini/Haisch/Schmitt/Pasquini/Randich, Guglielmo/Epstein/Le Bertre, Catalano F. A./Leone/Kroll, Courvoisier/Bouchet/Blecha.

February 1993: Courvoisier/Bouchet/Blecha, Reinsch/Beuermann/Motch/Pakull, Gieren/Moffett/Barnes, Di Martino/Zappalà/Manara/Blanco.

March 1993: Di Martino/Zappalà/Manara/Blanco, Oblak et al. (7-009-49K), Alcalá/Wichmann / Krautter / Covino / Schmid / Zinnecker, Courvoisier/Bouchet/Blecha, Alcalá / Wichmann / Krautter / Covino / Schmid / Zinnecker, Lagerkvist/Magnusson/Erikson.

50-cm ESO Photometric Telescope

October 1992: Carrasco/Loyola, Sinachopoulos.

November 1992: Sinachopoulos, Magnan/Menessier/Laverny, Oblak et al. (7-009-49K), Poretti/Bossi/Mantegazza/Zerbi.

December 1992: Poretti/Bossi/Mantegazza/Zerbi, Magnan/Menessier/Laverny, Carrasco/Loyola, Bruch/Niehues, Cutispoto/Leto/Giampapa/Pagano/Pasquini.

January 1993: Cutispoto/Leto/Giampapa/Pagano/Pasquini, Magnan/Menessier/Laverny, Lorenz R./Drechsel/Mayer.

February 1993: Lorenz R./Drechsel/Mayer, Wolf B./Mandel/Stahl/Szeifert/Zickgraf/Sterken.

March 1993: Wolf B./Mandel/Stahl/Szeifert/Zickgraf/Sterken.

GPO 40-cm Astrograph

October 1992: Vidal-Madjar et al.

November 1992: Vidal-Madjar et al.

December 1992: Vidal-Madjar et al.

January 1993: Vidal-Madjar et al.

February 1993: Vidal-Madjar et al.

March 1993: Vidal-Madjar et al.

1.5-m Danish Telescope

October 1992: Mayor et al. (5-001-43K), Nordström, J. Andersen et al., Jørgensen et al., Nissen/Schuster.

November 1992: Nissen/Schuster, Surdej et al. (2-003-43K), Pagel/Copetti/Schmidt/Castaneda, Richtler/Gieren/Grebel, Hunt/Malkan/Rush/Spinoglio, Richter/Capaccioli/Ferrario/Thänert, Danziger/Bouchet/Gouiffes / Lucy / Fransson / Mazzali / Della Valle, Longo/Busarello/Rifatto/Richter/Tenjes, Warren / Loveday / Williger / Møller, Vidal-Madjar et al.

December 1992: Vidal-Madjar et al., Surdej et al. (2-003-43K), Nordström/J. Andersen et al., Clausen et al., Jønh-Sørensen, Clausen et al.

January 1993: Surdej et al. (2-003-43K), Danziger / Bouchet / Gouiffes / Lucy / Fransson/Mazzali/Della Valle, Danziger/Carollo, Moffat / Leitherer / Drissen / Hubeny / Langer / Nota / Robert / St-Louis / Schmutz, West / Hainaut/Marsden/Smette, Surdej et al. (2-003-43K), Duquenooy/Mayor.

February 1993: Duquenooy/Mayor, Merrilliod/Mayor, Rasmussen/M. I. Andersen, Kjeldsen/Frandsen, Jønh-Sørensen/M. I. Andersen, Rasmussen/M. I. Andersen.

March 1993: Waelkens/Mayor, Jorissen/Mayor/North, Ardeberg/Lindgren H./Lundstroem, Ardeberg/Lindgren H./Lundstroem, Danziger/Bouchet/Gouiffes/Lucy/Fransson/Mazzali/Della Valle, Caon/D'Onofrio/Capaccioli, Tancredi/Lindgren M./Rickman/Kamél, Fusi Pecci/Cacciari/Bragaglia/Ferraro/Carretta.

50-cm Danish Telescope

October 1992: Rose/J. Andersen/Nordström, Group for Long Term Photometry of Variables.

November 1992: Group for Long Term Photometry of Variables, Jønh-Sørensen.

December 1992: Stefl/Baade/Balona.

January 1993: Stefl/Baade/Balona, Group for Long Term Photometry of Variables.

February 1993: Group for Long Term Photometry of Variables, Sterken/Jerzykiewicz, Jønh-Sørensen/M. I. Andersen, Ardeberg/Lindgren H./Lundstroem.

March 1993: Ardeberg/Lindgren H. Lundstroem, Group for Long Term Photometry of Variables.

90-cm Dutch Telescope

October 1992: Schuecker/Cunow/Naumann/Ungruhe.

November 1992: Oblak et al. (7-099-49K), Peletier/Burkert, Baade/Kjeldsen/Frandsen, Katgert/Mazure/Dubath/Le Fèvre/Den Hartog / Focardi / Giuricin / Rhee / Jones / Perea, Baade/Kjeldsen/Frandsen, Katgert/Mazure/Dubath/Le Fèvre/Den Hartog/Focardi/Giuricin/Rhee/Jones/Perea, Baade/Kjeldsen/Frandsen.

December 1992: Baade/Kjeldsen/Frandsen, Grebel/Richtler/de Boer/Roberts, Pakull/Beuermann/Motch/Schaeidt, De Ruiter/Lub, Turatto et al. (4-004-45K), Augusteijn/van Paradijs/van der Klis.

January 1993: Augusteijn/van Paradijs/van der Klis, Bomans/van Rossum.

February 1993: de Winter/Thé, Pettersson, Dettmar/Garcia-Barreto/Combes F./Koribalski, West M. J./Schombert, Lagerkvist/Dahlgren/Williams/Fitzsimmons, Wicenc/Snijders.

March 1993: Wicenc/Snijders, Oblak et al. (7-009-49K), Reimers et al. (2-009-45K), Alcalá / Wichmann / Krautter / Covino / Schmitt/Zinnecker, Turatto et al. (4-004-45K), Ferrari/Bucciarelli/Massone/Koornneef/Lasker/Le Poole/Postman/Siciliano/Lattanzi/Pizzuti.

SEST

October 1992: Knee/Mezger, Tornikoski, Valtaoja, Nyman, Olofsson, Fuller.

November 1992: Combes F., Casoli, Danziger, Boulanger, Cox, Lemke, Chini, Omont.

December 1992: Orgura, Valtaoja, Nyman, Haikala, Olofsson, Booth, Knee, Lindqvist, Olofsson, Wolstencroft.

January 1993: Wiklind, Galletta, Becker, Horellou, Cameron M., Olmi, Roueff, Henkel, Hron, Israel.

February 1993: Wiklind, Tornikoski, Valtaoja, Olberg, Harjunpää, Olofsson, Harju, Sahai, Bergman, Irvine, Olofsson, Rydbek, Knee.

March 1993: Wielebinski, Danziger, Henning, Krügel, Dahmen, Pfau, Water, Leone, Loup, Omont, van der Hucht, Kastner.

The Instituto Isaac Newton: A Highly Productive ESO-Chile Connection

G. ALCAINO and W. LILLER, Instituto Isaac Newton, Santiago, Chile

A bright occasion for Chile in 1978 was the founding of the Instituto Isaac Newton for Astronomical Research by Chilean astronomer Gonzalo Alcaíno. The Instituto, supported almost entirely by a contract with the Chilean Ministry of Education, now has for its staff Alcaíno as Director, William Liller, Associate Director and Senior Research Scientist, and Franklin Alvarado and Erich Wenderoth, Research Associates, plus a secretary. Located in suburban Las Condes in the eastern outskirts of Santiago, the Instituto offices are situated at the base of the Andes in a peaceful farmhouse surrounded by ancient trees and a rustic garden.

The primary research programme of the Instituto is the observational study of globular clusters in the Galaxy and in the Magellanic Clouds. That this fruitful field, which is providing fundamental answers to astronomical key questions, should be the Instituto's main activity was first suggested by Professor James Cuffey at the University of Indiana in the early 1960's when Alcaíno was carrying out graduate studies in astronomy. At the time, the pioneering work on globular clusters was being done at the Mount Wilson and Palomar Observatories by astronomers like Arp, Baum and Sandage, and during a visit to the Mount Wilson offices, Sandage and Alcaíno discussed the possibilities further. The decision was made: Do multi-colour photometry on the many globular clusters that lie at negative declinations (60 per cent of them south of -20°).

A few years later, in July 1968, Alcaíno was just completing an observing run on the Cerro Tololo 1.5-metre telescope when Harvard University professor, William Liller, arrived with a graduate student to begin work on the same instrument. This chance encounter grew into a close friendship between Alcaíno and Liller and led eventually to scientific collaborations several years later. In 1981–82 Liller took a year's leave of absence from Harvard where he had been for 21 years carrying out research in a wide spectrum of fields, including studies of planetary nebulae, comets, asteroids, cool stars and quasars. At the time he was working with Riccardo Giacconi and the group of investigators analysing early results from the Einstein Observatory. Liller was specifically involved in the optical identification of X-ray sources and had a

keen interest in globular cluster sources. The following year Liller took early retirement from Harvard, made Chile his permanent residence, and became a regular staff member of the Instituto.

In the early 1980s, in addition to the research on globular clusters, the Instituto expanded its activities to include the systematic search for novae in the Galaxy and the Magellanic Clouds, and supernovae in nearby clusters of galaxies, a project which Liller undertook first using nothing more than a Nikon camera in the garden of his home in Viña del Mar, located on the central coast of Chile 120 kilometres west of the Instituto's offices. A further activity of the Instituto grew out of Liller's 3-month stay on Easter Island, 3300 kilometres west of the Chilean coast, where he went to set up a small NASA observatory to observe Halley's Comet. While there, he became fascinated with the many ancient temples on the island, and that interest has developed into a broad programme of archaeoastronomy that has spread to many other Polynesian islands.

Since ESO's 1-metre telescope became operational in 1970, nearly all the Instituto's globular cluster data have been secured at La Silla. Since then, the

staff of the Instituto has had approximately 450 scheduled nights of observing time and has used telescopes ranging from the 1-metre to the 3.6-metre and the NTT. It is our personal pleasure and privilege to express in the *Messenger* not only our deep appreciation for the use of ESO equipment, but especially our gratitude to Directors General Adriaan Blaauw, Lodewijk Woltjer, and Harry van der Laan for their constant support and encouragement. Special thanks are also due to our good friend Daniel Hofstad, the current head of La Silla, as well as to all the personnel at the site.

In the following sections we describe in more detail the various programmes of the Instituto.

Globular Clusters in the Galaxy and the Magellanic Clouds

While the first telescopes at La Silla were not large, globular cluster photometry in the Southern Hemisphere was a virgin field, and many of the clusters that we worked on were being studied for the first time. It was at least possible in most clusters to reach below the horizontal branch, home of the RR Lyrae stars, thereby permitting us to derive

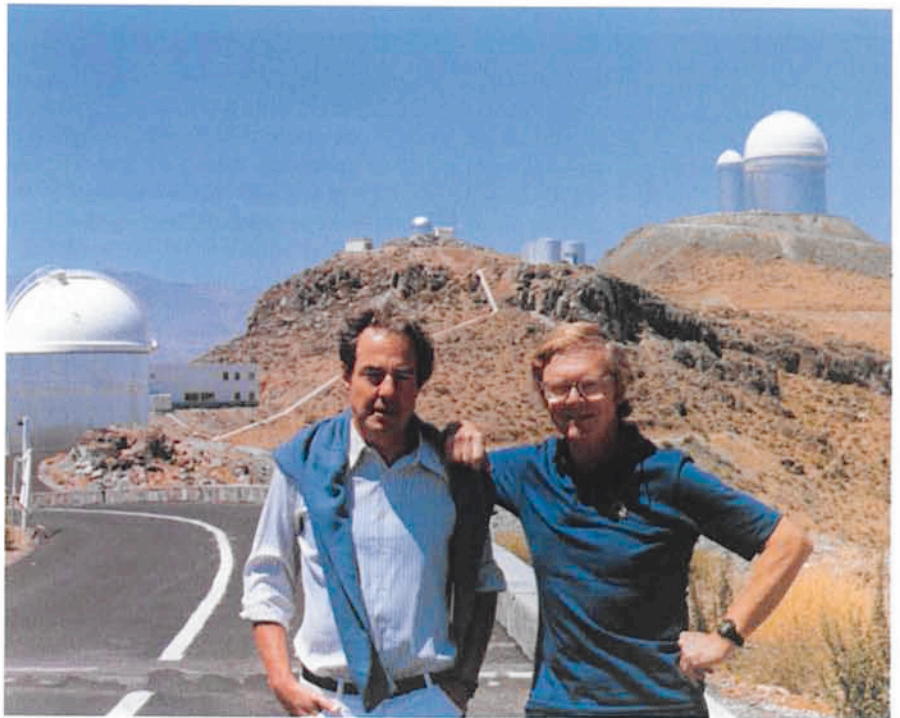


Figure 1: The authors in front of the ESO-La Silla 3.6-m dome (Alcaíno at left).

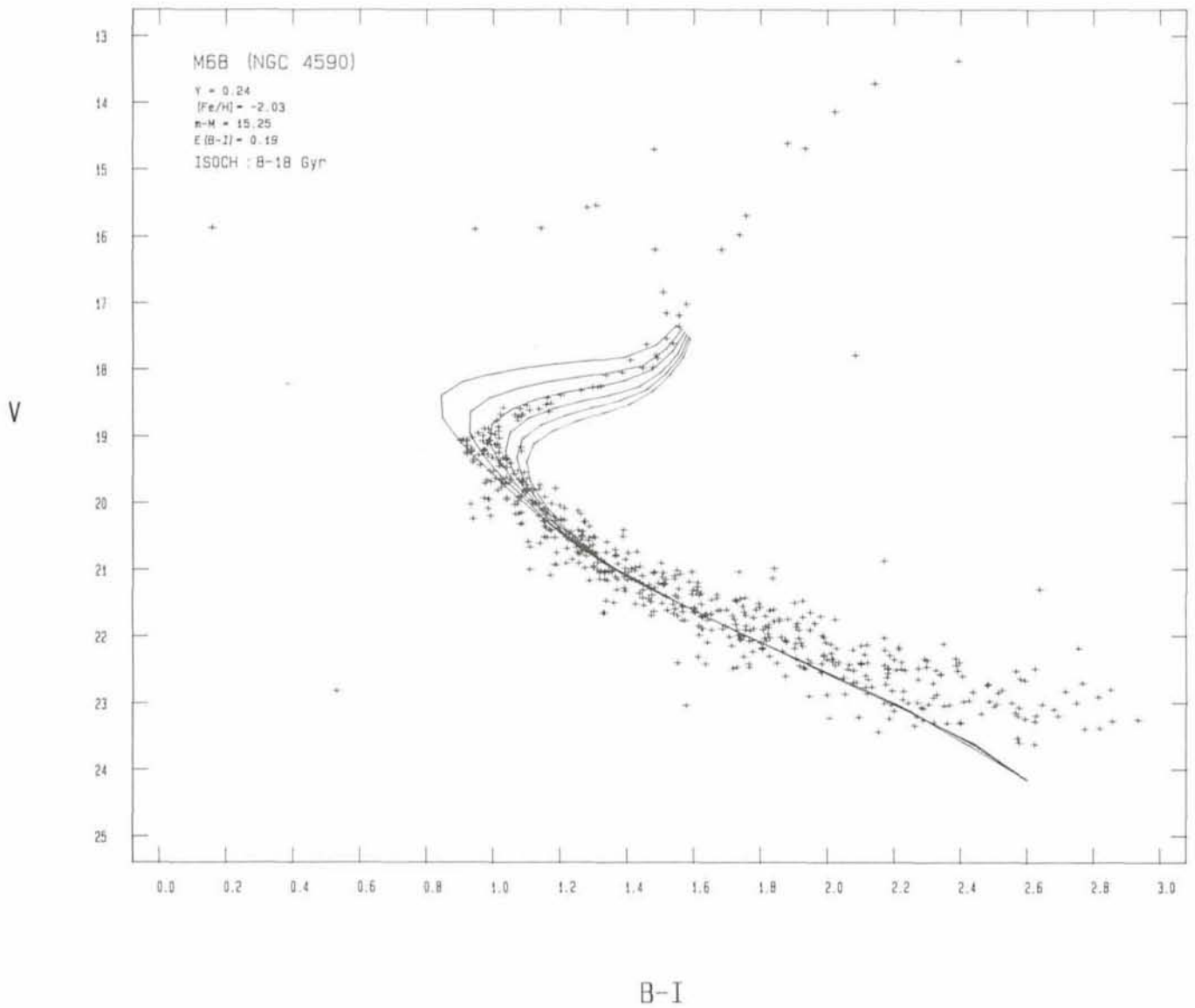


Figure 2: The V vs. $B-I$ colour-magnitude diagram for NGC 4590 (Alcaino et al., 1990).

reasonably reliable distances and interstellar reddenings for these objects. Also, approximate metallicities could be determined. This work culminated in the publication of the book, *Atlas of Galactic Globular Clusters with Colour Magnitude Diagrams* (Alcaino 1973).

The early photometry was carried out arduously in several steps. First, a dozen or so stars were measured photoelectrically (UBV usually) covering as wide a range of colour and magnitude as possible. Then photographs were taken and star images measured with an iris photometer such as had been developed by Cuffey and which had been loaned to us by ESO. On some telescopes a thin-wedge prism could be placed before the objective thereby producing a second, much fainter image of each star. Thus, in a boot-strap manner, the relatively bright photoelectric sequence could be extended to fainter magnitudes.

Then came charge-coupled devices (CCDs). Suddenly it became possible to carry out photometry with substantially higher precision owing to the stability and the linearity of these marvelous detectors, especially at low light levels. Also, the sensitivity range extended beyond 1 micron making it possible to work with ease in more colours than B and V which had been the workhorse wavelength bands for many years.

One of the weaknesses of the BV system is that metallic line absorption in the blue and violet can be significant, especially for metal-rich clusters. The interpretation of observations in the context of stellar evolution theory rests heavily on model stellar atmospheres which must correctly predict the effects of this metallic absorption in stars where the metallicity is often not well known. It should be emphasized that the metallicity of globular clusters, usually expressed by the parameter $[Fe/H]$ has

a range of over two orders of magnitude. Fortunately, Vandenberg and Bell (1985) and Demarque and his colleagues have carried out the calculations needed to predict the location of isochrones in the longer wavelength bands where there is much less metallic absorption than in the blue-violet.

Other advantages are realized by working into the red and infrared: an enlarged colour baseline results which enhances effects seen less clearly and less accurately with a smaller range in colour. Additionally, observational uncertainties are reduced by having several independently derived colour-magnitude diagrams of the same cluster. With the separate evaluations of the age of a single cluster, one not only can assess more reliably the accuracy of the final result, but also can derive ages with a higher precision than attained previously or with only two colours.

Since the mid-1980s we have had

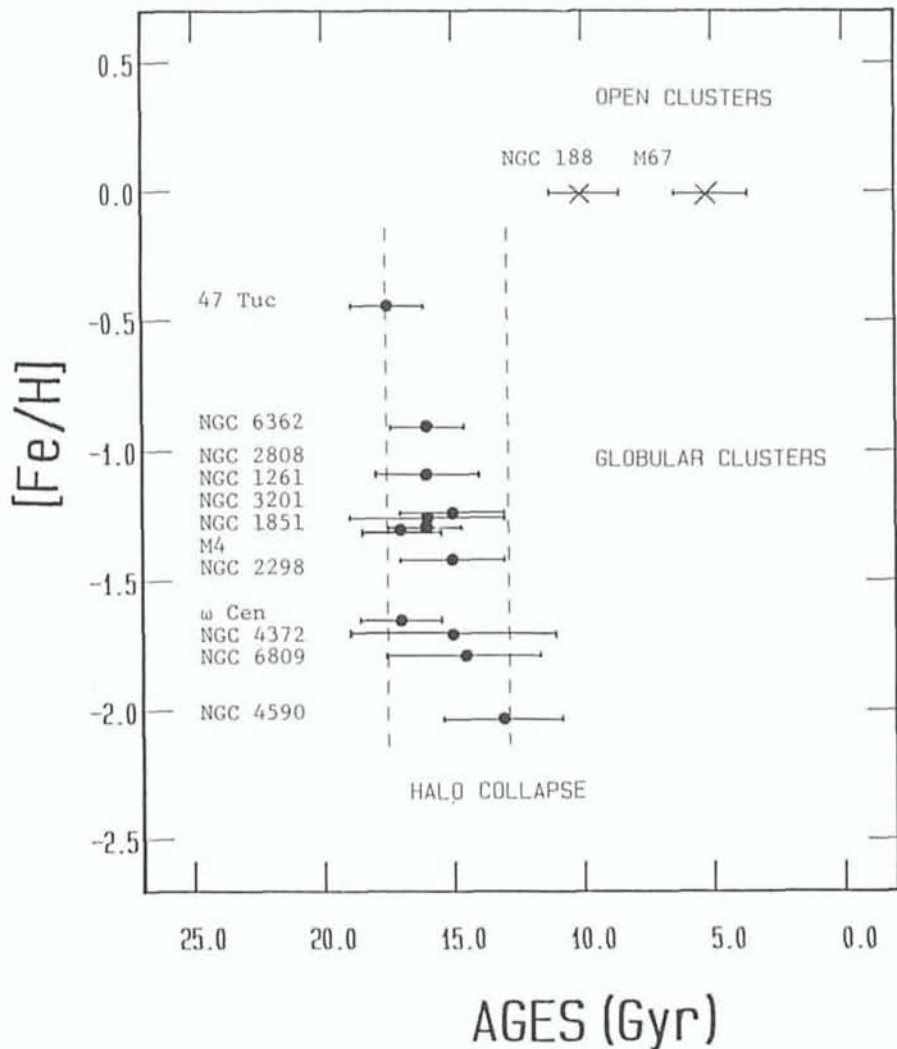


Figure 3: The age versus metallicity of the galactic globular clusters that we have so far analysed, plus these same quantities for the two oldest known open clusters, M67 and NGC 188. It can be seen that the ages derived for all these objects are 16 ± 2 Gys equivalent to $H_0 = 61 \pm 8 \text{ km s}^{-1} \text{ Mpc}^{-1}$ ($q_0 = 0$).

The majority of our cluster data has been collected with either the 3.6-m, the 2.2-m (Max-Planck), and the 1.54-m telescopes at ESO La Silla. Much of the recent observing and reduction work has been done expertly and efficiently by our colleagues at the Instituto, Franklin Alvarado and Erich Wenderoth. Besides being now very well known and highly respected at La Silla, they have often assisted others in the sophisticated data reduction techniques available to visiting astronomers.

To date we have published multi-colour results for the galactic globular clusters NGC 104 (47 Tucanae), 1851, 2298, 2808, 3201, 4372, 4590, 5139 (Omega Centauri), 5946, 6121, 6362 and 6809. We also have accumulated data for a large number of Magellanic Cloud clusters. In all we have published over 100 articles in *Astronomy and Astrophysics*, the *Astronomical Journal*, and the *Astrophysical Journal*.

One of the most significant results of this on-going research programme is shown in the accompanying figure where we have plotted the age versus metallicity of the galactic globular clusters that we have analysed plus these same quantities for the two oldest known open clusters, M67 and NGC 188. It can be seen that the ages derived for all these objects are 16 ± 2 Gys; hence it is still an open question if the time scale of the galactic collapse was brief or as long as 4 Gys. These ages set a lower limit for the age of the Universe and an upper limit for the Hubble constant of $H_0 = 61 \pm 8 \text{ km s}^{-1} \text{ Mpc}^{-1}$, assuming $q_0 = 0$.

underway a programme of BVRI photometry of globular clusters using CCDs and the excellent reduction software (MIDAS-INVENTORY) provided by ESO. For each cluster, and using most often the ESO 1-metre reflector, we set up photoelectric standards in the same cluster fields that we intend to observe with CCDs. Thus, the effects of inaccurately known or varying atmospheric extinction are totally avoided, and errors that might arise from slightly variable exposure times are eliminated. Perhaps most importantly, valuable large telescope time is not wasted moving back and forth between widely separated fields.



Figure 4: ESO Director General Harry van der Laan (r.) with Dr. and Mrs. Liller in front of the dome housing the 0.2-m Schmidt camera in Viña del Mar.



Figure 5: Liller and the NASA-loaned 0.2-m Schmidt posed in front of a moai head and altar platform on Easter Island.

The Viña del Mar Nova Search

In April 1981 the late and highly successful comet and nova discoverer, Minoru Honda, discovered a seventh-magnitude nova in the southern constellation of Corona Australis at a declination of -37 degrees. His latitude in Japan was 33° North; Viña del Mar, Chile, is situated at 33° South. Consequently, Liller decided to take advantage of his far more advantageous location and devote spare evenings to patrolling the rich Southern Milky Way using nothing more than a store-bought Nikon camera.

This project has since grown into an extremely fruitful search programme and has expanded to include the use of a 0.2-m f/1.5 Schmidt telescope on indefinite loan from NASA. (As mentioned above, Liller had set up an observing station on Easter Island in 1986 and employed this Schmidt to photograph Halley's Comet). Today, the same Nikon camera is used to patrol the Milky Way; the Schmidt is employed to photograph on a regular basis the Magellanic Clouds and several clusters of galaxies. All the equipment is mounted permanently next to Liller's home in a small dome financed partially by the Instituto and partially by a grant from NASA. Many of the photographic supplies have been kindly supplied by the Director R.E. Williams of the Cerro Tololo Interamerican Observatory.

As of July 1992, Liller has discovered or co-discovered 15 galactic novae or nova-like objects, more than any other single person in the history of as-

tronomy. Two additional novae were found in the Large Magellanic Cloud, one of them, discovered in April 1991, becoming the brightest nova (visual magnitude 8.7) ever recorded in the LMC. Liller (1991) has analysed the recent discoveries of galactic novae and estimates that on the average, each year in our Galaxy, some 75 ± 25 novae occur, considerably more than what Arp once estimated for our near-twin galaxy, M31 in Andromeda.

The recently inaugurated search for supernovae in nearby galaxy clusters produced its first find in January 1992, a thirteenth magnitude Type Ia SN in the S0/Sa galaxy NGC1380, a member of the Fornax Cluster. In late 1991 the Schmidt camera was equipped with a CCD detector, and Liller has now begun to patrol the hundred or so nearest and most massive southern galaxies not located in clusters. With the CCD Liller can also do more precise photometry of novae and supernovae, thereby adding to the scientific output of this humble annex of the Instituto Isaac Newton in Viña del Mar.

Polynesian Archaeoastronomy

Shortly after Liller arrived on Easter Island in 1986 the distinguished archaeologist and Governor of the island, Don Sergio Rapu Haoa asked Liller if he would measure the orientation of Ahu Nau Nau, the magnificent ancient stone temple (with several colossal statues, or *moai*) that Rapu had recently restored. By chance, archaeologist Dr. Georgia Lee arrived a few days later with a tour

group, and she in turn persuaded Liller to measure orientations of another curiosity of the island, the "sun stones" of Orongo.

These initial and totally unexpected adventures whetted Liller's appetite, and together with his Chilean wife Matilde, he began a detailed study of all of the more than three hundred temples on the island in order to discover if some had been designed to be used as astronomical observatories. Several had been considered earlier, but Liller's more thorough study led to the conclusion that over a dozen – perhaps as many as twenty – temples had been intentionally oriented with rising or setting solstices or equinoxes.

The question then arose as to whether similar results would be found elsewhere in Polynesia. Between 1987 and May 1992 the Lillers have travelled to a number of islands in the vast expanse of the Pacific Ocean – twenty so far – trips frequently made possible by support from the Instituto Isaac Newton. Of all the monuments measured to date, the best candidates for structures intentionally oriented astronomically are the massive trilithon, Ha'amonga, in Tongatapu in the Friendly (Tonga) Islands, and several long alignments of standing stones on Aitutaki in the Cook Islands, reminiscent of those found in France's Brittany. The holiest of ancient Polynesian shrines, Taputapu'atea on Rai'atea in the Society (Tahitian) Islands, and

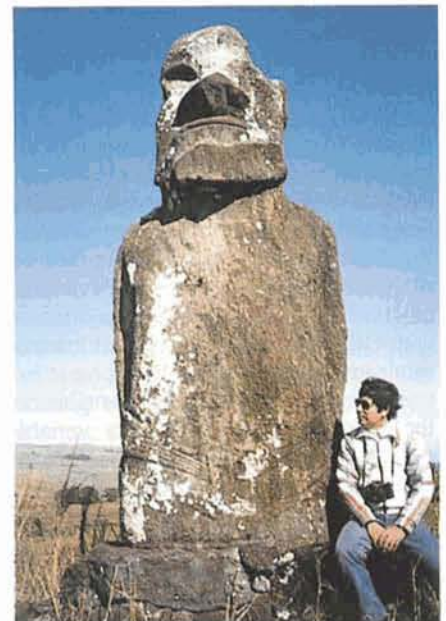


Figure 6: The astronomically-oriented moai at the ceremonial centre of Ahu Huri A Urenga on Easter Island. The statue looks almost precisely in the direction of the rising winter solstice and a sharply peaked hill in the distance. Chilean meteorologist Julio Duarte (at right) worked with Liller at this site.



several similar temples in neighbouring islands share a common orientation towards a rising declination of -9° . Perhaps the sun rose at that declination on the date of a since forgotten holy festival.

But of the several hundred temples elsewhere in Polynesia studied so far, few, if any others, appear to have an astronomical connection. (See Liller 1990). The people of Easter Island, called the most remote inhabited island

Figure 7: Erich Wenderoth (standing) and Franklin Alvarado analysing CCD data at the Instituto.

on Earth, seem to have had a special desire to record fundamental directions.

References

- G. Alcaïno, W. Liller, F. Alvarado and E. Wenderoth: 1990 *Astron. J.* **99**, 1831.
 G. Alcaïno: 1973, *Atlas of Galactic Globular Clusters with Colour Magnitude Diagrams*, Univ. Católica de Chile.
 W. Liller: 1990, "Orientations of Religious and Ceremonial Structures in Polynesia", paper delivered at the Third International Conference on Archaeoastronomy, St. Andrews, Scotland, U.K.
 W. Liller: 1991, "The Viña del Mar Nova Search: 1982–1991", paper delivered at the Workshop on Cataclysmic Variable Stars, Viña del Mar.
 D.A. Vandenberg, R.A. Bell: 1985, *Astrophys. J. Suppl.*, **58**, 561.

Sporty ESO

The victorious ESO Teams are feared by the competitors!

No, this is neither the translation of a phrase in a Latin reading book, nor does it refer to the technological and scientific achievements of our organization. It describes how sporty ESO staff members have repeatedly destroyed the common myth that astronomy is the realm of old men who stumble over long and white beards!

Football has always been one of our strengths and ESO teams on two continents have taught their adversaries many a lesson. ESO-La Silla tennis players are reputed to have the fastest serves above 2300 metres, and long-distance ESO-runners have been seen on many a road in Chile and Germany.

Bicycling, that noble art of ecological propagation, is in the coming, and ESO people are among the pioneers. At the ESO Headquarters just outside Garching, more and more of these elegant machines are seen, shining in all colours and in a great variety of shapes. Concerned car-drivers (a few are still left) have noticed an increasing spill-over onto the sparse parking space. New speed records are being set during the early morning race from Garching to the ESO Headquarters. And there are unconfirmed rumours that some ESO staff members spend an important part of their free time, riding along the beautiful roads in the hilly Bavarian countryside.

But nowhere has the impact been so great as in the 4th region of Chile! Read the following story to learn how the ferocious La Silla mountainbike team conquered the hearts of the Chilean public, won (almost) all of the honours at Tololo, all while representing ESO in the best possible way. Racing up (and down) the mountains in the dry Atacama desert, they have shown the world that at ESO power, transmission and response refer to more than telescopes and CCD's.

Because of the international nature of our organization, the International Astronomical Union some years ago decided that ESO astronomers participating in international IAU meetings may be registered as belonging to "ESO", rather than to a particular country.

It is at this moment not known whether the International Olympic Committee will follow this example, when the first ESO athletes show up . . . and what about the anthem?

Another Aficionado

The Other Face of La Silla

THE ESO AFICIONADOS

There used to be a time when driving a car up to La Silla one would hardly meet a living soul, and the only occasional *obstacles* of appreciable size were some donkeys. Not anymore. Several La Silla visitors and most of the La Silla staff have lately seen cyclists on the local roads, any time of the day, and going quite a bit faster downhill than uphill.

Although a solitary cyclist could be observed here and there already years

ago, this activity on the present scale is new for La Silla. So what's behind the display of these hairy legs? A sudden increase of interest in a healthy pastime, or does it go further than that?

The answer is in fact better known by the amateur cyclist of the 4th Region in Chile than by many of the ESO staff and visitors. Since about a year and a half ago, these ESO mountainbikers have won all competitions that have been organized in this area.

It all started with the arrival of the mountainbikes in Chile. As a robust and all-terrain version of the traditional bike, a mountainbike is particularly well suited to wheel on unpaved roads. Although the unpaved parts of the access road to La Silla are among the best maintained of Chile, they are still unsuitable for race-bikes with narrow tires. Hence some of the ESO personnel with interest in biking brought such a mechanical piece of art up to La Silla, and a couple



Figure 1: Start of 70 cyclists at the gate of Cerro Tololo Interamerican Observatory. (Photos 1 and 2 by Claudia Astorga; photos 3 and 4 by Nelson Muñoz).

of them actually started using it a few times a week. A similar situation was seen in other parts of this country, abounding with dirt tracks, and especially also in Tololo.

The Tololo Experience

Things became a little more serious in the beginning of 1991, when Tololo people talked about organizing a bike-race on the Tololo roads. The original idea came from Bob Williams, director of Tololo and lifetime jogger. More than a real race, he saw it as a personal challenge for all the participants, including himself. Knowing how tough an exercise this is, he stated: "This is where the *real* men are separated from the ordinary guys". He couldn't know then that also women would participate, even some of his own female employees. Where are you, ESO girls?

Not exactly unfamiliar with this type of road, six ESO cyclists quickly inscribed for this test. At the time of the event, end of April 1991, some of the ESO participants had been riding a mountainbike for only a week or so. Which was of course still a lot better than most of the 55 participants. The 34 km race, from the Tololo gate up to the top of the mountain, rising from 600 m to 2200 m above sea level, was really too much for many unprepared adventurers. But not for five of the six participants of ESO. Hans Gemperlein won easily, Luis Wendegass was third, Walter Rosenfeld sixth, Andrea Moneti eighth and Eric Allaert eleventh. Stimulated by this overwhelming success, the La Silla sports commission knocked immediately on the ESO management doors to get per-

mission for the organization of a similar event on the ESO premises.

The La Silla Continuation

It didn't take too long to convince the decision takers, and off went the sports commission to organize this event. Followed many letters and phone calls pleading for sponsorship, collaboration and/or participation, meetings to set up regulations and the like, TV interviews, text processing of all documents, etc. A lot of manhours later, on the 20th of October 1991, La Silla opened its doors for its biggest non-astronomical event ever: 60 cyclists, 120 companions, and

about 30 volunteers made this day a real treat. Now on their own territory, ten ESO pedallers participated. The success of the organization itself was fully complemented by the results of these racers: again Hans Gemperlein comfortably first, Luis Wendegass second, Eric Allaert third, Walter Rosenfeld seventh (and first senior), Andrea Moneti eighth, Eduardo Matamoros eleventh, Bruno Altieri sixteenth, Eduardo Robledo twenty-second, Ricardo Otto thirty-third and Rainer Donarski thirty-eighth. Many of the outside participants still talk wonders about the organization of this event, where "nothing nor nobody was left unattended". Which is not surprising considering the efforts of the organizers and the support of the ESO management.

But success has its price: if you want to keep it up, you must do something for it, i.e. keep on training, more, longer, harder. That didn't seem to bother many of the iron-horse enthusiasts. Especially not during Chilean summer, when the after-work training consisted in riding to La Frontera, to have a cold beer and a sandwich, or to the world-famous telephone booth in Cachiuyuyo. And the good results kept on coming: Luis Wendegass won the 1st La Serena mountain race (August 1991), Hans Gemperlein the 1st race to Andacollo (November 1991), Eric Allaert the Cendyr circuit in La Serena (February 1992) and the 1st race Vicuña – El Pangue (March 1992). DIGEDER, the sports department of the Chilean government, awarded Hans Gemperlein as the best mountainbiker in 1991 for the fourth region.

So what about the second race to Tololo? Postponed for the absence of its inventor, Bob Williams, and en-

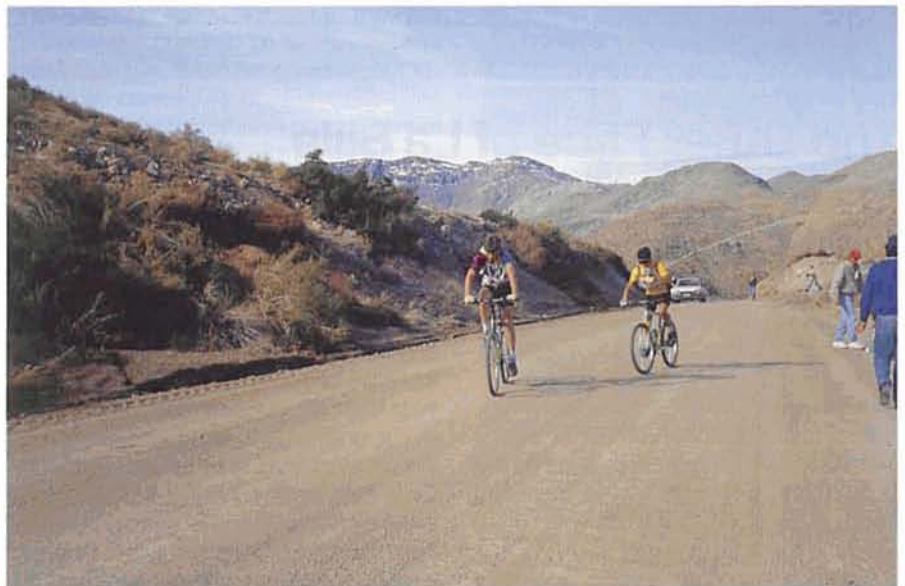


Figure 2: Hans Gemperlein and "compañero" 2 kilometres before the arrival.



Figure 3: The (unquiet) ESO bike team just before the start of the La Silla race.

dangered by *El Niño* – a periodic Pacific ocean stream spelling meteorological disaster – this race was finally scheduled for the 21st of June 1992. Expectations were high from many sides, as ESO racers had better-than-ever preparation, but at the same time were looked at as the ones to beat.

Tololo Again!

The night before the big event, again six ESO cyclists went down from La Silla to La Serena, and took off early next morning towards Vicuña. At the Tololo gate, on a cold but sunny Sunday morning, they saw many familiar faces half a metre above the 70 mountainbikes. Now with experienced organizers and perfectly assisted by Jorge Santana and Roberto Rojas in an ESO carry-all (thanks, boss!), the ESO racers had no one to blame in the case of a defeat. Nobody really worried, as Hans had said he was "feeling pretty good", quite opposite to all the other races. Where he had won anyhow. Halfway it didn't look bad at all with 3 racers a few minutes ahead: Hans, Eric, and – wait a minute – an unknown guy hanging on the rear wheel of Hans. Half an hour later Eric had to let the two other go: "Either I hook off and get up there, or I hang on and drop dead 1 km further." This scenario continued until about 250 m before the finish. In a spectacular sprint Hans left his opponent 20 seconds behind. He finished exhausted in about 10 minutes less than last year. When asked how he felt, he barely lifted his head to see who dared to ask him such a misplaced question. Eric came in third, 4 minutes behind Hans, Walter 4th (11 min), Luis 6th (12 min), Eduardo 8th (19 min), and Bruno 19th (42 min). Although a real fine result, this one was

tougher than ever, and the distances between the participants are vanishing. So do not take it for granted that ESO racers will keep on winning for ever. After all, between the training sessions

there is some work to be done on La Silla!

Citius – Altius – Fortius

The story does not end here yet. The sports commission already started to organize the second ascension of La Silla, after getting an informal approval from the management. Keep your thumbs up for the end of next October!

Most of the more conventional articles in the *Messenger* end with acknowledgements. This one is no exception. In their constant effort to offer healthy and active entertainment on La Silla, the sports commission would like to express its gratitude towards the ESO management for its continuous support. Of course we should not forget the main actors of these events, i.e. the fine sportsmen who defend the ESO colours also when the subject is not astronomy, and their colleagues for the encouragement. Also thanks to all the car drivers who take care and slow down on the La Silla roads, because there might be a cyclist just behind the next curve!



Figure 4: The (smiling) winners at La Silla.

Alive and Kicking into the 90's

During the past decade in Germany, ESO has established for itself a reputation of a dynamic and successful organization, with a relatively young staff of highly motivated people. Apart from the astronomy field, this found confirmation on several occasions on the Bavarian football fields. The ESO team integrated the best of the different national styles and proved that this can be done effi-

ciently and successfully, besides giving a lot of fun.

Some of the matches against the strong team of the Universitäts-Sternwarte München, led by its powerful director R. Kudritzki, have not been recorded in the Annual Report of the Organization, but are part of the legacy that we are passing to the future ESO generations, together with EFOSC, the

NTT and the quality of the food in the La Silla cafeteria.

Entering the 90's, we started to fear that the driving core of the team was softening with increasing age, that motivations were on the low side, that new arrivals did not integrate in the possibly obsolete working schemes: in short that we might not be up to the new challenges that ESO is facing.

On a hot Saturday in July, on the Max Planck field in Garching, an ESO team with a shaken self-confidence and an average age dangerously approaching 40, entered the ASTRO CUP, a one-day competition with the teams of our neighbours and friends of the Max Planck Institutes für Astrophysik and für Extraterrestrische Physik and of the Observatory of the University of Munich.

At the end of the day, after four strenuous games where we scored 5 goals and suffered 2, we stood as battered but clear winners with the cup at our feet and glasses of excellent Bavarian beer in our hands (both courtesy of the sponsor CONVEX). We might well lose the Cup next year to one of our excellent contenders, but we are satisfied to have proved this time that we are not at our wit's end and that we still



The ESO team who successfully competed in the 92 Astro-Cup, from the left, top: M. Klaus, C. Gouiffes, a visitor to ESO, E. Zolti (a friend from NET), A. Wallander, F. Koch, J. Quebatte; bottom: L. Noethe, F. Zigmann, B. Delabre, S. D'Odorico, M. Quattri, M. Basbilir (other team members not included in this picture: B. Buzzoni, D. Chittim, A. van Dijsseldonk, G. Fisher, P. François, B. Jørgensen, P. Møller, T. Oosterloo and R. Warmels).

have energies to spend when needed.

We are too realistic to claim that this victory is a good omen for other ac-

tivities of the Organization, but it does not hurt to secretly play with this feeling. Long live ESO! S. D'ODORICO, ESO

Astrometry with ESO Telescopes

A Contribution to the Construction of the New Extragalactic Reference Frame

Chr. DE VEGT, Hamburg Observatory, Germany

Astronomical research is strongly dependent on the availability of a unique all-sky reference frame though most astrophysicists do not explicitly take notice of this complex astrometric problem.

However, the necessity of very precise pointing of new generation large telescopes from ground or space and the unambiguous identification of very faint objects in all spectral regions accessible from ground and space, in particular in the radio and infrared region, has sensitized the astronomical community to this problem.

During the IAU General Assembly in Buenos Aires a resolution by the Working Group on Reference Systems has been adopted (IAU 1992) which describes the properties of a new, inertial, extragalactic reference frame and a new intercommission working group has been established to provide a practical solution within the coming three years to

be presented to the IAU during the 1994 General Assembly in The Hague.

1. Main Properties of the New Reference Frame

Contrary to the present fundamental system which is based on the positions and proper motions of bright stars – the basic FK5 contains 1535 bright stars –, the future extragalactic system will be based primarily on the positions of a carefully selected small number of compact extragalactic radio sources; almost all of these sources will display optical counterparts, mainly quasars and BL Lac's but also some compact galaxies.

This choice is based on the generally agreed assumption of cosmic distances of these objects with the consequence of negligible proper motions and therefore fixed space directions for a long period. This idea already has a long

history, but only in the last decade the practical realization of this concept became feasible through the mature technique of VLBI radio astrometry.

Using a global net of suitably distributed radio telescopes, positions of these primary radio sources can now be determined in a routine way to milli-arcsecond (mas) precision and an absolute global reference frame can be established and maintained for the future.

At the same time the high angular resolution of VLBI provides comprehensive information on source structure and their temporal changes with sub-mas resolution.

A second group of objects is of equal importance for solving this problem; namely selected radio stars, the cm radio emission of which has to be strong and steady enough to be measured with mas precision by VLBI, the VLA and future VLBA-net on a routine basis.

Absolute positions, proper motions

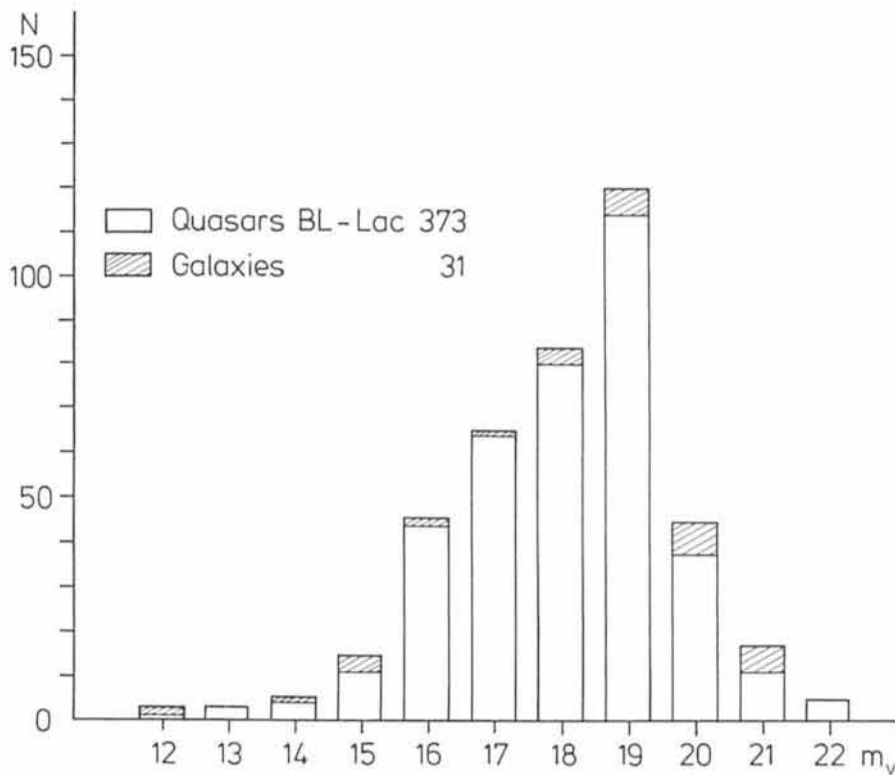


Figure 1: Magnitude distribution of 404 radio sources for the Extragalactic Reference Frame.

and parallaxes of those stars are obtained then in the primary extragalactic frame. At the same time these galactic objects can be easily accessed by optical astrometry because of their brightness thus providing a natural link to the optical spectral region.

While being optimal candidates in the radio domain, the primary sources are not very suitable to work with in the optical spectral range directly. The reasons are obvious: firstly, the faintness of their optical counterparts (mostly beyond 18th magnitude, see Fig. 1), which requires large telescopes for observation, the astrometrically usable field of which is $\ll 1$ degree, with an additional dramatic decrease of usable field size when CCDs are used instead of the photographic plate. Therefore the object of interest and the reference frame sources have to be very close in the sky, a situation which will allow only very occasionally to link any other object directly to the primary reference frame.

Secondly, there is no realistic measuring technique presently available in the optical domain to determine object positions relative to these very faint primary sources over large arcs, contrary to the radio. Therefore a practical realization of the new reference frame must be based in addition on a dense, global net of fairly bright stars. At the same time this net should be of comparable precision with the radio positions. The anticipated HIPPARCOS stellar net will be the natural choice and will be superior to

any previous fundamental catalogue, provided it can be linked in a unique way to the VLBI based primary reference frame.

Thus a multi-step approach is necessary for the construction of this new reference frame, on the other hand, dealing again with stars which will reflect kinematically their galactic origin and the earth's and solar system's motion, precise proper motions (p.m.) and parallaxes have to be determined. Because of unavoidable systematic and random errors in this process, the stellar net will deteriorate substantially as a function of changing epoch. To maintain the initial high precision of the HIPPARCOS net and to improve the precision (2 mas/yr) of the HIPPARCOS proper motions, future astrometry satellite missions are indispensable. Furthermore, a continuous improvement of the main astronomical constants as for example precession and nutation are of crucial importance to maintain a high-precision reference frame.

Although the selection of the about 120,000 HIPPARCOS programme stars was based primarily on astrophysical proposals, the scanning principle used by the satellite and the requirement to monitor continuously the satellite orientation by a large set of so-called star-mapper stars fortunately had the consequence that the selection of the programme stars had to be made as uniformly as possible on the sphere. A large body of stars with well-known as-

tronomical history is therefore included in the programme stars; for a recent overview see (A & A, 1992).

Thus the HIPPARCOS mission will provide automatically a homogeneous and fairly dense stellar net of about 2.7 stars/sq.deg., mainly in the magnitude interval 7–10 (see Fig. 3).

Furthermore, the Tycho Mission will add some 500,000 fainter stars with precise photometry although reduced astrometric accuracy. However, if we recall for example that already the AGK3 on the northern hemisphere and the CPC2 on the southern hemisphere provide stellar densities of ≥ 10 stars/sq.deg. it is obvious that the HIPPARCOS net should soon be made denser and extended to much fainter limiting magnitudes by further catalogue projects to keep up with the needs of large telescopes with their small-field, highly sensitive area detectors.

2. Linking HIPPARCOS to the VLBI System

The rigidly constructed HIPPARCOS stellar net still may contain a small unknown rotation of some mas/year which will be reflected in the HIPPARCOS proper motions. After this residual motion has been taken out, the HIPPARCOS net will be adjusted to a fixed origin, close to that of the FK5/J2000 system. Because none of the VLBI primary sources is observed by HIPPARCOS directly, a number of indirect approaches has been worked out to provide the link to the inertial (rotation-free) extragalactic system (see Table 1). With a view to the ongoing problems with HST, several ground-based, large observing programmes are underway to provide this link. (Froeschle and Kovalevsky, 1982; A & A, 1992; de Vegt et al., 1991).

However, whereas the extragalactic VLBI net does not display a net rotation because of the inertial nature of its target objects, the zero point of the R.A. system has to be adjusted, because VLBI provides only R.A. differences, although absolute declinations. According to the quoted IAU resolution, the R.A. zero point shall be adjusted to the FK5/J2000 zero point at epoch J2000. To achieve this goal, precise optical positions of a suitable subset of the radio sources have to be determined in the FK5 system. Furthermore, the physical nature of the radio and optical emission and the morphology of the sources have to be studied in detail to ensure that the optical and radio emission centres will coincide to the precision of the VLBI measurements, i.e. within mas. At present, knowledge is lacking in this respect, therefore the number of objects and object types (quasars, BL Lac's,

- Galaxies
- Quasars, BL-Lac's

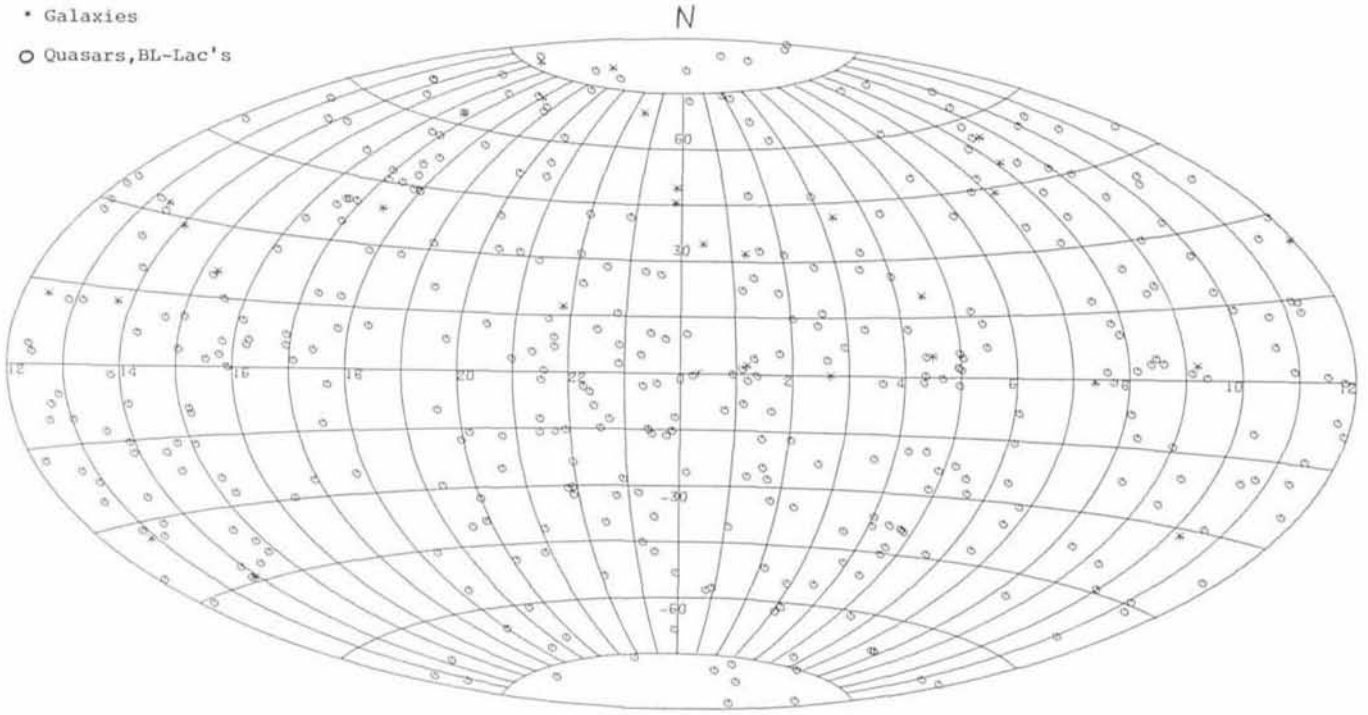


Figure 2: Distribution of 413 radio sources for the new Extragalactic Reference Frame.

AGN's . . .) should be as large as possible with the result that possible differences of the emission centres in the various wavelengths will hopefully average out. The same situation obviously will be met with radio stars, although here the source geometry is easier to evaluate.

Any successful link method therefore must be a statistical approach, because no ideal objects do exist with point source properties in all wavelength regions.

In our long-term programme to establish a VLBI-based reference frame (Johnston et al., 1991; de Vegt et al., 1991) we have been using long exposure plates to determine positions of compact radio sources from this primary VLBI net in the FK5 optical fundamental system. Figure 2 shows the source distribution as presently selected for this reference frame. A subset of these objects has already been used successfully for the orientation of a first high-precision VLBI reference frame catalogue. (Ma et al., 1990). Although the optical positions are less precise by about a factor 10 (some 0.01 arcsec) than the corresponding radio positions, the large number of sources available (some 100) will allow to determine the R.A. zero point, also with mas precision.

As Figure 1 clearly demonstrates, most optical counterparts are fainter than 18th magnitude. To link these objects directly to the FK5 system is impossible because almost all FK5 stars are brighter than 6th magnitude and the

low catalogue density of about 1 star/30 sq. deg. will provide only a vanishing probability to find a fundamental star in the telescope field ($\ll 1$ deg. diam.) together with the target object and in addition no detector can handle the enormous magnitude differences. A multi-step approach therefore has to be used. In the first step we are using high precision wide field astrographs in both hemispheres to provide a dense system of secondary reference stars in the magnitude $m_v = 12-14$. The primary reference stars to be used for the astrograph plates solutions are taken from the AGK3RN and SRS catalogues in the northern and southern hemispheres respectively.

These transit circle based catalogues form the main body of the global IRS reference system and are transformed to the IAU FK5/J2000 system.

The reference stars are mostly from the magnitude interval $m_v = 6-9$ with an average density of 1 star/sq. deg. Both astrographs are used with a 6-mag objective grating, therefore we can measure first-order diffraction images of all reference stars together with their central images and also diffraction images of the 1-3 FK5 stars which often will be in the astrograph field also. The plate constants obtained therefore allow to determine the positions of the secondary reference stars very precisely in the FK5 system. As a very important additional step we are measuring all HIPPARCOS programme stars in the astrograph field (about 80-100) for a

final HIPPARCOS-based plate solution. It should be recalled here that most of the IRS stars are already among the HIPPARCOS programme stars.

3. Astrometry of Source Plates Using ESO Telescopes

To obtain high-precision astrometric plates for the radio sources, we have used the 3.6-m telescope in the prime focus mode very successfully and currently are using the ESO-Schmidt telescope, because the 3.6-m telescope unfortunately is no more available for direct photography. Although both telescopes provide the necessary limiting magnitude and plate field size to guarantee a sufficient number of secondary reference stars for the determination of precise positions of the target source, the much larger scale of the 3.6-m and the plane image field are more favourable for precise astrometry than the Schmidt, although some accuracy can be regained by averaging a larger number of Schmidt plates. However, concerning possible object structure and problems with crowded fields there is no compensation for the favourable scale of the 3.6-m telescope.

3.1 3.6-m Prime Focus Astrometric Model

The 3.6-m was used with the 3-lens red-triplet corrector which provides a usable field of about 50 arcmin diameter and a flat image plane, 24×24 cm,

Table 1. Main Programmes to link the HIPPARCOS Net to the Extragalactic System.

Object class	Technique	N	M	Orientation	Rotation
Radio stars	VLBI	<20	D	yes	yes
	VLA	<100	D	yes	yes
Extragal. radio sources with opt. counterparts	VLBI	<400	I	yes	partly
	Opt. astrometry				
H [*] -quasar-pairs	VLBI	<100	I	partly	yes
	Opt. astrometry				
	HST-FGS				
Lick p.m. stars (mainly N. Hem.)	Opt. astrometry	<20,000	D	no	yes

N = approximate number of objects available.
M = Mode D = direct link (objects observable in both systems).
I = indirect link (objects are not HIPPARCOS programme stars).

1.5-mm thick Kodak 098-04 plates have been used. However, the corrector introduces a strong third-order regular geometric distortion term which has to be taken into account in the plate model.

Furthermore, there is no possibility to calibrate the intersection of the optical axis on the plate, therefore two additional terms for the zero point of the distortion have to be included. Because of the limited field size and the position of the target object very close to the plate centre, a 6-constant affine plate model (de Vegt, 1991) will be sufficient for modelling differential refraction and aberration and the usual projection onto the tangential plane.

The linearized plate model therefore is:

$$\begin{aligned}
 XI &= ax + by + c + Lx(x^2 + y^2) - U(3x^2 + y^2) - V(2xy) \\
 ETA &= a'x + b'y + c' + Ly(x^2 + y^2) - U(2xy) - V(x^2 + 3y^2)
 \end{aligned}$$

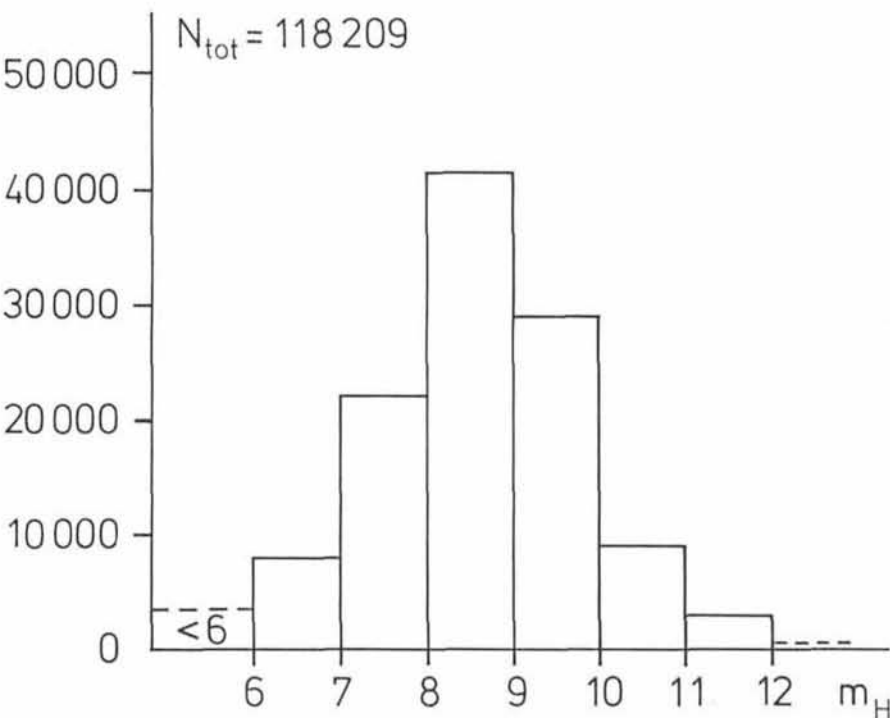


Figure 3: Magnitude Distribution of Hipparcos Programme Stars.

3.2 Schmidt Plates

Global astrometric modelling of Schmidt plate geometry is a major problem and in addition different solutions may be required for the different optical configurations of various Schmidt telescopes. At least one fact is obvious: any successful solution requires a dense net of very accurate reference stars which in addition have to be chosen from a magnitude range where the diffraction spikes of Schmidt plate images are negligible which means that these reference stars should be at least >12th magnitude for practical exposure conditions. Unfortunately a precise global reference star catalogue in this magnitude range is still lacking, although definite plans are available but on hold because of recent financial problems (de Vegt, 1989, 1991).

In our application we are only interested in modelling the central plate area of about 1×1 deg. As in the case of the 3.6-m, our system of secondary reference stars is perfectly suited for this purpose. Because of the small size of the 3rd-order term and the restricted field size, a statistically significant determination of the distortion zero point terms is not possible. Furthermore, as practical experience has shown, even the third-order term can be pre-corrected without affecting the position of the central target object significantly, provided the origin of the rectangular plate measurements x, y is carefully adjusted to the plate centre a priori.

The appropriate choice of the plate model can be limited therefore to a 6-constant affine model, with a possible extension to the 3rd-order term, if the geometry of the particular Schmidt telescope is not well known at the beginning, or the adopted plate-filter combination changes (see above-quoted model, without the U, V terms).

In the current Schmidt observing programme high quality plates for 29 sources have already been obtained. Normally 3 plates/object are taken using a 098-04+OG550 emulsion-filter combination. Plates are unhypered, exposure times are ≤ 40 minutes each. All plates are measured on our modernized 422F-MANN comparator which uses a CCD camera for direct image digitization (for details see Winter et al., 1992). A measuring accuracy of 0.5 microns is obtained in routine operation. In addition, a new type of astrometric measuring machine is under development which will allow to digitize a complete Schmidt plate in less than 1 hour with submicron accuracy.

As an example of our current work, results for the QSO 748+126 ($m_v = 17.8$, $z = 0.889$) are presented. This primary

reference frame radio source shows a stellar appearance on the plates. Using the quoted reduction model, a m.e. of unit weight for the plate solution of <0.1 arcsec could be obtained. The final FK5/J2000 position, based on 3 plates, is

RA(J2000) $7^{\text{h}} 50^{\text{m}} 52.051^{\text{s}}$;
DEC(J2000) $+12^{\circ} 31' 04.84''$

Using the corresponding VLBI position from (Ma et al., 1990), the system difference in the sense "optical minus radio" then is:

$\Delta\text{Cos(DEC)} = +0.073$ arcsec;

$\Delta\text{DEC} = +0.01$ arcsec

which is in good agreement with earlier results (Johnston et al., 1985) and the recently quoted first preliminary results of a HIPPARCOS-FK5 comparison in that sky region (Lindgren, 1992). However, a dense grid of some 100 com-

parison points, as will be provided by our reference frame programme is required for a more detailed conclusive analysis.

Acknowledgements

The author wants to thank H.E. Schuster and B. Reipurth of ESO for their continuous help with the observing programme. Financial support by BMFT under grant 1000018-3 (HIPPARCOS) is gratefully acknowledged.

References

- IAU, 1992, *IAU Inf. Bull.* **67** (Jan. 1992), 7, Resolution 4.
A & A, 1992, *Astron. Astrophys.* **258**, No. 1, (May I), special HIPPARCOS Vol.
Froeschlé M., Kovalevsky J., 1982, *Astron. Astrophys.* **116**, 89.

- de Vegt Chr., Zacharias N., Johnston K.J., 1991, *Adv. Space Res.* **11**, 133.
Johnston K.J., Russell J.L., de Vegt Chr., Zacharias N., Hindsley R., Hughes J., Jauncey D.L., Reynolds J.E., Nicholson G., Ma C., 1991, *Proc. IAU Coll.* **127**, 123.
de Vegt Chr., 1991, *Astrophys. Space Science* **177**, 3 = *Proc. IAU Coll.* 100.
de Vegt Chr., 1989, Conference on Digitized Sky Surveys, Geneva = *Bull. Inf. CDS* **37**, 21.
de Vegt Chr., Winter L., Zacharias N., 1992, Digitized Optical Sky Surveys = *Astrophys. Space Sc. Lib.* **174**, 115 (Kluwer Acad. Publ.).
Winter L., de Vegt Chr. Steinbach M., Zacharias N., 1992, *ibid.* p. 123.
Johnston K.J., de Vegt Chr., Florkowski D., Wade C.M., 1985, *A.J.* **90**, 2390.
Ma C., Shaffer D., de Vegt Chr., Johnston, K.J., Russell J., 1990, *A.J.* **99**, 1284.
Lindgren L., 1992, ESA SP-349, in press.

The ESO Minor Planet Sky

L. D. SCHMADEL, *Astronomisches Rechen-Institut, Heidelberg, Germany*

The European Southern Observatory was established in 1962 to operate the powerful La Silla observatory for the benefit of many fields of astronomy and astrophysics. Only a few programmes were directly concerned with the survey of the solar system and the discovery of minor bodies like comets and minor planets. In many cases, observations of these objects were made only as valuable by-products of other campaigns. It was especially the wide-field telescopes, the 1-m ESO Schmidt and the 40-cm GPO Astrograph, which yielded an enormous amount of positional data. During the last decades ESO has always maintained a leading position in the world, as far as the number of minor planet observations is concerned.

In 1988, Commission 20 of the IAU established a special study group to elucidate the meanings of minor planet names. This endeavour, which comprises a lot of data for the first 5012 minor planets numbered until the end of 1991, has now reached completion (L.D. Schmadel, *Dictionary of Minor Planet Names*, X+687 p., Springer-Verlag, 1992).

Since all information in this work has been archived in a computer-readable data base, it is very easy to extract material which directly or indirectly pertains to ESO. I have here used the data base and some recently published, additional material to illustrate the "ESO minor planet sky".

The many thousands of observations at ESO have inevitably produced quite a few discoveries. However, there is a long way from the detection of a new solar system object until it can be definitively numbered and named. The new planet has to be observed in – at least – three oppositions before it can be numbered. Therefore, the majority of new detections remain in a "dormant" stage in the Minor Planet Center's computer files. In some cases it is possible to identify new positions with planets observed earlier; this shortens the process. Nowadays, it is a rare exception when a newly discovered planet can be quickly identified with a long series of prior observations.

The statistics show that until July 1992, some 186 ESO discoveries have reached the status of "established", i.e. numbered, minor planets. Table 1 records these objects in ascending order together with the name (or preliminary designation), the year of discovery and the discoverer(s). Whereas the great majority was found by Belgian astronomer Henri Debehogne during special surveys for minor planets, most others were found by chance, mainly with the Schmidt telescope, and during the various ESO atlas projects. A total of 16 astronomers earned discoverer merits; they are shown in Table 2 together with the overall numbers of discoveries and co-discoveries (in parentheses).

It is interesting to note that in the very near future ESO is likely to rank fifth (behind Heidelberg, Crimea, Palomar and the Anderson Mesa Station of Lowell Observatory) on the list of the most successful minor-planet discovering observatories. In the ranking list of the most successful discoverers of minor planets of all times, Henri Debehogne now occupies the 13th place – one place ahead of the famous visual planet hunter A. Charlois in Nice, who detected some 99 planets between 1887 and 1904.

The right to name a minor planet essentially belongs to the discoverer. As can be seen from Table 1, only a small fraction of ESO discoveries honours ESO astronomers. This has to be done by other colleagues, and there are in fact a lot of names which together constitute a kind of "ESO minor planet sky". While it is very easy to extract all ESO successes from the data base, it is nearly impossible to find among the 4,000 existing minor planet names those which have been accorded to ESO officials, staff astronomers, etc.

The list in Table 3 gives all those which are mentioned in the book about the ESO history, recently written by Adriaan Blaauw. Still, it cannot be considered to be a complete compilation. It shows, however, that it is not very exaggerated to speak about the ESO minor planet sky!

Table 1: Discoveries of numbered minor planets made at ESO

(2052) Tamriko	1976 R. M. West	(3573) Holmberg	1982 C.-I. Lagerkvist
(2053) Nuki	1976 R. M. West	(3610) Decampos	1981 H. Debehogne and G. De Sanctis
(2105) Gudy	1976 H.-E. Schuster	(3625) Francastoro	1984 W. Ferreri
(2115) Irakli	1976 R. M. West	(3631) Sigyn	1987 E. W. Elst
(2116) Mtskheta	1976 R. M. West	(3634) Iwan	1980 C.-I. Lagerkvist
(2117) Danmark	1978 R. M. West	(3646) 1985 RK4	1985 H. Debehogne
(2145) Blaauw	1976 R. M. West	(3679) 1984 DT	1984 H. Debehogne
(2146) Stentor	1976 R. M. West	(3683) Baumann	1987 W. Landgraf
(2147) Kharadze	1976 R. M. West	(3705) 1984 ET1	1984 H. Debehogne
(2148) Epeios	1976 R. M. West	(3740) Menge	1981 H. Debehogne and G. De Sanctis
(2187) La Silla	1976 R. M. West	(3778) Regge	1984 W. Ferreri
(2234) Schmadel	1977 H.-E. Schuster	(3788) 1986 QM3	1986 H. Debehogne
(2275) 1979 MH	1979 H.-E. Schuster	(3820) 1984 DV	1984 H. Debehogne
(2329) Orthos	1976 H.-E. Schuster	(3821) 1985 RC3	1985 H. Debehogne
(2364) Seillier	1978 H. Debehogne	(3848) 1982 FH3	1982 H. Debehogne
(2461) Clavel	1981 H. Debehogne and G. De Sanctis	(3852) 1987 DR6	1987 H. Debehogne
(2526) Alisary	1979 R. M. West	(3865) 1988 AY4	1988 H. Debehogne
(2543) Machado	1980 H. Debehogne	(3866) 1988 BH4	1988 H. Debehogne
(2567) Elba	1979 O. Pizarro and G. Pizarro	(3870) Mayré	1988 E. W. Elst
(2589) Daniel	1979 C.-I. Lagerkvist	(3871) Reiz	1982 R. M. West
(2590) Mourão	1980 H. Debehogne	(3908) 1980 PA	1980 H.-E. Schuster
(2595) Gudiachvili	1979 R. M. West	(3916) 1981 QA3	1981 H. Debehogne
(2596) Vainu Bappu	1979 R. M. West	(3919) 1984 DS	1984 H. Debehogne
(2608) Seneca	1978 H.-E. Schuster	(3933) Portugal	1986 R. M. West
(2673) Lossignol	1980 H. Debehogne	(3984) 1984 SB6	1984 H. Debehogne
(2694) Pino Torinese	1979 C.-I. Lagerkvist	(4016) Sambre	1979 H. Debehogne and E. R. Netto
(2707) Ueferji	1981 H. Debehogne	(4030) 1984 EO1	1984 H. Debehogne
(2765) Dinant	1981 H. Debehogne and G. De Sanctis	(4036) 1987 DW5	1987 H. Debehogne
(2788) Andenne	1981 H. Debehogne and G. De Sanctis	(4038) Kristina	1987 E. W. Elst
(2795) Lepage	1979 H. Debehogne and E. R. Netto	(4060) Deipylos	1987 E. W. Elst
(2814) Vieira	1982 H. Debehogne	(4061) Martelli	1988 W. Ferreri
(2852) Declercq	1981 H. Debehogne	(4099) 1988 AB5	1988 H. Debehogne
(2902) Westerlund	1980 C.-I. Lagerkvist	(4120) 1985 RS4	1985 H. Debehogne
(2926) Caldeira	1980 H. Debehogne	(4123) 1986 QP1	1986 H. Debehogne
(2935) Naerum	1976 R. M. West	(4169) Celsius	1980 C.-I. Lagerkvist
(2958) Arpetito	1981 H. Debehogne and G. De Sanctis	(4172) 1982 FC3	1982 H. Debehogne
(3002) Delasalle	1982 H. Debehogne	(4191) Assesse	1980 H. Debehogne
(3004) 1976 DD	1976 R. M. West	(4192) Breysacher	1981 H. Debehogne and G. De Sanctis
(3005) Pervictoralex	1979 C.-I. Lagerkvist	(4199) 1983 RX2	1983 H. Debehogne
(3016) Meuse	1981 H. Debehogne and G. De Sanctis	(4202) 1985 CB2	1985 H. Debehogne
(3121) Tamines	1981 H. Debehogne and G. De Sanctis	(4206) 1986 QL	1986 H. Debehogne
(3138) Ciney	1980 H. Debehogne	(4210) 1987 DY5	1987 H. Debehogne
(3175) Netto	1979 H. Debehogne and E. R. Netto	(4211) 1987 RT	1987 H. Debehogne
(3235) Melchior	1981 H. Debehogne and G. De Sanctis	(4216) Neunkirchen	1988 H. Debehogne
(3266) 1978 PA	1978 H.-E. Schuster	(4218) Demottoni	1988 H. Debehogne
(3268) De Sanctis	1981 H. Debehogne and G. De Sanctis	(4252) 1985 RG4	1985 H. Debehogne
(3271) 1982 RB	1982 H.-E. Schuster	(4310) Strömholm	1978 C.-I. Lagerkvist
(3274) Maillen	1981 H. Debehogne	(4313) Bouchet	1979 H. Debehogne
(3288) Seleucus	1982 H.-E. Schuster	(4328) 1982 SQ2	1982 H. Debehogne
(3308) Ferreri	1981 H. Debehogne and G. De Sanctis	(4334) 1983 RO3	1983 H. Debehogne
(3331) Kvistaberg	1979 C.-I. Lagerkvist	(4342) Freud	1987 E. W. Elst
(3365) Recogne	1985 H. Debehogne	(4344) Buxtehude	1988 E. W. Elst
(3374) Namur	1980 H. Debehogne	(4345) Rachmaninoff	1988 E. W. Elst
(3389) Sinzot	1984 H. Debehogne	(4349) Tiburcio	1989 W. Landgraf
(3390) Demanet	1984 H. Debehogne	(4378) Voigt	1988 W. Landgraf
(3398) 1978 PC	1978 H.-E. Schuster	(4398) 1984 HC2	1984 W. Ferreri
(3411) Debetencourt	1980 H. Debehogne	(4443) 1985 RD4	1985 H. Debehogne
(3450) Dommangot	1983 H. Debehogne	(4444) 1985 SA	1985 H. U. Norgaard-Nielsen, L. Hansen and P. R. Christensen
(3456) 1985 RS2	1985 H. Debehogne	(4474) 1981 QZ2	1981 H. Debehogne
(3457) 1985 RA3	1985 H. Debehogne	(4478) Blanco	1984 W. Ferreri
(3458) 1985 RT3	1985 H. Debehogne	(4479) 1985 CP1	1985 H. Debehogne
(3465) 1984 SQ5	1984 H. Debehogne	(4501) Eurypylos	1989 E. W. Elst
(3477) Kazbegi	1979 R. M. West	(4535) 1986 QV2	1986 H. Debehogne
(3496) Arioso	1977 H.-E. Schuster	(4545) 1989 SB11	1989 H. Debehogne
(3519) 1984 DO	1984 H. Debehogne	(4546) Franck	1990 E. W. Elst
		(4571) Grumiaux	1985 H. Debehogne
		(4593) Reipurth	1980 C.-I. Lagerkvist
		(4599) 1985 RZ2	1985 H. Debehogne
		(4600) 1985 RE4	1985 H. Debehogne
		(4608) 1988 BW3	1988 H. Debehogne

Table 1 (continued)

(4609) Pizarro	1988 E. W. Elst	(4938) 1986 CQ1	1986 H. Debehogne
(4611) Vulkaneifel	1989 M. Geffert	(4939) 1986 QL1	1986 H. Debehogne
(4627) 1985 RT2	1985 H. Debehogne	(4942) 1987 DU6	1987 H. Debehogne
(4633) 1988 AJ5	1988 H. Debehogne	(4985) 1979 QK4	1979 C.-I. Lagerkvist
(4636) Chile	1988 E. W. Elst	(4993) 1983 GR	1983 H. Debehogne and G. De Sanctis
(4668) 1987 DX5	1987 H. Debehogne	(4994) 1983 RK3	1983 H. Debehogne
(4684) 1978 GJ	1978 H. Debehogne	(4999) MPC	1987 E. W. Elst
(4695) 1985 RU3	1985 H. Debehogne	(5003) 1988 ER2	1988 W. Ferreri
(4697) 1986 QO	1986 H. Debehogne	(5022) 1984 HE1	1984 W. Ferreri and V. Zappalà
(4744) 1988 RF5	1988 H. Debehogne	(5056) 1986 RQ5	1986 H. Debehogne
(4761) 1981 QC	1981 H.-E. Schuster	(5057) 1987 DC6	1987 H. Debehogne
(4784) 1984 DF1	1984 H. Debehogne	(5088) 1979 QZ1	1979 C.-I. Lagerkvist
(4793) 1988 RR4	1988 H. Debehogne	(5098) 1985 CH2	1985 H. Debehogne
(4798) Mercator	1989 E. W. Elst	(5099) 1985 DY1	1985 H. Debehogne
(4800) 1989 TG17	1989 H. Debehogne	(5107) 1987 DS6	1987 H. Debehogne
(4804) Pasteur	1989 E. W. Elst	(5108) Lübeck	1987 E. W. Elst
(4817) 1984 DC1	1984 H. Debehogne	(5109) 1987 RM1	1987 H. Debehogne
(4821) Bianucci	1986 W. Ferreri	(5115) Frimout	1988 E. W. Elst
(4825) Ventura	1988 E. W. Elst	(5127) Bruhns	1989 E. W. Elst
(4830) 1988 RG4	1988 H. Debehogne	(5160) 1979 YO	1979 H. Debehogne and E. R. Netto
(4843) 1990 DR4	1990 H. Debehogne	(5184) Cavallé-Coll	1990 E. W. Elst
(4864) 1988 RA5	1988 H. Debehogne	(5204) 1988 CN2	1988 E. W. Elst
(4931) 1983 CN3	1983 H. Debehogne and G. De Sanctis	(5229) 1987 DE6	1987 H. Debehogne
(4933) 1984 EN1	1984 H. Debehogne	(5248) 1983 GQ	1983 H. Debehogne and G. De Sanctis
(4937) 1986 CL1	1986 H. Debehogne		

Table 2: Ranking list of ESO discoverers

1. Debehogne, H.	109 (19)
2. Elst, E. W.	20
3. West, R. M.	18
4. De Sanctis, G.	15 (15)
5. Lagerkvist, C.-I.	12
Schuster, H.-E.	12
7. Ferreri, W.	8 (1)
8. Netto, E. R.	4 (4)
9. Landgraf, W.	3
10. Christensen, P. R.	1 (1)
Geffert, M.	1
Hansen, L.	1 (1)
Norgaard-Nielsen, H. U.	1 (1)
Pizarro, G.	1 (1)
Pizarro, O.	1 (1)
Zappalà, V.	1 (1)

Table 3: The ESO minor planet sky

(3496) Arioso	(4380) Geyer	(1679) Minnaert	(1637) Swings
(1501) Baade	(3371) Giacconi	(1691) Oort	(3765) Texereau
(2358) Bahner	(1894) Haffner	(1738) Oosterhoff	(2154) Underhill
(2145) Blaauw	(1650) Heckmann	(1629) Pecker	(2842) Unsöld
(1983) Bok	(4924) Hiltner	(4609) Pizarro	(2823) van der Laan
(1543) Bourgeois	(3573) Holmberg	(3933) Portugal	(2203) van Rhijn
(3363) Bowen	(3282) Spencer Jones	(2884) Reddish	(1946) Walraven
(4192) Breysacher	(1776) Kuiper	(4593) Reipurth	(2022) West
(1120) Cannonia	(2187) La Silla	(3871) Reiz	(2902) Westerland
(4636) Chile	(1851) Lacroute	(2605) Sahade	(2301) Whitford
(1594) Danjon	(1448) Lindblad	(1542) Schalerh	(1795) Woltjer
(3450) Dommangot	(1334) Lundmark	(1743) Schmidt	
(1761) Edmondson	(4386) Lüst	(1235) Schorria	
(4385) Elsässer	(1527) Malmquista	(2018) Schuster	
(3433) Fehrenbach	(2131) Mayall	(837) Schwarzschilda	
(1561) Fricke	(4065) Meinel	(1422) Strömgrenia	

A Honeycomb in the Large Magellanic Cloud

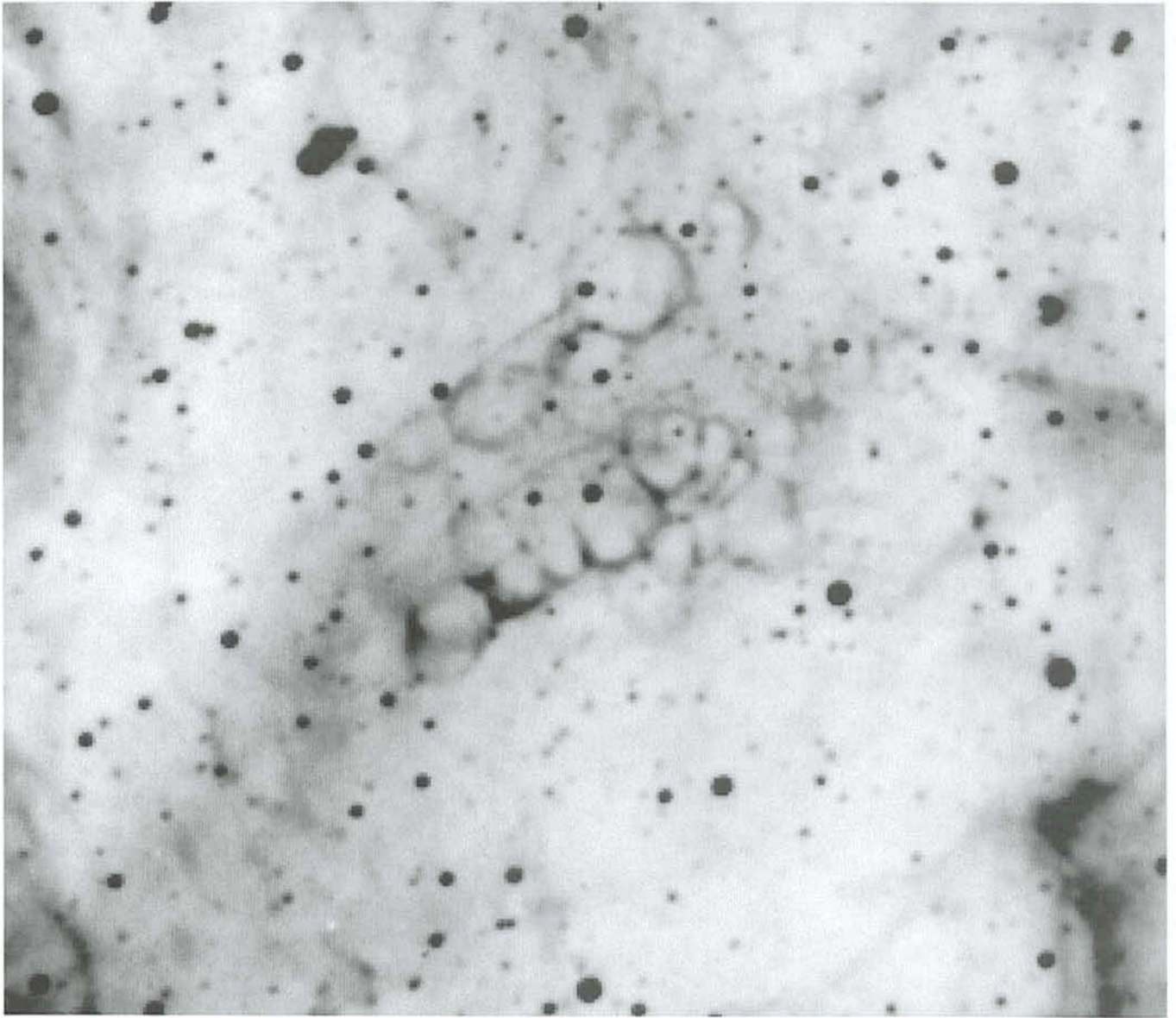
L. WANG, Department of Astronomy, University of Manchester, UK

The beautiful image shown in the centre of this page was taken by the ESO NTT on January 17, 1992. It was obtained with the ESO Multiple Mode Instrument (EMMI), in a narrow H α filter and the integration time was 10 minutes. The original purpose was to observe the inter/circumstellar material around SN1987A; the results of that work can be found in the paper by Wang and Wampler (1992).

It is purely by chance that this strange nebulosity, reproduced in negative in the picture on the opposite page, was in the field of our CCD detector. As shown in the picture, it consists of over ten loops with a size of around 12 arcsec, or about 3 parsec at the distance of the LMC. The most remarkable features are: (1) all the bubbles are clustered along a filamentary nebula, 1.5 arcmin long and 30 arcsec wide; (2) the bubbles have

roughly the same size; (3) they are rather circular. These features have led F. D. Kahn to suggest that this is a "honeycomb" in the LMC. The same bubbles were also observed in a narrow-band [OIII] 500.7 nm filter image.

Bubbles in the interstellar medium are not a rare phenomenon, especially in the LMC. The present "honeycomb" nebula is in fact located in a complex environment which is full of bubbles with sizes



Negative reproduction of the newly found "honeycomb" structure in the Large Magellanic Cloud, as seen in the light of $H\alpha$. North is up and east is to the left.

up to 30–40 pc across. These "super" bubbles may be due to OB associations or supernova explosions (Dyson and de Vries, 1972; Weaver et al., 1977).

Still, the origin of the "honeycomb" may be quite different, although it seems that there are only two possibilities – it is either related to the activities of the underlying stellar objects or it is independent of, or weakly dependent on, the stellar activity.

However, direct images taken in the continuum band do show an enhancement in the number densities of stellar objects in the neighbourhood of the "honeycomb". This implies that something peculiar might be happening here, and that the "bees" who made the "honeycomb" are perhaps the swarm of stars that is resident in the cloud. Bubbles of similar size can be easily pro-

duced by the stellar winds from massive stars.

If the "honeycomb" is indeed due to stellar activity, it will set very strong constraint on the nature of the underlying stellar objects. In order to produce a cluster of bubbles of similar size, the underlying stars have to be born at the same time, with the same initial mass and they must evolve at the same rate. The "honeycomb" will then be a unique object for the study of sequential star formation (see, for example, Elmegreen and Lada, 1977).

The morphology of the "honeycomb" makes it an interesting object in its own right. More work will now have to be done, both observational and theoretical.

This work is supported by SERC. I am thankful for several helpful discussions with J. Danziger of ESO.

References

- Dyson, J. E., de Vries, J.: 1972. *A & A*, **20**, 223.
 Elmegreen, B. G., Lada, C. J.: 1977. *Ap.J.*, **214**, 725.
 Wang, L. and Wampler, J. E.: 1992. *A & A*, **262** L9.
 Weaver, R., McCray, D., Caster, J., Shapiro, P., Moore, R.: 1977. *Ap.J.*, **218**, 377.

Centrefold

10-min $H\alpha$ frame, obtained with the NTT and EMMI. The frame has been rotated 30° clockwise for typographical reasons; the north direction is therefore at 1 o'clock. SN 1987A is at the centre and the strange "honeycomb" is visible in the lower left area. ▶





Comet P/Grigg-Skjellerup Observations at ESO La Silla During the GIOTTO Encounter Period

H. BOEHNHARDT, *Universitäts-Sternwarte, München, Germany*

K. JOCKERS, N. KISELEV, *Max-Planck-Institut für Aeronomie, Katlenburg-Lindau, Germany*

G. SCHWEHM, N. THOMAS, *ESTEC, Noordwijk, the Netherlands*

Introduction

On July 10, 1992, the GIOTTO spacecraft of the European Space Agency (ESA) became the first satellite to pass within 500 km of the nucleus of a comet. GIOTTO encountered the periodic comet P/Grigg-Skjellerup and returned a wealth of interesting *in situ* measurements of the cometary coma to Earth. After the fly-by of comet Halley on March 14, 1986, the spacecraft completed the first ever Earth gravity assist manoeuvre on July 2, 1990, placing it on course for an encounter with comet P/Grigg-Skjellerup. At launch, operations after the fly-by of comet P/Halley were unforeseen but the remarkable performance of the spacecraft and its instrumentation allowed the extension of the mission. GIOTTO has now completed 7 successful years in space.

Unlike comet P/Halley, comet P/Grigg-Skjellerup was previously a largely unexplored comet (for a summary of the results published so far see Birkle and Boehnhardt, 1992; additional information can be found in Osip et al., 1992, Schmidt and Wegmann, 1992). ESO has supported the GIOTTO fly-by at comet P/Grigg-Skjellerup by providing urgently needed astrometric positions before the encounter and by granting observation time to four authors of this article for physical observations. In this article we give a preliminary account on these observations and provide some highlights of the spacecraft encounter.

The Observing Programme

The main scientific goals of our observing programme at ESO-La Silla were: to determine production rates of the very abundant H₂O molecules and other gaseous coma species, to provide direct images of the comet for the encounter period which could be used for an analysis of the coma geometry and overall dust environment, and to collect information on the cometary ion tail. Because of the damage of two important onboard experiments (the Halley Multicolour Camera and the Neutral Mass Spectrometer) GIOTTO was unable to collect detailed data on the questions addressed by our observing programme.

In total 4 half nights (from 7/8 to 10/11 July 1992) at the ESO 3.6-m telescope and at the ESO 1.5-m spectroscopic telescope were devoted to observe comet P/Grigg-Skjellerup. Two evenings were lost due to clouds over La Silla. In the night July 9/10, 1992 some direct images could be obtained through cirrus clouds. Only the last night of July 10/11, 1992 gave reasonably good atmospheric conditions for our observations. However, the small elongation of the comet from the Sun (about 45 deg.) restricted the observing window to just 1 hour after evening twilight with the comet positioned low above the western horizon (below 25 deg. elevation). In fact, special precautions were needed to operate the 3.6-m telescope at such large zenith distances and even then guiding on the comet with non-siderial rate was not at optimum.

Comet P/Grigg-Skjellerup reached its perihelion of 0.99 AU on 22 July 1992. It was predicted to show a late onset of its nuclear activity and to exhibit a steep brightness increase (Green, 1991) before perihelion. Actually, it looks as if the comet only initiated significant coma development by the beginning of June 1992 (that was 1½ months later than expected) when it was already at a heliocentric distance of about 1.2 AU. However, the steepness of the light-curve was approximately as predicted (n of about 30 to 40). Before perihelion the total coma brightness was estimated to be about 1 mag fainter than the light-curve prediction published by Green (1991). At a wavelength of 620 nm the brightness of the comet in a square aperture of 20 arcsec was 15.5 mg on July 11, 1992.

In the night July 9/10, 1992, just 15 hours before the GIOTTO encounter with P/Grigg-Skjellerup, 4 broad-band R filter CCD images were obtained with the ESO 3.6-m telescope at La Silla through cirrus clouds low at the western horizon (below 20 deg. elevation). The images were processed at La Silla and immediately transmitted via satellite link to ESO-Garching. The co-added coma image of these exposures is shown in Figure 1. Thanks to the night work of people from the ESO Information Service and by staff at ESO-La Silla a hard-copy version of Figure 1 could be distri-

buted only 10 hours after the observations and about 5 hours before the encounter to the GIOTTO experimenters, to the scientists and to the press who were following the fly-by at the GIOTTO control centre, the European Space Operations Centre (ESOC), in Darmstadt/Germany (Jockers, 1992).

On the day of the GIOTTO encounter (see Figure 1) an ellipsoidal coma of about 30 × 20 arcsec apparent extension surrounded the central brightness condensation which contained the cometary nucleus. The major axis of the coma ellipsoid pointed towards position angle 130 deg. (counted east from north), i.e. about 15 deg. out of the anti-solar direction. Numerical simulations of the dust tail orientation for the encounter day support the interpretation of the elongated coma as being formed mainly by cometary dust particles. No indications of a plasma tail were detected in any of our exposures. This is partly caused by the moon-lit sky which does not allow to reach the low surface brightness of the plasma tail (a plasma tail was detected by GIOTTO) and also limits the extent of the visible coma. The radial renormalization method was applied to the superimposed CCD image of P/Grigg-Skjellerup of Figure 1. However, apart from the dust tail extension no further structure was found in the otherwise symmetric cometary coma. An analysis of the radial profile of the integrated coma brightness exhibited a rather linear increase with aperture diameter. Both phenomena (the elongated coma towards the dust tail direction and the radial coma brightness profile) support ideas that most of the light in the R filter exposures of July 9/10, 1992 arose from sunlight scattered by the dust. An analogous image processing of the R filter CCD observation of P/Grigg-Skjellerup obtained on June 29, 1992 at the ESO New Technology Telescope NTT (Storm and Meylan, 1992) has been performed by one of the authors and led to similar results as for our images of July 9/10, 1992.

In the night July 10/11, 1992 7 images (exposure time 30 s each) through a wide-band red filter (dust + NH₂) and 3 plasma filter exposures (10 minutes each, but trailed due to guiding problems) were obtained at the ESO 3.6-m

telescope. The photometric calibration and the analysis of these data is still in progress. While the cometary imaging continued at the 3.6-m telescope, 2 CCD spectra in the 370 to 1000 nm wavelength range were exposed on July 10/11, 1992 at the ESO 1.5-m spectroscopic telescope. The spectra show the strong emission band of CN at about 388 nm and also the C₂ emission around 517 nm. A weak dust continuum was found in the red part of the spectra. For the spectra the calibration and data analysis is presently performed.

ESO has also supported the fly-by targeting of the GIOTTO spacecraft by providing high-quality astrometric positions of the comet to ESO before encounter. The data were measured by Richard West from CCD frames obtained with La Silla telescopes. Post-fit residuals of 0.1 to 0.2 arcsec were derived for the ESO data from the comet orbit determination at ESOC Darmstadt. Astrometric positions of the comet were also determined from our CCD frames of July 9/10, 1992. These data were also transmitted to ESOC Darmstadt and can be used together with data from other observers for the post-encounter analysis of the GIOTTO fly-by trajectory at the comet.

The GIOTTO Fly-by at the Comet

On July 10, 1992 15:30:36 UTC* (± 46 sec) GIOTTO passed within about 200 km of the nucleus of comet P/Grigg-Skjellerup. During the P/Grigg-Skjellerup encounter GIOTTO was actually overtaken by the comet in its orbital motion around the Sun. At the same time it passed through the orbital plane of the comet from north to south. The relative velocity during the fly-by was about 14 km/s which was almost 5 times slower than during the Halley encounter in 1986. The heliocentric distance of the comet at encounter was 1.01 AU, the Earth distance 1.43 AU. GIOTTO approached the nucleus from 11 deg. behind the terminator. For on-board power reasons and because of communications constraints (the high-gain antenna needed to be kept Earth pointing) GIOTTO had to fly through the coma of comet P/Grigg-Skjellerup almost side-on with the solar cells fully exposed to the cometary dust and gas environment (at comet P/Halley the bumper shields of the spacecraft were front-on in order to protect the experiments and the other satellite hardware from damage by cometary particles).

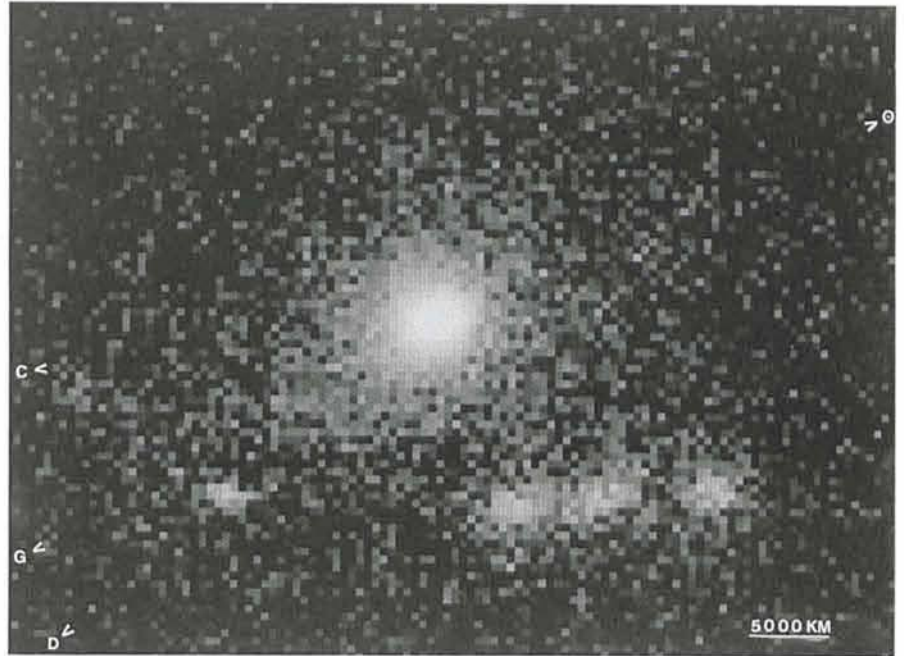


Figure 1: Comet P/Grigg-Skjellerup on July 10, 1992, just 15 hours before the GIOTTO encounter.

The image is a composite of 4 R filter exposures obtained at the ESO 3.6-m telescope. The field of view is about 70×50 arcsec ($73,000 \times 52,000$ km at the comet). North is up and east to the left. The Sun direction is indicated by symbol O, that of the dust tail by symbol D. The direction of the cometary motion on the sky is given by symbol V, that of the GIOTTO spacecraft by symbol G. The four trails in the lower image section are background stars.

Further details on the GIOTTO Extended Mission to comet P/Grigg-Skjellerup have been given in Schwehm et al. (1991). Spacecraft orbit and attitude aspects of the fly-by have been described by Morley (1991).

The payload was switched on in the evening of July 9, 1992. 7 out of the original complement of 11 on-board experiments were operated during the encounter: the Magnetometer (MAG), the Johnstone Plasma Analyser (JPA), the Energetic Particle Analyser (EPA), the Optical Probe Experiment (OPE), the Reme Plasma Analyser (RPA), the Dust Impact Detection System (DID), the Ion Mass Spectrometer (IMS). In addition, the signals from the spacecraft were analysed for perturbations by members of the GIOTTO Radio Science Experiment (GRE) team.

At about 600,000 km from the nucleus (12 hours before closest approach), JPA detected the first presence of cometary ions. At a distance of 18,000–15,000 km both JPA and RPA reported what looked like a bow shock or a bow wave of the coma, much more distinct than had been predicted for such a faint comet. MAG measurements carried out during the inbound trajectory could not confirm this finding, but reported interesting wave phenomena not seen in a natural plasma before. However, on the outbound trajectory MAG saw clear indications of a shock.

OPE started to detect emissions from the gas coma about 50,000 km from the nucleus. The first indication of entering the dust coma occurred around 20,000 km from the nucleus (at about the same distance as the dust coma extent in our ground-based observations). Data from OPE provided the first estimate of the spacecraft-nucleus distance at closest approach. A value of approximately 200 km was derived. In combination with the MAG data, there is good evidence that GIOTTO passed the nucleus on the anti-sunward side, i.e. through the tail forming region of the coma. The data from OPE also suggested that closest approach occurred a few seconds after the nominal predictions.

DID reported its first impact at 15:30:56 UTC – probably after closest approach. A total of three impacts were recorded, the first being the largest. It is conceivable that the impacts occurred when GIOTTO crossed the orbital plane of the comet.

At 15:31:02 UTC, shortly after the first impact, the High-Gain Antenna of GIOTTO appeared to be oscillating slightly around its nominal value. An increase of the spin rate by 0.003 RPM was also observed while the solar aspect angle readings were fluctuating between 89.26 and 89.45 deg., indicating a nutation of about 0.1 deg. This was also recorded by the GRE and is awaiting further evaluation.

* All times in this section are station-receive times of the GIOTTO signals in UTC. The time for signals to reach Earth from GIOTTO at the time of the encounter was 11 minutes 52.6 seconds.

EPA saw clear indications of the acceleration regions and surprising differences in the structures between P/Halley and P/Grigg-Skjellerup. Last but not least IMS recorded good data; however, the data analysis for this instrument is quite cumbersome and complex, due to the comparatively low encounter velocity.

A thorough test of the Halley Multicolour Camera (HMC) onboard GIOTTO on 7 July 1992 could only confirm that the optical path was very effectively blocked. However, on July 12, 1992 a number of tests were performed with the detectors of the MMC, which provided engineering and calibration data on the long-term behaviour of CCD's in space.

The Future of GIOTTO

About one week later than previously planned, on July 21, 1992, another major orbit manoeuvre put the spacecraft into an orbit that will bring it close to Earth (distance about 200,000 km) in July 1999. There are still 4 kg of fuel left onboard for attitude and further orbit correction manoeuvres. This leaves, though with rather hard constraints, the door open for some further activities in 1999. After a final orbit trim manoeuvre on July 23, 1992 at 17:07 UTC the GIOTTO spacecraft was put into hibernation for the third time.

Meanwhile, spacecraft experimenters and telescope observers have started the scientific evaluation of their data, which may still hold surprises. The next space exploration of comets, after cancellation of the American CRAF (Comet Rendezvous Asteroid Flyby) project will be ESA's ROSETTA mission which is supposed to bring a cometary sample back to Earth. It will take place in the next century. Meanwhile, cometary exploration will continue from the ground and we expect that, together with other branches of astronomy, it will profit from ESO's progress in telescope technology.

Acknowledgement

The authors like to thank very much the staff at ESO-La Silla and at ESO-Garching who supported – partly in night work – the fast data transmission and hardcopy production of our P/Grigg-Skjellerup observations on the encounter day. We would also like to acknowledge the help of Richard West from ESO-Garching in obtaining the astrometric positions of the comet from our CCD frames.

References

- K. Birkle, H. Boehnhardt: 1992, *Earth, Moon and Planets* **57**, 191.
D.W.E. Green: 1991, *International Comet Quarterly* **13**, 91.
K. Jockers: 1992, ESO Press Photo 06/92.
T. Morley: 1991, Proceedings of the 3rd International Symposium on Spacecraft Flight Dynamics, ESA SP-326, 487.

- D.J. Osip, D.G. Schleicher, R.L. Millis: 1992, *Icarus*, in press.
H.U. Schmidt, R. Wegmann, D.C. Boice, W.F. Huebner: 1992, MPA 670.
G. Schwehm, T. Morley, H. Boehnhardt: 1991, *The Messenger* **65**, 37.
J. Storm, G. Meylan: 1992, ESO Press Photo 05/92.

A Minor Planet with a Tail!

R. WEST, H.-H. HEYER and J. QUEBATTE, ESO

Minor Planet 1979 VA was discovered by Eleanor Helin at Palomar on November 15, 1979 as a "fast-moving object" of magnitude 11 (IAC 3422). Further observations were made, and when a reasonably accurate orbit became available, it was found that 1979 VA belonged to the select "Apollo" class of Earth-crossing minor planets. Its perihelion was just inside the Earth orbit, at 0.98 AU, and it had passed within 0.1 AU, or less than 15 million km, of the Earth in late October 1979. The eccentricity was rather large, 0.63, and the orbit was therefore very elongated; the period was somewhat over 4 years.

After more observations had become available in the 1980's, 1979 VA was duly assigned the definitive number 4015, but it has not yet received an official name.

Nothing very exciting about that. But this August, Minor Planet (4015) suddenly became an object of intense interest among solar system astronomers!

The Palomar 1949 Observations

Extrapolating the motion of (4015) backwards in time in the hope of finding earlier recorded images of this object, Ted Bowell of the Lowell Observatory at Flagstaff, Arizona, USA, found that it should be visible on a pair of plates, obtained with the 48-inch Palomar Schmidt telescope for the first Palomar Sky Survey on November 19, 1949. These plates were some of the first obtained with this telescope, red-sensitive no. 9 (45 min; 103a-E + a red plexiglass filter) and blue-sensitive no. 10 (12 min; unfiltered 103a-O).

The image of (4015) was easy to find, but Bowell and his colleagues were most surprised to discover that it did not look like a normal minor planet trail – it had a tail!

When a hint was passed to Brian Marsden at the Minor Planet Center

(Center for Astrophysics, Cambridge, Mass., USA) that the earlier images were "unusual", he immediately recalled that an object on the Nov. 19 Palomar plates had already been catalogued in 1949 as Comet Wilson-Harrington (1949 III). There was also the strange circumstance, however, that this comet was described as having a point-like appearance on plates obtained the following nights.

So here was an object that was a seemingly normal minor planet in 1979 and thereafter, but which looked like a comet on a pair of plates in 1949. How could this be explained? Were the tails perhaps some kind of plate fault, or was this a real effect?

Brian Marsden asked about our opinion and we decided to have a very careful look at the glass copies of the POSS I Atlas plates, stored in the vault at the ESO Headquarters in Garching.

Our first conclusion was that the "tails" are unlikely to be photographic faults. Although a great variety of artificial dots, lines, etc. is often found on the very sensitive emulsions used in astronomy – the first Palomar Atlas contains many so-called "Kodak stars" – the emulsion structure around the "tail" is uniform on both plates and does not indicate any artificial origin. It is of course true that we were only able to study second-generation copies of the original plates in the plate vault at Caltech in Pasadena, but from our experience with many thousand Schmidt plates over the years, this conclusion still seems quite safe.

The tail is rather weak, especially on the red plate, and we therefore photographically enhanced the two Palomar plates in order to see the structure more clearly. The amplified images are reproduced in Figure 1a and 1b. There is no doubt that on both plates, the "tail" has the normal appearance of a cometary tail. It extends only to one side of the trail, is attached to the trail over the full

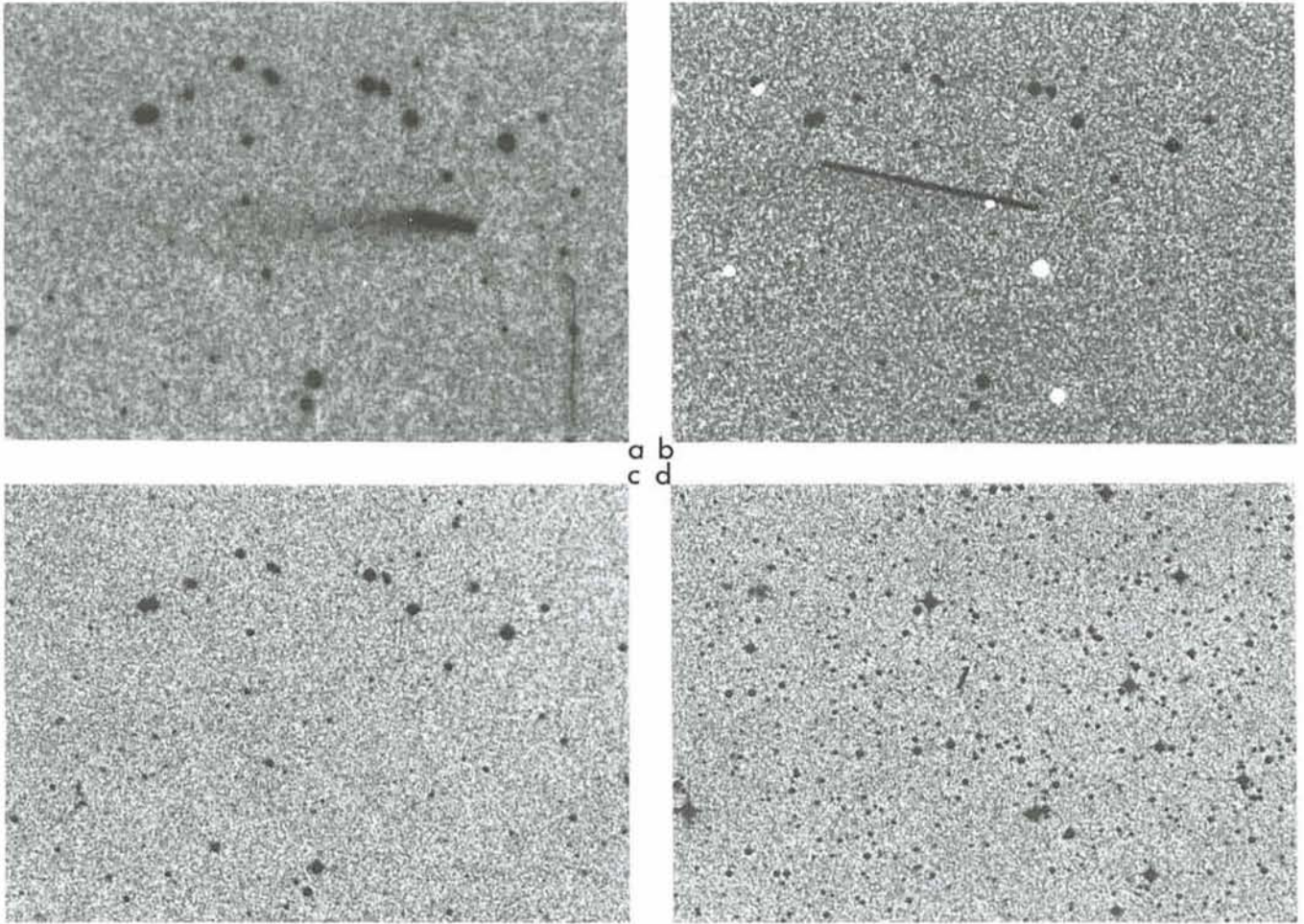


Figure 1: These photographically enhanced photos show Minor Planet (4015) = Comet Wilson-Harrington on (a) a blue- (12 min) and (b) a red-sensitive (45 min) plate, obtained on November 19, 1949, with the 48-inch Schmidt telescope at Palomar. The tail is well visible below and to the left of the trail. The vertical line in the lower right corner of (a) is an emulsion fault. In (c), the same sky field is shown on a recent plate obtained with the same telescope for the POSS II; there is no diffuse object in the field. In (d), a 1979 image of minor planet (4015) from a plate obtained with the 48-inch UK Schmidt telescope demonstrates the sharpness of the short trail (at the centre) – there is absolutely no tail visible. On (a) and (b), the distance from the Earth and the Sun was 34 million km and 172 million km, respectively; on (d) the corresponding distances were 58 million and 178 million km. The object appears brighter in 1949 (a, b) than in 1979 (d), partly because it was closer to the Earth, but most probably also because it was at that time surrounded by a small dust cloud.

All photos are reproduced at the same scale, approximately 6.5 arcsec/mm; north is up and east is to the left.

The photo was prepared at ESO from the Palomar Observatory Sky Surveys I and II and the ESO/SERC Survey of the Southern Sky (©California Institute of Technology (c) and UK Science and Engineering Research Council (SERC) (d)).

length, does not extend beyond the trail ends and has the same general direction on the two plates. In other words, the tail really “moves” with the object and it is therefore very unlikely to be a ghost reflection from a bright star in the field. Moreover, a look at the same sky field on the J plate (Figure 1c), recently obtained for the POSS II survey (which is now being reproduced at ESO) shows that there are no nebulae or galaxies in this area which might simulate a comet tail.

It is also important to note that the weakness of the tail on the red plate does not necessarily mean that the tail consists of gas only. Even dust tails which shine by reflected sunlight, and which are generally redder than gas tails, are normally weaker on red than on blue photographic Survey plates be-

cause of the different emulsion sensitivity. It is for this reason that comets are much easier to discover on blue-sensitive plates; that is also why very few comets were found on the ESO(R) survey. This does not apply to comet observations with CCDs, since these detectors are more sensitive in the red spectral region.

So we are convinced that minor planet (4015) really had a dust tail in 1949.

Minor Planet/Comet Interrelations

Until now, the object (4015) had fulfilled all requirements for classification as a minor planet; its trail (Figure 1d) was perfectly sharp, without any hint of a coma or a tail. But the 1949 observa-

tion proves that it must at least once have had an outburst of some kind, giving it the (temporary) appearance of a perfectly normal comet. So what is it really, a minor planet or a comet?

Possibly both. There has recently been a growing interest in studying the relationship between these two types of solar system objects and various evidence for interrelation has become available during the recent years. For example, minor planet (2060) Chiron, in a 50-year orbit between Saturn and Uranus, developed a large coma in 1988 on its way towards perihelion in 1996. Earlier this year, another minor planet with an even larger comet-like orbit was found and was provisionally designated as 1992 AD (cf. *The Messenger* 67, p. 34, March 1992). It has in the meantime received the number (5145) and

the name Pholus (another Centaur), but contrary to Chiron, Pholus has not shown any activity (yet).

Other minor planets are known to move in highly eccentric comet-like orbits much nearer the Sun. One of them, (3200) Phaeton (discovered by IRAS in 1983 and designated 1983 TB), moves in the same orbit as the Geminid meteor stream. It seems that it is the parent body of the material in this stream. This is strange, because only a comet, and not a solid minor planet, is thought to be able to disperse dust along its orbit.

Several comets in well-known orbits have been found to disappear from view, probably because their source of volatiles is exhausted. One of the most well-documented cases is that of Biela's

comet, first discovered in 1826. It was seen to split into two pieces in 1846, it faded in 1852 and was not seen at all at its predicted return in 1866. When no more ice is available on the surface of the nucleus of a comet, or if the Sun's heat can no longer penetrate through the insulating surface to the reservoirs of ice that may still be present inside the nucleus, no coma and tail will develop. The comet will have become "inactive" and its small nucleus will only shine by reflected sunlight. This implies that it will be very faint and its image, if observable at all, will from then on be indistinguishable from that of a minor planet. This type of object is appropriately referred to as a "dead" or "dormant" comet.

It is widely believed that at least some of the minor planets, now in comet-like

orbits in the inner solar system, are in fact dead comets. It may well be that we actually witnessed the death throes of comet 1949 III, and that its inactive nucleus was "re-discovered" in 1979 as minor planet 1979 VA. It is the first direct observation of this kind and it will surely stimulate much activity in this interesting research field.

Minor planet (4015) again passed through its perihelion in late August 1992. There is little doubt that it will be extensively observed during the coming months. Unfortunately, it will be located in the northern sky and will not be easily accessible from La Silla. Initial observations (IAUC 5585 and 5586, August 14, 1992) have not revealed any signs of activity whatsoever.

A Very Low Resolution Spectrophotometric Nova Survey

A. BIANCHINI, *Dipartimento di Astronomia, Università di Padova, Italy*

M. DELLA VALLE, *ESO*

H. W. DUERBECK, *Astronomisches Institut der Westfälischen Wilhelms-Universität, Münster, Germany*

M. ORIO, *Osservatorio Astronomico di Torino, Italy*

The Aims of the Survey

A very low resolution spectrophotometric survey of classical novae at minimum is of great interest for a more thorough understanding of these objects. As it was stressed in a previous account (Bianchini et al., 1991), up to now only Williams (1983) studied a number of spectra of old novae. There is therefore a strong need of a systematic study of the post-outburst spectra of a large number of these objects, in order to be able to derive statistical conclusions.

With very low resolution spectroscopy we can cover a wide wavelength range for many novae at minimum, obtaining a statistically meaningful sample, and detect the following features:

- the slope of the continuum;
- the ratios of the intensities of different emission lines of H, HeI and HeII, all meaningful to understand the accretion mechanisms;
- the presence of a nebular spectrum if this still exists;
- sometimes the spectrum of the secondary;
- the possible discovery of peculiar variabilities (see Bianchini et al., 1991).

Since we are engaged also in the systematic study of novae at minimum in other wavelength ranges, especially UV and X (Bianchini et al. 1991, Orio et al. 1992), this survey in the optical range becomes an important tool when the level of the continua is correlated with that in UV and IR or certain details of the optical spectra are used to understand the mechanisms of X-ray emission (the typical example is the HeII $\lambda 4686$ line, which has been shown by Patterson and Raymond (1984) to be the result of reprocessed soft X-ray emission for high accretion rates). Moreover, many objects were poorly studied at maximum and their classification is uncertain. Using the ESO 1.5-m telescope, we are able to distinguish between the spectrum of an old nova and that of a symbiotic star or a red variable up to $M_V = 20$; a proposed classification as dwarf nova (with long cycle length) instead of classical nova can be rejected on the basis of a strong $\lambda 4686$ HeII emission line, which is typical only of classical novae or magnetic CV's and is an indicator of accretion rates $\dot{m} > 10^{16} \text{ g s}^{-1}$ (Patterson and Raymond 1984).

A systematic study of classical novae at minimum is therefore extremely im-

portant to understand the physical mechanisms powering novae and the nature of the different systems.

First Results

The spectral atlas we are building consists already of 50 different objects, all observed in the range $\lambda 3000-9000 \text{ \AA}$. In three observing runs at the ESO 1.5-m telescope (February 1991, December 1991, July 1992) we have been able to study 31 novae using a CCD detector and the Boller & Chivens spectrograph. In addition there are spectra of 23 objects taken by Duerbeck in the years 1986-1988 with the same telescope and B & C spectrograph; the majority was observed with the somewhat ageing image dissector scanner (IDS) instead with a CCD, resulting in a poorer S/N and a lower spectral resolution. However, these observations are useful in order to establish secular trends in the data - e.g. declining continuum fluxes and decreasing strengths of He II emission. Such findings are useful to find indications for a secular decrease in the accretion rate, which is postulated by the hibernation hypothesis (Priainik and Shara 1986, Shara et al. 1986). Accord-

Table 1

Nova	Year	Mag _v (observed)	Run	Classification
CI Aql	1925	15–16	1, 4	(new)
DO Aql	1925	18.5	1, 4	(new) DN?
V356 Aql	1936	17.8	1	
V368 Aql	1936	17.3	1	
V603 Aql	1918	11.8	1	
VY Aqr	DN	17.0	1, 4	DN
QY Ara	1910	18.5	1, 2	(new)
T Aur	1891	15.9	1	
CG CMa	1934	16.5	1, 2, 3	(new)
V411 Car	1953	17.5	2	
V812 Cen	1973	19	1	(new)
V840 Cen	1986	15.0	1, 2, 4	Symb
V842 Cen	1986	14.4	1	
WX Cet	DN	17.0	1, 3	DN
AR Cir	1906	14.2	2	star close to 18-mag old-nova
V655 CrA	1967	15.7–16.2	1, 4	(new)
HR Del	1967	12.6	1	
DM Gem	1903	17.0	2	(new)
nova Her	1991	18.9	4	
GW Lib	1983	16.6	1	DN?
BT Mon	1939	17.0	1, 3	
GI Mon	1918	16.2	1, 2	(new)
V616 Mon	RN	16.5–17	2, 3	stronger variability in the red
GQ Mus	1983	16.5	1, 2	
IL Nor	1983	17.4	1	(new)
RS Oph	RN	10.9	1, 4	
V841 Oph	1848	13.5	1	
V849 Oph	1919	18	1	
V942 Oph	1957	16.6	1, 4	(new), red variable?
BD Pav	1934	15.2	1, 4	DN?
RR Pic	1925	12.2	1, 2	
CP Pup	1942	15.1	1, 3	
HS Pup	1963	18	2, 3	(new)
HZ Pup	1963	17.4	1, 2	(new)
nova Pup	1673	19.5	2, 3	not yet confirmed
T Pyx	RN	15.5	1, 2, 3	
SS Sge	1926	17.8	1	Symb?
BS Sgr	1917	15.4	1	
GR Sgr	1924	16.5	1	Symb?
HS Sgr	1900	17	4	(new)
V522 Sgr	1931	16.8	1, 4	
V999 Sgr	1910	16.6	1	
V1017 Sgr	1919	13.7	1	
V1059 Sgr	1898	17.5	1	
V697 Sco	1941	19	4	(new)
EU Sct	1949	19.5	1	
GL Sct	1925	16.1	1	(new), uncertain
nova Sct	1938	14.0	4	(new), not a nova
V427 Sct	1958	16.7	1, 4	Mira
X Ser	1903	15.2	1	
FH Ser	1970	17–18	1, 4	
XX Tau	1927	18.5	2, 3	
RR Tel	1908	16	1, 4	Symb
DC Vel	1905	17.2–18.4	1, 2, 3	(new)

(new) = observed for the first time / Symb = Symbiotic Star / DN = Dwarf Nova
1 = First survey by Duerbeck, 1986–1988 / 2 = February 18–22, 1991 / 3 = December 1–5, 1991 / 4 = July 4–7, 1992

ing to this, novae should decrease in brightness and accretion rate in the centuries after outburst, and “hibernate” for several millennia before they experience another nova outburst.

All the observed objects have been localized using the finding charts provided by Duerbeck (1987). Table 1 lists (a) the name of the novae, (b) the year of

their outbursts, (c) an estimate of the observed visual magnitude, (d) the observing runs, and (e) comments and the proposed classification for those objects for which the identification as a nova cannot be confirmed on the basis of our spectra. Unfortunately this is the case for the oldest objects of our sample, N Pup 1673, which we were able to

detect at $V = 20$, but for which no emission lines or other peculiarities could be detected. The identification is thus not yet clear, and the use of this object for a proof of the validity of the hibernation scenario is still not yet possible.

Objects like V840 Cen or BS Sgr appear like symbiotics, quite alike the famous RR Tel, a symbiotic nova that erupted in the late 1940s.

We also started analysing the possible correlation between the type of nova and the intensity of the $\lambda 4686$ He II emission line relative to H α or H β . The correlation of the intensity of the He II line with the level of soft X-rays is undoubtedly confirmed: all the objects that were detected during the *Rosat* All-Sky Survey that appear in our sample, show a very intense $\lambda 4686$ in emission: RR Tel, GQ Mus, CP Pup, V603 Aql, V841 Oph, N Her 1991 (see Orío et al., 1992, Lloyd et al., 1991). The correlation with the type of nova is, however, less clear. Other objects with a strong He II feature are DO Aql, the DQ Her type nova T Aur, the moderately fast nova HZ Pup and the fast nova GI Mon. Finally, also the recurrent nova T Pyx has a strong He II $\lambda 4686$ line, perhaps favouring the interpretation of the outburst as a thermonuclear runaway.

An Example: Detection of a Puzzling (and Important) Variability

An example of variability of a nova during the survey is reported in Bianchini et al., 1991. As another example of the use of such a systematic survey we shall bring now the spectrum of an object that is not a classical nova, but was included in our survey because of its relationship with classical novae and its puzzling, interesting nature: the X-ray nova and black hole candidate V616 Mon, or A0620-00 (McClintock et al., 1987). It is the prototype of what seems a spectacular class with at least three more members: GS2023+338 = V404 Cyg, GS 1124-68 = N Mus 1991, and GS 2000+25. During its outburst of 1975, detected by *Ariel V* and followed by SAS-3, it was the brightest X-ray source in the sky with a peak X-ray luminosity $L_x \geq 10^{38}$ erg s $^{-1}$ in the range 1-18 KeV, after a rise time of about 10 days. The determination of the position with a precision of 1 arcsec by SAS-3 allowed Boley et al. (1976), to identify it with a source in outburst again in the optical in 1975 after a previous eruption in 1917. The amplitude, $\Delta M = 8$ mag, and the decline in optical light in about 15 months, resembled the behaviour of classical novae. The spectrum, however, without absorption lines, did not

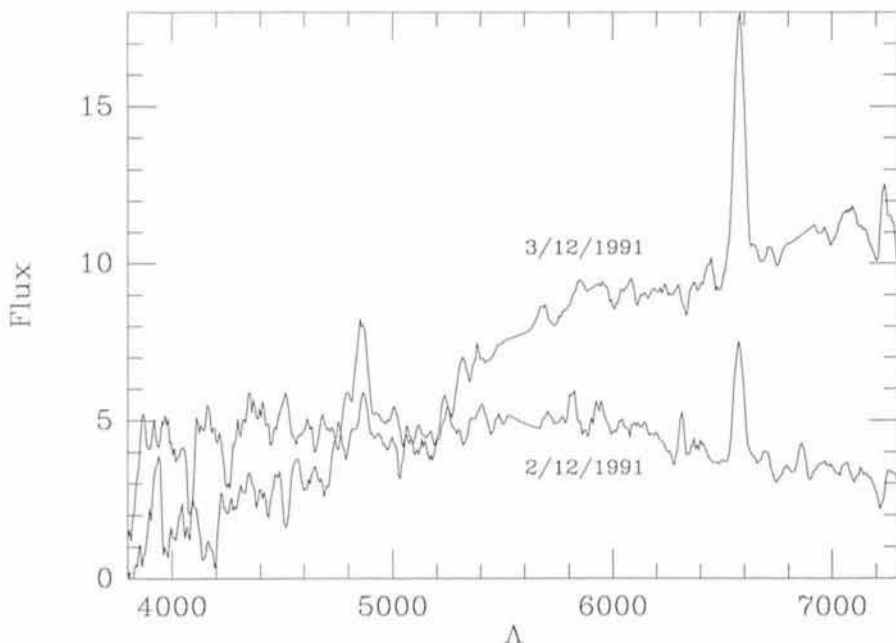


Figure 1: Two spectra of V616 Mon (A0620-00) taken in December 1991. Fluxes in $10^{-14} \text{ erg cm}^{-2} \text{ sec}^{-1} \text{ \AA}^{-1}$.

resemble a classical or recurrent nova: the only feature was the late appearance of emission lines quite like those of dwarf novae (Duerbeck 1977). Modelling the physical mechanism powering the outburst of A620-00 and its associate sources has always appeared a challenge because there are problems both with mass overflow instability models implying X-ray heating of the secondary by the compact object (Hameury et al., 1986, 1990), and with disk instability models (Mineshige and Wheeler, 1989, Huang and Wheeler, 1989, Mineshige et al., 1991) that need a higher mass transfer rate to work than the one inferred by Fu and Taam (1989). For a detailed discussion see Haswell, 1992.

Two spectra were obtained on February 18 and 19, 1991, three on December 2, 3 and 4, 1991, and two more at an interval of a few hours on December 5, 1991. Although the two spectra of February are alike and their slope and characteristics appear to match those of Haswell of November 1987 (see Haswell, 1992), the spectrum of December 2 shows that the flux in the red can decrease significantly and re-increase on a time scale of one day (see Fig. 1, where the two spectra were taken at the same orbital phase). On December 5, the decrease of the red flux occurred again, but a second spectrum reappeared "normal" again after a few hours. The luminosity fluctuations in the red region of the spectrum were up to 1 mag (larger amplitude at longer wavelengths?) and the slope of the continuum totally changed (see Fig. 1). Such sudden, irregular variations in the flux and in the slope of the continuum

were never noticed before and they were not correlated with the orbital phase. An explanation for the phenomenon could be a sudden variation in the mass transfer rate, causing a shrinking of the disk that appears bluer, but less luminous. However, the contribution of the disk to the total flux does not seem to exceed 15% in any band (Haswell, 1992). These results appear therefore very puzzling and they should be connected also with the secondary star, which must have undergone some kind of instability. For better understanding it is undoubtedly necessary to study possible new spectral variations, monitoring the object regularly. This could offer a key to understanding the complex phenomena that are happening and the mechanism that powers the outbursts, because it is crucial for any model to know if and how there is variability of the mass transfer rate and what is the nature of the disk.

Such serendipitous discoveries of variability, already known not to be infrequent for certain symbiotics and X-ray binaries, can be detected also for classical novae during a survey of this kind and certainly be meaningful to understand the nature of the systems.

References

- Bianchini, A., Della Valle, M., Orio, M., Ögelman, H., Bianchi, L., 1991 *The Messenger* No. 64, 32.
 Boley, F., Wolfson, R., Bradt, H., Doxsey, R., Jernigan, G., Hiltner, W.A., 1976, *Ap.J.*, 203, L13.
 Duerbeck, H.W., 1977 in *Novae and Related Stars*, ed. M. Friedjung, Dordrecht: Reidel, p. 150.

- Duerbeck, H.W., 1987, *Space Sci. Rev.*, 45, 1.
 Fu, A., Taam, R., 1989, *Ap.J.*, 349, 553.
 Hameury, J.M., King, A.R., Lasota, J.P., 1986, *Ap.J.*, 353, 85871.
 Haswell, C.A., 1992, Ph. D. Thesis at the University of Texas at Austin.
 Huang, M., Wheeler, J.C., 1989, *Ap.J.*, 343, 229.
 Lloyd, H.M., O'Brien, T.J., Bode, M.F., Predehl, P., Schmitt, J.H.M.M., Trümper J., Watson, M.G., Pounds, K.A., 1991, *Nature*, 356, 222.
 McClintock, J.E., Remillard, R.A., 1986, *Astrophys. J.*, 308, 110.
 Mineshige, S., Wheeler, J.C., 1989, *Ap.J.*, 343, 241.
 Mineshige, S., Kim, S.W., Wheeler, J.C., 1990, *Ap.J.*, 358, L5.
 Orio, M., Ögelman, H., Pietsch, W., Bianchini, A., Della Valle, M., Krautter, J., Starrfield, S., contributed paper to the Cospar Meeting, Washington, September 1992.
 Patterson, J., Raymond, J.C., 1984, *Ap.J.*, 292, 550.
 Prialnik, D., Shara, M.M., 1986, *Ap.J.*, 311, 172.
 Shara, M.M., Livio, M., Moffat, A.F.J., Orio, M., 1986, *Ap.J.*, 311, 163.
 Williams, G., 1983, *Ap.J. Suppl. Ser.*, 53, 523.

STAFF MOVEMENTS

Arrivals

Europe

- BEDDING, Timothy (AUS/GB), Fellow
 CONZELMANN, Ralf (D), Designer-Draughtsman (Mechanics)
 HAINAUT, Olivier (B), Student
 KJELDSEN, Hans (DK), Fellow
 RASMUSSEN, Bo (DK), Technician (Software)
 RODRIGUEZ ULLOA, Jesus (E), Operation Technician (Remote Control Equipment)

Transfers

- ALLAERT, Eric (B), Engineer (Software) (from La Silla to Garching)

Departures

Europe

- LIU, Xiaowei (RC), Associate
 MAZZALI, Paolo (I), Fellow
 PRAT, Serge (F), Mechanical-Project Engineer
 STEFL, Stanislav (CS), Associate
 VAN MOORSEL, Gustaaf (NL), Scientific Programmer/Analyst
 WARREN, Stephen (GB), Fellow
 ZEILINGER, Werner (A), Fellow

Erratum (*Messenger* 68, p. 2, June 1992)

The 6.5-m MMT mentioned in the list of large telescope projects is of course located on Mt. Hopkins, not on Mt. Graham.

Observation of the Central Part of the β Pictoris Disk with an Anti-Blooming CCD

A. VIDAL-MADJAR, A. LECAVELIER DES ETANGS-LEVALLOIS, G. PERRIN, R. FERLET,
F. SÈVRE, Institut d'Astrophysique, CNRS, Paris, France

F. COLAS, J.-E. ARLOT, Bureau des Longitudes, CNRS, Paris, France

C. BUIL, CNES, Toulouse, France

H. BEUST, Service d'Astrophysique, Saclay, France

A.-M. LAGRANGE-HENRI, Observatoire de Grenoble, France

J. LECACHEUX, Observatoire de Paris, Meudon, France

1. The β Pictoris Disk

Since the discovery with the IRAS Satellite of a number of main-sequence stars which show an infrared excess, direct imaging has proved, in the only case of the southern A5-type star β Pictoris, that this excess is caused by a disk of dust surrounding the star (Smith and Terrile, 1984). The favourable orientation of the disk, viewed nearly edge-on from Earth, has permitted the further detection of its gaseous counterpart, with a typical density $n(\text{H}) \sim 10^5 \text{cm}^{-3}$ (Hobbs et al., 1985; Kondo and Bruhweiler, 1985; Vidal-Madjar et al., 1986). Subsequent observations have emphasized the complex time variations of the circumstellar (CS) lines, both in the visible and the UV (Ferlet, Hobbs and Vidal-Madjar, 1987; Lagrange, Ferlet and Vidal-Madjar, 1987).

In order to interpret the extensive data set gathered on the β Pictoris proto-planetary system, we have proposed a model in which the sporadic redshifted events are the result of the evaporation in the vicinity of the star of solid comet-like bodies falling into the star (La-

grange-Henri, Vidal-Madjar and Ferlet, 1988; Beust et al., 1989). Numerical simulations of infalling bodies which evaporate when grazing the star are able to reproduce the observational data and provide constraints on the bodies' nearly parabolic orbits: for instance, a specific direction of the orbit's axis with respect to the line of sight is required, along with close perihelia ≥ 10 stellar radii. We then came to the conclusion that the numerous events seen could be due to the presence of a giant planet (or proto-planet) in the β Pictoris disk which perturbs a lot of small passing-by objects and throws some of them towards the star (see e.g. Beust, Vidal-Madjar and Ferlet, 1991, and references therein), thus possibly clearing up the inner part of the disk.

From their coronagraphic study, Smith and Terrile (1984) have shown that an $r^{-4.3}$ power law was well representing the dust distribution within the disk. However, at less than 6 arcsec from the star (100 AU), i.e. behind the coronagraphic mask, they showed that if this law was extrapolated to less than 30 AU, a too strong extinction of the

direct starlight (passing through the edge-on disk) would result. Therefore, they claimed that a cleared-up region was probably present within 30 AU from the star, possibly due to planetary formation. Later on, Diner and Appleby (1986), using the same coronagraphic data but coupled with the IRAS observations, produced a disk model coherent with both dust scattering and emissivity, and found that within 100 AU no strong constraint was present in the data: dust distributions presenting very small cleared-out inner regions were certainly acceptable. This is due to the fact that, similarly to the coronagraphic observations, the low resolution IRAS data are sensitive to relatively cool (outer and extended) dust. Then, Artymowicz, Burrows and Paresce (1989), using new coronagraphic data (Paresce and Burrows, 1987) still limited to more than 6 arcsec from the star, along with the IRAS data, confirmed the radial power law (although slightly less steep, in $r^{-3.6}$) and the Diner and Appleby (1986) conclusions, i.e. a 5 to 15 AU cleared inner region is compatible with the observations.

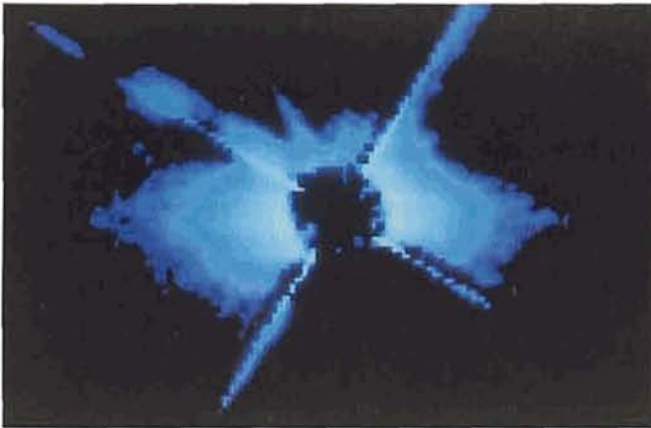


Figure 1a: 20-sec exposure (V filter) of β Pictoris corrected for the diffuse light level by the use of a template star (see text). The bright spikes due to the secondary spider cannot be completely corrected, but do not perturb disk brightness evaluations due to their angular separation.

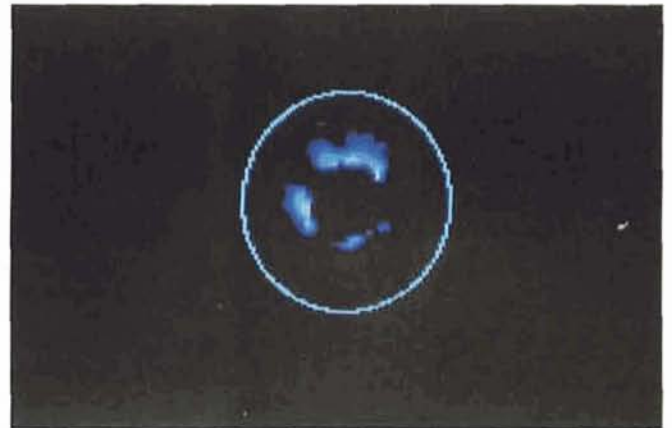


Figure 1b: Same correction made on another star (with similar light levels) obviously shows no circumstellar disk. A 6-arcsec-radius circle is drawn around the star to visualize the limit of previous coronagraphic observations.

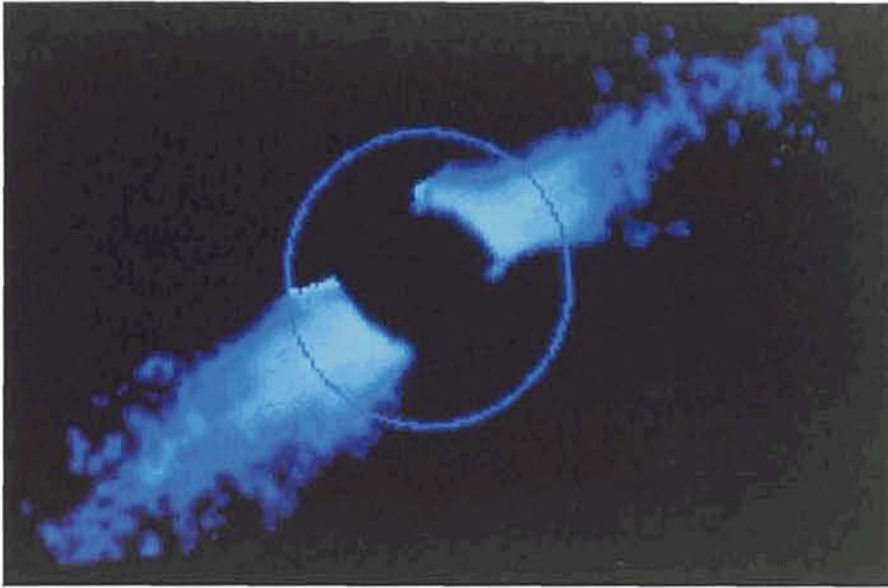


Figure 2: The β Pictoris disk image without the spikes, radially flattened to strengthen the weakest parts of the disk. North is up. A 6-arcsec-radius circle is drawn. This disk is clearly seen down to 2.5 arcsec from the star. Shorter exposures reveal the disk down to 2 arcsec (30 AU).

Simultaneously, Telesco et al. (1988), completing 10 and 20 μ ground-based observations with 5 arcsec resolution, were able to constrain more strongly the different models: the β Pictoris inner disk is relatively clear of dust, possibly up to 50 AU (3 arcsec from the star). However, more recent observations from 8 to 12 μ by Telesco and Knacke (1991) led to a possible detection of a spectral signature related to silicates, but only seen within 3 arcsec from the star.

From all these observations, it is plausible to assume that a dust-free zone exists in the inner regions of the β Pictoris disk.

Observations with an Anti-Blooming CCD

To observe the disk closer to the star, we decided to use an anti-blooming CCD (THX 7852), instead of a classical one associated to a coronagraphic approach. In effect, all the observations published with coronagraphs give very good results far from the star (Smith and Terrile, 1984; Paresce and Burrows, 1987), but fail close to it, the limit being around 6 arcseconds. The difficulty to get closer is due to the diffuse light around the mask which is extremely sensitive to the star position behind the mask, a position difficult to control without any adaptive optical device. Fluctuations producing unrepeatably changes of diffuse light levels around the mask make difficult to achieve quantifiable observations with such techniques very close to the star.

On the contrary, the use of an anti-blooming CCD which avoids the contamination of pixels adjacent to saturated ones, allows the direct observation of the disk next to the star without the use of any coronagraph. Stellar light simply saturates some pixels while the nearby ones collect charges related to the light coming from the vicinity of the star. This technique was well developed in planetary studies by Colas (1991), and led to the detection of very faint satellites ($V \sim 16$) near the giant planets.

The size of the stellar image is thus simply defined by the seeing and the exposure time. Typical values are between one and two arcseconds, representing roughly the limit of that observational approach. Use of adaptive optics could further reduce the effect of the seeing, and observations of the disk at less than one arcsecond from the star should become possible. The limitation is then only due to the diffuse light characteristics in the telescope, produced by both the cleanliness of the mirrors and the induced diffraction pattern.

The recorded images with such a CCD must be simply centred on the stellar images in order to give the possibility to either add them and improve S/N by selecting sharp images (always corresponding to shorter exposures), or correct for the diffuse light effect within the telescope by subtracting the properly centred images of a template star which was in our case the nearby star α Pictoris.

The observations were performed in October 1991, at the 2.2-m Telescope

at La Silla. To probe the disk at different distances, series of images were taken with exposure times ranging from 0.5 s (to see as close as possible to the star) to 300 s (to detect the disk as far as possible and have an overlap with the previous coronagraphic images). This has been done with the four standard filters: B (440 nm), V (550 nm), R (700 nm) and Ic (800 nm). More than 450 CCD images were taken, and an average of 10 was gathered for each filter and exposure time. Additional exposures were recorded with different angular position of the bonette in order to test the effect of the CCD orientation relative to the disk. No changes were observed.

Data Analysis

After the classical bias and flat fielding corrections of the CCD frames (see e.g. Buil, 1989), one of the difficulties was to properly correct for the diffuse light level by using the template star, observed almost simultaneously with the same instrument setting. This correction was done by scaling properly the diffuse light level of one star relative to the other in the two quadrants where the disk is not observed. This is not a simple linear correction. The radial variation of the correction factor was evaluated assuming, in a first approximation, that the diffuse light (away from the obvious spikes due to the telescope spider) presents a circular symmetry.

The result is shown in Figure 1a, in which the image was rotated in order to have the disk horizontal. The disk detection is obvious, particularly when comparing with Figure 1b in which the same correction was applied to another template star with no disk at all, and in which all light levels are at most equal to 10% of the ones in Figure 1a, at similar angular distances from the central stars. It is also very clear in Figure 1 that the correction process is unable to perfectly eliminate the very bright spikes in the case of β Pictoris because they are partly due to scattered light from the disk itself.

The final image of the β Pictoris disk is shown in Figure 2, where the brighter spikes were simply taken out, and the disk luminosity is flattened by an r^{-3} power law in order to better illustrate its radial extent. The superimposed circle represents a region of 100 AU (6 arcsec) around the star, corresponding to the inner limit of the coronagraphic studies. The disk is seen down to 2.5 arcsec from the star. Shorter exposures allow a precise evaluation of the disk brightness down to 1.8 arcsec, i.e. down to less than 30 AU.

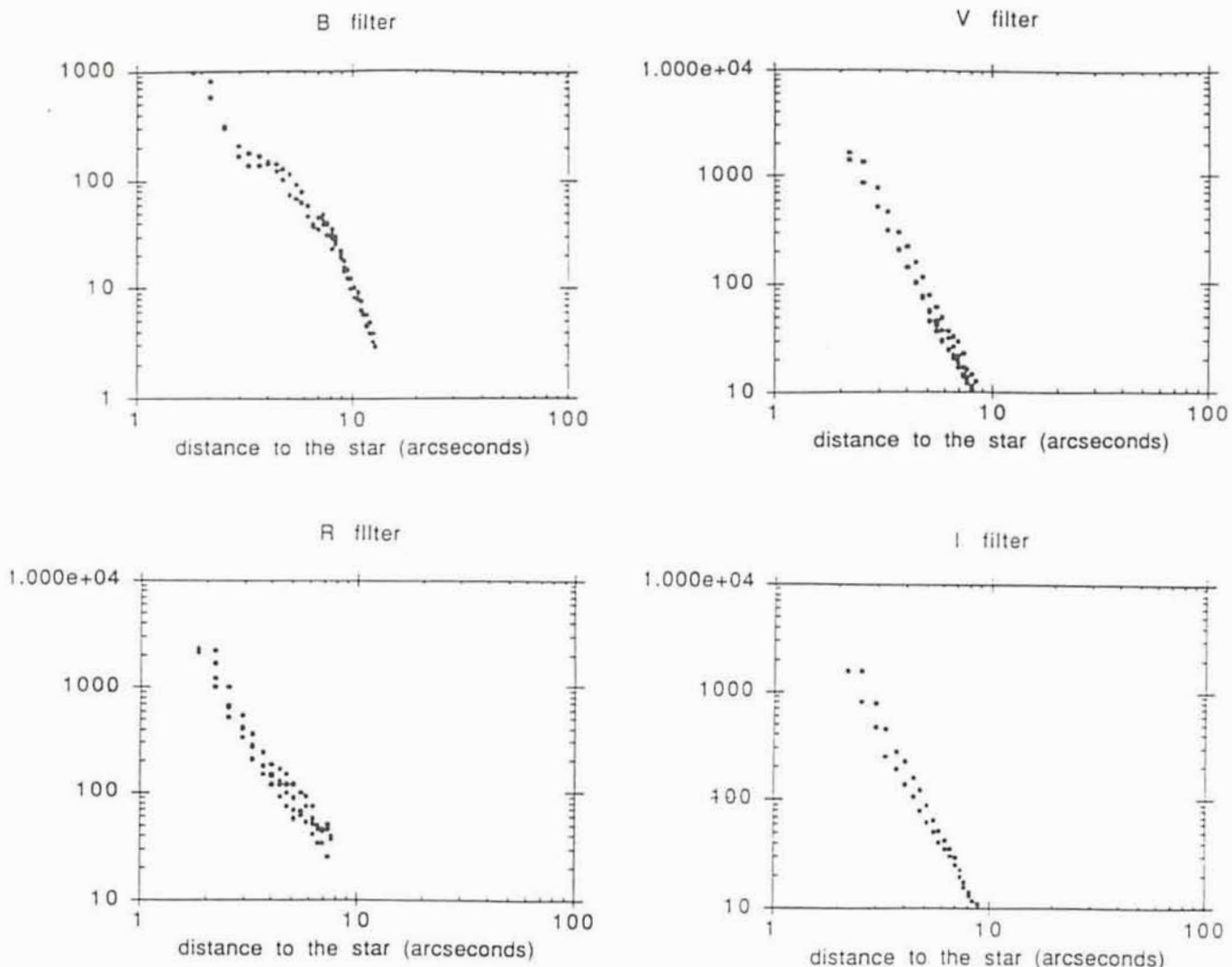


Figure 3: Disk brightness in arbitrary units for the four filters as a function of the stellar distance in arcsec. In V, R, and I filters, an $r^{-3.6}$ power law is found, while in the B filter, departure from this power law is clearly detected at less than 5 arcsec from the star (60 AU).

Preliminary Results

From these different images, it is possible to reconstruct the disk brightness between 2 and 12 arcsec by evaluating the total signal above background perpendicular to the disk plane. The results for the different filters are shown in Figure 3. Nearly an $r^{-3.6}$ power law is found in V, R and I, in excellent agreement with the previous observations of Artymowicz, Burrows and Parasce (1989).

The striking difference is seen in the B filter. The power law found at more than 6 arcsec from the star matches very well the one found in the other filters and confirms also the previous coronagraphic results: the disk colour does not vary with the distance to the star. Furthermore, these disk colours are shown in Figure 4 after normalization with the stellar colours themselves. Our result thus confirms the flat albedo of the dust particles, demonstrating again the probable large size of the grains present in the outer disk ($> 1 \mu$).

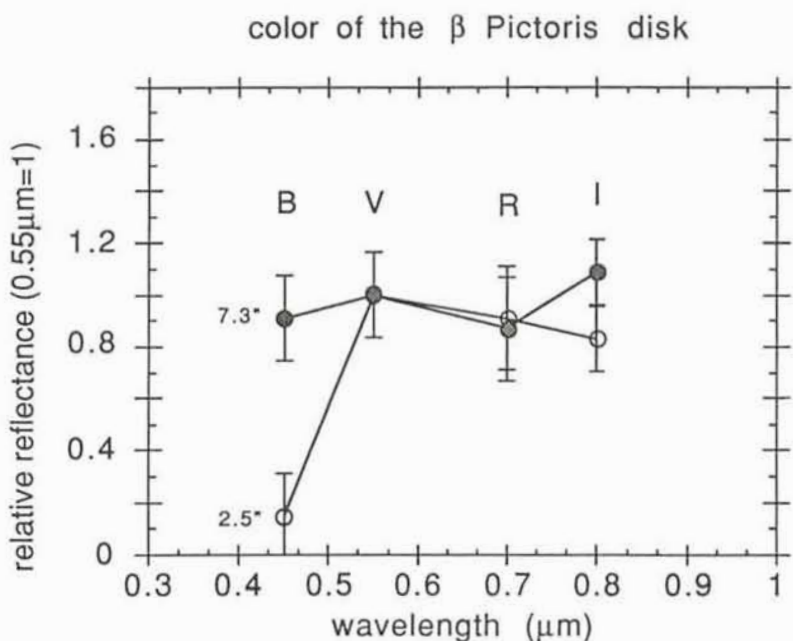


Figure 4: The disk colour is given at two different locations in the disk and in the four filters (after normalization with the stellar light). Neutral colour is seen at large distances, while a drop in the B filter is clearly observed in the inner regions.

However, at shorter distances from the star, we observe a very clear drop in the B filter, showing that the dust albedo seems to decrease by at least a factor of 4 when moving from 7.3 arcsec to 2.5 arcsec. This slow drop of the B albedo is also clearly seen in Figure 3.

This is an extremely interesting and totally new result, which seems to indicate that the nature of the grains is changing when moving inward. More precisely, a change in the grain size could not explain such a variation because larger grains should induce no colour changes while smaller ones should, on the contrary, favour the blue. However, a change in surface albedo of the grains could easily explain such a behaviour; from material albedoes by Gaffey and McCord (1979), a similar behaviour could be found in icy material more and more covered with dust.

If this explanation is correct, it seems to indicate that the grains in the β Pictoris disk are ices more and more dusty when going inward. This might be a first direct indication that a different situation prevails in the inner regions of the disk, namely at less than about 75 AU (5 arcsec), where planets are possibly forming.

We also have confirmed a slight asymmetry in the disk from one side to the other, but noticed an inversion of that asymmetry in the inner regions, leading to an average symmetric disk. This may again be the signature of planetary formation processes within the β Pictoris disk.

Conclusions

We have shown that a new observational approach does exist to look for very faint features near bright objects. Compared to classical stellar coronagraphy, it allows observations closer to the star, particularly if quantitative results must be reached very close to it.

In the case of the β Pictoris disk, we confirmed previous results obtained at more than 6 arcsec from the star. Moreover, we were able to directly observe the disk down to 2 arcsec. The main results are:

- the disk extension continues down to 30 AU from the star, following an $r^{-3.6}$ power law;
- the disk colour is neutral in V, R and Ic at all observed distances;
- the disk colour drops down in the blue (B) when going inward, starting at about 75 AU from the star, to reach a factor of 4 reduction at 30 AU;
- a slight disk asymmetry (80%) is present, but is inverted within 100 AU from the star.

Obviously, this technique is very promising and a lot more is still to be done to further confirm these results and observe the disk even closer. From our first approach we are convinced that observing the β Pictoris disk down to less than one arcsec from the star is within the possibilities. Furthermore, this is potentially a very powerful technique to search for other protoplanetary disks around nearby stars, even if they are

more inclined, as the β Pictoris one is still a unique phenomenon.

References

- Artymowicz, P., C. Burrows, and F. Paresce, *Astron. Astrophys. J.*, **337**, 494, 1989.
- Beust, H., A.M. Lagrange-Henri, A. Vidal-Madjar, and R. Ferlet, *Astron. Astrophys.*, **223**, 304, 1989.
- Beust, H., A. Vidal-Madjar, and R. Ferlet, *Astron. Astrophys.*, **247**, 505, 1991.
- Buil, C., in *Astronomie CCD*, ed. S.A.P., 1989.
- Colas, F., *University of Paris*, Ph.D. Thesis, 1991.
- Colas, F., and J.E. Arlot, *Astron. Astrophys.*, **252**, 402, 1991.
- Diner, D.J., and J.F. Appleby, *Nature*, **322**, 436, 1986.
- Ferlet, R., L.M. Hobbs, and A. Vidal-Madjar, *Astron. Astrophys.*, **185**, 267, 1987.
- Gaffey, M.J., and T.B. McCord, in *Asteroids*, **688**, ed. T. Gehrels, 1979.
- Hobbs, L.M., A. Vidal-Madjar, R. Ferlet, C.E. Albert, and C. Gry, *Ap. J. Lett.*, **293**, L29, 1985.
- Kondo, Y., and F.C. Bruhweiler, *Ap. J. Lett.*, **291**, L1, 1985.
- Lagrange, A.M., R. Ferlet, and A. Vidal-Madjar, *Astron. Astrophys.*, **173**, 289, 1987.
- Lagrange-Henri, A.M., A. Vidal-Madjar, and R. Ferlet, *Astron. Astrophys.*, **190**, 275, 1988.
- Paresce, F., and C. Burrows, *Ap. J. Lett.*, **319**, L23, 1987.
- Smith, B.A., and R.J. Terile, *Science*, **226**, 1421, 1984.
- Telesco, C.M., E.E. Becklin, R.D. Wolstencroft, and R. Decher, *Nature*, **335**, 51, 1988.
- Telesco, C.M., and R.F. Knacke, *Ap. J. Lett.*, **372**, L29, 1991.
- Vidal-Madjar, A., L.M. Hobbs, R. Ferlet, C. Gry and C.E. Albert, *Astron. Astrophys.*, **167**, 325, 1986.

Spectroscopy of Arcs and Arclets in Rich Clusters of Galaxies

G. SOUCAIL, *Observatoire Midi-Pyrénées, Toulouse, France*

1. Introduction

Since 1987, the redshift determination of the giant arcs observed in rich clusters of galaxies has been a great challenge for observers, as it was initially the only way to confirm the nature of the gravitational phenomenon. But the faint surface brightness of most of the arcs, only slightly compensated by the extension of the image, is partly responsible for the slow progress of such observations although their scientific impact is quite large.

Let us begin this paper with some chronological steps in the discovery and

the observations of giant luminous arcs. The first main result, about one year after the discovery of giant arcs in two clusters of galaxies (Soucail et al. 1987, Lynds and Petrosian 1986), was the redshift measurement of the giant arc in Abell 370, a rich cluster at a redshift of 0.37. A strong emission line was detected all along the structure, with a curved slit punched with the PUMA system installed at the 3.6-m at La Silla. The line was immediately identified with the well-known [OII] line at 3727 Å, redshifted at 0.725. This important result was the confirmation of the hypothesis

that we were observing a gravitationally distorted image of a background source through the cluster of galaxies. One year later we continued our study by showing that many clusters were acting as giant lenses on the numerous population of faint blue galaxies detected at the same period by Tyson (1988). For example in A370, many weakly distorted blue objects were detected, with an orthoradial orientation with respect to the cluster centre (Fort et al. 1988). These so-called "arclets" were also supposed to be images of distant background galaxies. But in this case, the confirmation of this

idea is less obvious, because their magnitude is larger than 25, out of the capabilities of the present-day spectrographs. Many other clusters have now been observed by many people and a lot of them present similar structures. In particular, Tyson et al. (1990) have detected a strong excess of tangentially elongated objects in the very rich cluster A1689, mainly among the blue selected objects, by using very deep imaging in B and R.

The scientific interest in these examples of gravitational lensing is quite important, because it is a new tool for Observational Cosmology, and an approach of the mass distribution rather independent of other dynamical methods. The development of the new methods applied on lensed-clusters will be presented in a final report of the Key Programme 1-015-45K, "Arcs survey in distant clusters of galaxies", performed by the Toulouse group (Fort et al., 1990). The use of the "gravitational telescope" for probing the deep and distant Universe is also very promising and exciting and will be discussed here. A major goal of the spectroscopic observations is to derive the redshift of the largest and brightest arcs, and this for many reasons:

- It is the ultimate confirmation of the gravitational lensing hypothesis, especially in the cases for which other interpretations are possible (cluster galaxy seen edge-on, manifestations of galaxy-galaxy interactions, etc). In a few cases, such as the triple arc in C10024+1654, the identification of a change of parity in the different images (from high spatial resolution data) is also a clear evidence of the phenomenon (Kassiola et al., 1992).

- The redshift of one arc in a cluster fixes the geometrical scales of the lensing configuration and gives immediately the total mass within the critical radius. Consequently, the constraints obtained on the dark matter distribution are better (see for example the case of MS2137-23 in Mellier et al., 1992).

- The redshifts of two different arcs in one cluster could be very promising for constraining the value of q_0 , provided one is able to reconstruct the gravitational potential of the cluster, and the two redshifts are distant enough from each other.

- Last but not least, the arc sources form a sample of very distant field galaxies at redshift larger than 0.6. It is very important to study their properties in the framework of galaxy evolution and formation, and their stellar content must be compared with evolutionary models (Guiderdoni and Rocca-Volmerange 1987, Bruzual and Charlot 1992).

Here I will present some preliminary

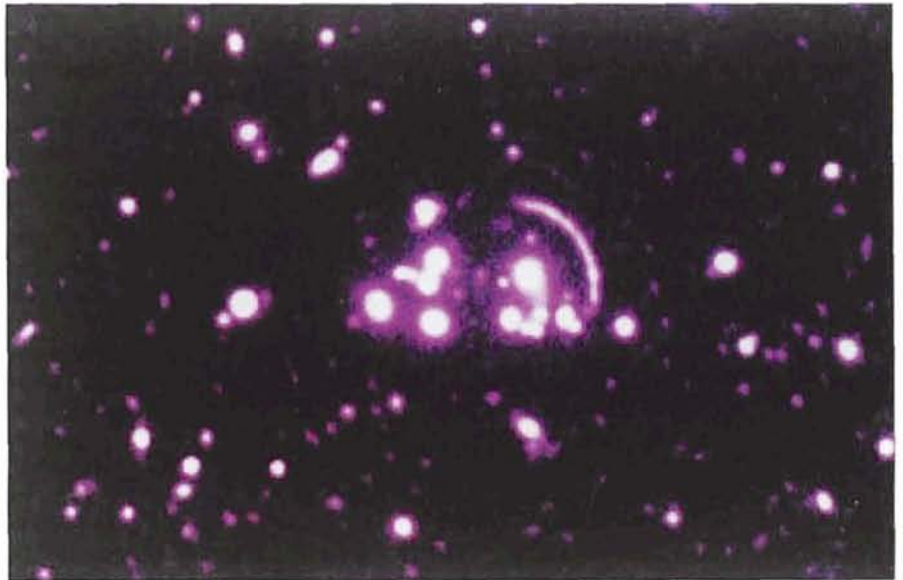


Figure 1: Ultra-Deep B image of the cluster of galaxies Cl2244-02, from CFHT. One can see some substructures along the giant arc.

results from the spectroscopic follow-up of the main arcs detected in our survey of rich clusters of galaxies (ESO Key Programme and CFHT Long-term Programme). The data have been collected on different telescopes with various instruments (3.6-m and NTT on La Silla, 3.6-m CFHT in Hawaii, 4.2-m WHT in La Palma), but they all correspond to faint objects and consequently low resolution spectroscopy with very long exposure times is required for each specific object.

2. Some Peculiar Cases of Redshift Determination

2.1 The Giant Arc in the Cluster Cl2244-02

The blue giant arc detected in the centre of Cl2244-02 ($z = 0.329$) is one of the most spectacular cases of gravitational lensing (see Fig. 1). Its very circular shape extends over more than 100° and its B-R colour index of 0.8 makes it one of the bluest arcs ever observed. More than 10 hours of integration were necessary at the 3.6-m with EFOSC in order to obtain a good signal on the continuum. An emission line was finally detected at a wavelength of 3940 Å and identified with Ly α redshifted at 2.238. This identification was also confirmed by the detection of several absorption lines (CIV 1549, SiII and SiIV) and the continuum observed in the rest-frame wavelength range of 1200–2000 Å is compatible with what is expected from starburst galaxies.

This rather secure identification makes the source of this arc one of the most distant field galaxies known up to

now (Mellier et al., 1991). The stellar content seems "normal" with a star formation rate of a few tens of solar masses per year, a value far from the high numbers derived from the spectra of distant radio-galaxies!

2.2. The "Straight" Arc in Abell 2390

The spectroscopic data on this peculiar arc were collected at the 4.2-m William Herschel Telescope in La Palma. The surprising straight shape of the arc made the slit positioning easy! A total integration time of about 10 hours led to the detection of an emission line at 7130 Å and an underlying continuum, both compatible with a redshift of 0.913 (Pelló et al. 1991). We were also able to detect a velocity gradient along the arc with a line shift of 10 Å which we confirmed further with observations on EFOSC at a better resolution. This gradient is presently interpreted as an intrinsic velocity gradient inside the source, stretched by the gravitational distortion of the cluster field. If so, it is the confirmation of the existence of a rotating disk with a maximum velocity of about 200 km/s (uncorrected for inclination). It has also been used tentatively to derive the Hubble constant H_0 through the Tully-Fisher relation (Soucail and Fort 1991).

Our first interpretation of the straight shape of the arc was the existence of a bi-modal deflecting potential with a source positioned in the saddle region between the two clumps of matter. Unfortunately we did not detect any overdense region of galaxies on the external side of the arc, which was somehow problematic. Another possibility was

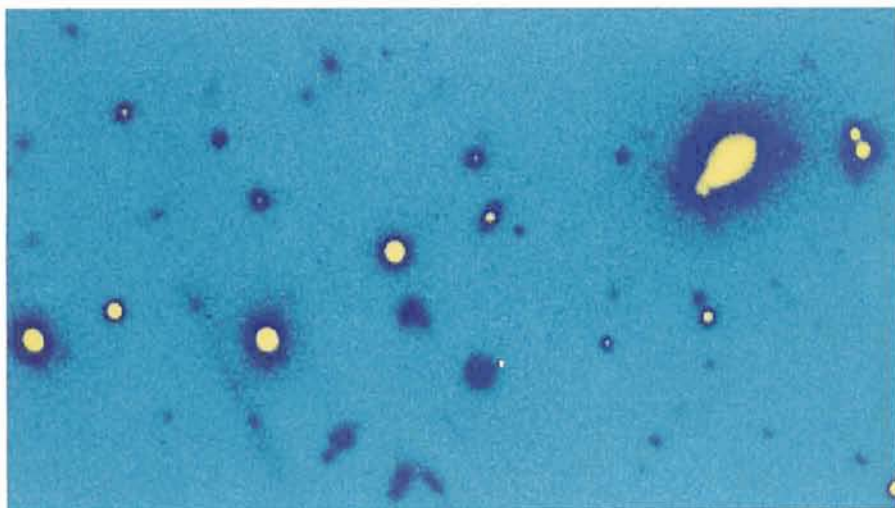


Figure 2: High-resolution image of the centre of Abell 2390, from CFHT and with a I-band filter. The separation between the images of the two galaxies forming the arc is visible and also a slight change in the orientation of each image.

suggested recently by Kassiola et al. (1992) that we see two interacting galaxies at $z = 0.913$. This hypothesis is reinforced by the infrared data (see below) because the arc presents a strong colour gradient in K (Smail et al. 1992) and also from high-resolution CCD frames collected at CFHT last year (Fig. 2). The separation between two smaller images is clearly evident in the I-band.

2.3. The Multiple Arc System in A2218

This cluster ($z = 0.175$) is one of the richest clusters of the Abell catalogue, with a giant cD in its centre. It shows many arclets in the central region, located around the cD and also around the second giant galaxy. A spectroscopic survey of the cluster has been performed at the 4.2-m WHT (La Palma) by Pelló et al. (1992). They collected spectra of several arclets, and got two source redshift measurements with a secure determination. The first one is located near the central cD and presents the spectrum of an E/Sa galaxy redshifted at $z = 0.702$. Its colours are redder than those of the cluster member, contrary to the other known arcs. The fact that the cluster redshift is only 0.17 also favours efficient magnification on rather low redshift sources. The second arclet is very blue and it lies around the second brightest galaxy. A strong emission line has been detected at 7580 \AA with an underlying blue continuum, giving an identification of the [OII] $\lambda 3727$ line at $z = 1.034$. More data are being analysed on this cluster, mainly by multi-colour photometry used on the numerous populations of very faint arclets, in order to evaluate their "photometric redshift" distribution.

2.4 Some Results from Other Clusters

Many other arcs or arclets were observed spectroscopically over the last three years, sometimes with less success. In most cases, we did not succeed to get a redshift for the arc spectra without emission lines, as it is extremely difficult to detect absorption lines on a low S/N continuum. This means that it will be very difficult to measure redshifts between 1.1 and 2.3: [OII] $\lambda 3727$ is too far in the red ($\lambda > 7800 \text{ \AA}$) and Ly α is not redshifted enough ($\lambda < 4000 \text{ \AA}$). Between these two typical emission lines, no other emission lines are prominent in normal galaxies and we only expect to see absorption lines.

Presently two arcs fall in this category:

- The arclet A5 in the cluster A370 is the largest one of the weakly distorted images detected by Fort et al. (1989). Its B-magnitude reaches 22.7, but the surface brightness is only $25.5 \text{ mag. arc-sec}^{-2}$. A spectrum was obtained with EFOSC, with the tentative detection of absorption lines giving a preliminary redshift of 1.305 (Mellier et al. 1991). The [OII] line was then predicted at a wavelength of 8590 \AA . Our last data collected in December 1991 on EFOSC using a grism with a higher dispersion (R150, 3 \AA per pixel) are rather inconclusive: no emission line is visible at the expected wavelength, and the continuum level is only at 1σ above zero. Anyway, even if the redshift of A5 is not confirmed, the photometric information available makes this object very peculiar and exciting. The colour indices (B-R) and (R-K) are very blue, the continuum in the optical range is flat and featureless. It is now quite improbable that this

corresponds to a cluster member at $z = 0.374$. Its very low flux in the near infrared (I and K bands) makes it rather "intriguing" and it should possibly correspond to a very distant and/or young galaxy, which needs to be re-observed. – The giant arc in the cluster C10024+1654 ($z=0.39$) is the most interesting one to study in view of its large spatial extension and its splitting into 3 pieces. A curved slit was punched with PUMA (October 1989) in order to follow the three main parts of the arc, and despite a total integration time of 6 hours, a featureless spectrum was obtained, with no evident emission lines. A recent analysis of the image formation in this cluster by Kassiola et al. (1992) led them to predict the redshift of the arc source to be between 1.4 and 1.9 from theoretical arguments. Deeper data are expected in order to test their predictions.

Let us also present one counter-example of what was initially suspected to be an arclet. From deep imaging in the cluster of galaxies A483 ($z = 0.29$) we noticed several extended blue images around the cluster centre. In particular, two structures were detected, one going through the envelope of the cD, and the other one extended over $9''$ located a bit more than $1'$ north of the cD. In December 1991, we got 4 hours exposure in spectroscopy on the second of these objects. After data reduction we found a redshift of 0.274! This object is most probably an edge-on spiral galaxy belonging to the cluster and not an arclet. One must conclude that people have to be very careful when they announce the discovery of arcs or arclet candidates. Only detailed multi-colour photometry and/or spectroscopic data can give some confidence in the gravitational arcs hypothesis, if one cannot detect a clear multiple arc system with a counter-image or possibly a parity change between the images.

3. Gravitational Lensing and Distant Galaxies

The sources of the gravitational arcs and arclets are potentially a very useful sample of very distant galaxies, from which we begin to gather extensive spectrophotometric data. At least ten of them are presently spectroscopically confirmed and the spectra generally include information on the continuum or the large-scale spectral energy distribution (Table 1).

We must also consider the possible selection biases introduced in the sample before any analysis and comparisons with other surveys. The arcs and arclets are generally detected by their blue colour ($B-R < 1$) with respect to the

Table 1. Summary of the spectrophotometric survey of arcs and arclets.

Cluster	z_{cl}	z_s	B	R	B-R	R-K	μ_B	γ	B_{int}	R_{int}
A370 (A0) ¹	0.374	0.725	21.1	19.4	1.7	4.1	24.6	12	23.8	22.1
A370 (A5) ²	0.374	1.305?	22.7	22.3	0.4	-3.0	25.4	6	24.7	24.2
Cl2244-02 ²	0.336	2.237	21.2	20.4	0.8	3.0	25.3	20	24.5	23.7
A2390 ³	0.231	0.913	21.9	20.0	1.9	4.2	25.3	12	24.6	22.7
A2218 (# 359) ⁴	0.176	0.702	24.3	21.4*	2.9	—	25.0	4	25.8	22.9
A2218 (# 289) ⁴	0.176	1.034	22.5	21.7*	0.8	—	24.2	5	24.2	23.4
A963 N ⁵	0.206	0.771	23.6	23.1	0.5	3.5	25.5	4	25.1	24.6
Cl0024+1654 ²	0.391	?	23.0	22.3	0.7	3.3	25	4	24.5	23.8
S506 (Cl0500-24) ⁶	0.321	0.91?	21.0	19.8	1.2	<3.0	—	8	23.2	22.0
A2163 (A1) ⁷	0.203	0.742	24.2	21.8	2.4	—	—	3	25.4	23.0
A2163 (A2) ⁷	0.203	0.728	23.1	21.2	1.9	—	—	3	24.3	22.4

¹Gunn r filter; ²Soucaill et al., 1987; ³Mellier et al., 1991; ⁴Pelló et al., 1991; ⁵Pelló et al., 1992; ⁶Ellis et al., 1991; ⁷Giraud 1992, preprint; ⁸Soucaill G., Amaud M., Lachièze-Rey M., Mathez G., in preparation.

redder cluster members but this is not always the case (see for example the "red arc" in A2218, Pelló et al. 1992). More important is the fact that the sample is limited in surface brightness more than in magnitude; this is due to the fact that to detect the continuum of the spectra of these objects in a reasonable exposure time implies that the surface brightness does not exceed $\mu_B = 25.5$. Remember that in gravitational lensing, surface brightness is conserved and that magnification means extension of the image of the source. Finally the sample is only based on galaxies with redshift larger than 0.7 because it roughly corresponds to the minimum redshift above which lensing is efficient, for a typical deflector at a redshift of 0.2 to 0.4 ($z_{Source} > 2z_{Cluster}$).

But the sources of the arcs belong to the family of FIELD galaxies (which are not detected by their radio emission for example), and their intrinsic magnitudes, corrected from the gravitational magnification, are in the range [24; 25] in B. This range is at least one magnitude fainter than the magnitude range of the deepest spectroscopic surveys of field galaxies performed by Cowie et al. (1991) for example. So it is interesting to explore the redshift distribution which is centred around 1 in our sample. One should note for example that with the exception of the peculiar case of Cl2244-02, about 70% of the galaxies have a redshift smaller than 1, and the median redshift is 0.9. Moreover, in view of their spectra, these objects are not observed in a phase of violent star formation although emission lines typical of HII regions are present in most of them. Moreover, when we have high-resolution images of the giant arcs, we often see sub-structures inside the arcs. This still preliminary result could suggest either that we see merging clumps at large z or that inside the distant galaxies disks or spiral arms are already formed.

4. Infrared Photometry of Large Arcs

In order to increase the observed spectral range of the galaxies, a photometric survey of the arcs has been performed by our colleagues from Durham (UK) in the K band (Smail et al., 1992). The main advantage of the K band at 2.2 μm is that it scans a portion of the spectrum dominated by the old stellar population, and is more indicative of the history of star formation than blue photometry, very sensitive to recent star formation. Anyway, the combination of both magnitudes as well as the redshift indication give a good tool to study the distant galaxies and their entire spectral content. Then it is shown that although most of the arcs have blue colour indices, none of them remain undetected in K. But for those at $z > 1$, the old population does not contribute significantly to the K flux, so the sample is not consist-

ent either with a non-evolutionary model of galaxy or a model with a single initial burst of star formation. This probably means that the history of star formation in these galaxies is rather continuous, up to a redshift of about 1.

5. Conclusions

I have presented in this article the status of the survey in 1992, and I should emphasize the fact that the increase of the sample of arcs with a secure redshift measurement is very slow, due to the difficulties of the observations and the long exposure times involved for these faint objects. But the detection of new arcs and arclet candidates still goes on, especially in the framework of the ESO Key Programme "Arcs and arclets survey" and the similar one at CFHT. We expect some new, very exciting data over the next year. In particular, we are very excited by the new arc system discovered in the cluster MS2137-23 (Fort et al. 1992, Figure 3): a long tangential arc has been detected as well as the first case of a radial arc candidate. This peculiar lensing configuration has been expected for a long time, but as radial images are supposed to form near the cluster centre, in most cases they fall in the envelope of the giant central galaxies. In the case of MS2137-23, the radial arc candidate was detected by its blue colour, and a modelling of the gravitational potential of the cluster was proposed by Mellier et al. (1992) which takes into account a large number of observational parameters. The spectroscopic confirmation of the radial image would fix one

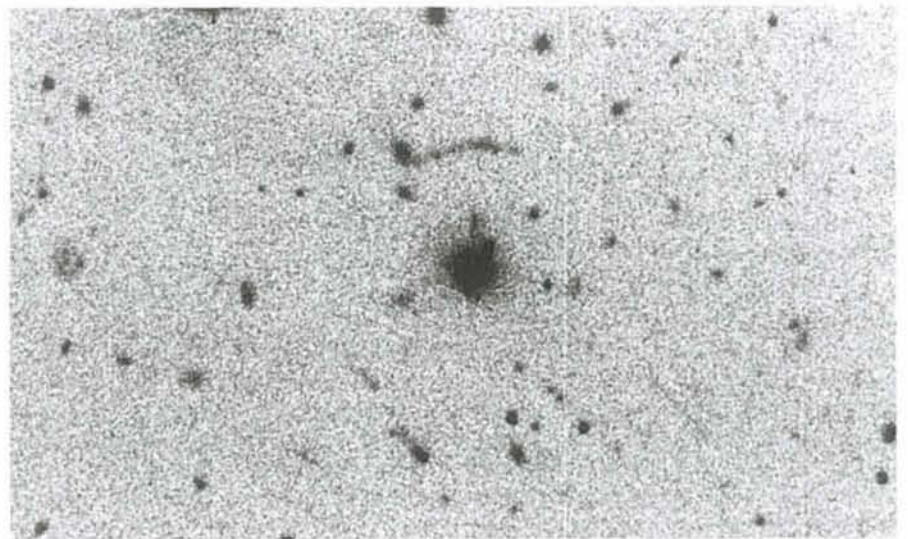


Figure 3: Image of the arc system in MS2137-23 ($z=0.315$) discovered during a run at the NTT in August 1991 for the Key-Programme "Arcs survey in clusters". Good resolution images show evidence for a blue "radial arc" near the central galaxy, the first case ever detected of this peculiar lensing configuration.

of the still unknown parameters, increasing the number of constraints of the model.

For the arclets or the weakly magnified galaxies which are too faint to be observed spectroscopically, we also expect some progress by using multi-colour photometric data spread over a large spectral range, such as B, R and I colours. In that case we can compare the colour indices of the objects with the predictions of spectrophotometric models of galaxy evolution, in order to evaluate a "photometric redshift". This method is being calibrated with the known arcs, and we are conscious that it is only useful in a statistical way, when a large number of arclets is being observed. The preliminary results of the method, applied in the field of A370 show that most of the galaxies have colours compatible with galaxies at redshift around 1, reinforcing the results presented above (Fort et al., in preparation).

Last but not least, in a few optimal cases, we expect to get a complete set of data in some clusters: high-resolution X-ray map with ROSAT, multiple arcs and a lot of arclets and weakly distorted images of background galaxies for a reconstruction of the 2D gravitational potential of the Dark Matter from the centre to the external radius of the cluster. The redshift of the giant arcs is in this case fundamental in order to fix the scaling of the potential in the lens modellings.

The use of the gravitational telescope for the study of distant galaxies appears to be a powerful and original tool, which is probably not yet fully used. For example, we can also expect to find some "exotic" magnified objects, such as very distant quasars (La Borgne et al., 1990) or we hope to "see" some spatial structures in galaxies at $z = 1$ through the distortion of the clusters. The arc survey opened for us a new window in the $z = 1$ Universe!

Acknowledgements

I wish to thank all my colleagues from the Toulouse-Barcelona group, namely B. Fort, H. Bonnet, J.P. Kneib, J.F. LeBorgne, G. Mathez, Y. Mellier, R. Pelló, J.P. Picat and B. Sanahuja with whom I have worked on arcs and lenses for many years in such a friendly environment! Also many thanks to our collaborators T. Tyson (Bell Labs), G. Bernstein (Tucson), R. Ellis, M. Fitchett and I. Smail from Durham for all the data provided and the exciting discussions we had about observations of gravitational lenses.

References

Bruzual G., Charlot S., 1992, submitted to *Ap.J.*
Cowie L.L., Songaila A., Hu E.M., 1991, *Nature* **354**, 460.

Guiderdoni, B., Rocca-Volmerange B., 1987, *A & A* **186**, 1.
Ellis R.S., Allington-Smith, J.R., Smail I., 1991, *M.N.R.A.S.* **249**, 184.
Fort B., Prieur J.L., Mathez G., Mellier Y., Soucail G., 1988, *A & A* **200**, L17.
Fort B., Le Borgne J.F., Mathez G., Mellier Y., Picat J.P. Soucail G., Pelló R., Sanahuja B., 1990, *The Messenger* **62**, 11.
Fort B., Le Fèvre O., Hammer F., Cailloux M., 1992, *Ap.J.*, submitted.
Kassiola A., Kovner I., Blandford R.D., 1992, *Ap.J.*, in press.
Kassiola A., Kovner I., Fort B., 1992, *Ap.J.* in press.
Lynds R., Petrosian V., 1986, *B.A.A.S.*, **18**, 1014.
Le Borgne J.F., Pelló R., Sanahuja B., Soucail G., Mellier Y., Breare M., 1990, *A & A* **229**, L13.
Mellier Y., Fort B., Soucail G., Mathez G., Cailloux M., 1991, *Ap.J.* **380**, 334.
Mellier Y., Fort B., Kneib J.P., 1992, *Ap.J.*, in press.
Pelló R., Le Borgne J.F., Soucail G., Mellier Y., Sanahuja B., 1991, *Ap.J.* **366**, 405.
Pelló R., Le Borgne J.F., Sanahuja B., Mathez G., Fort B., 1992, *A & A*, submitted.
Smail I., Ellis R.S., Aragón-Salamanca A., Soucail G., Mellier Y., Giraud E., 1992, *M.N.R.A.S.*, in press.
Soucail G., Fort B., Mellier Y., Picat J.P., 1987, *A & A* **172**, L14.
Soucail G., Mellier Y., Fort B., Mathez G., Cailloux M., 1988, *A & A* **191**, L19.
Soucail G., Fort B., 1991, *A & A* **243**, 23.
Tyson J.A., 1988, *A.J.* **96**, 1.
Tyson J.A., Valdes F., Wenk R.A., 1990, *Ap.J.* **349**, L1.

Quasar Absorption Spectra: The Physical State of the Intergalactic Medium at High Redshifts

E. GIALLONGO, Osservatorio Astronomico di Roma, Monteporzio, Italy

S. CRISTIANI, Dipartimento di Astronomia, Università di Padova, Italy

A. FONTANA, Dipartimento di Fisica, Il Università di Roma, Italy

D. TRÈVESE, Istituto Astronomico, Università di Roma "La Sapienza", Italy

1. Introduction

An important source of information on the distribution and the physical state of the intergalactic medium (IGM) up to redshift $z \approx 5$ is provided by the study of the absorption spectra of high redshift quasars. The crowd of narrow absorption lines seen shortward of the QSO Lyman- α emission is thought to be due mainly to Lyman- α absorptions caused by intervening clouds along the line-of-sight (Lynds 1971; Sargent et al. 1980).

Direct measures of column densities and doppler widths of the absorption

lines provide typical values of $N_{\text{HI}} = 10^{14}$ atoms cm^{-2} and $b = \sqrt{2}\sigma = 20-30$ km s^{-1} (Carswell et al. 1987, 1991) correspondent to $T_c \sim 2-5 \times 10^4$ K, assuming thermal broadening. However, Pettini et al. (1990) claim typical b values as low as $b = 17$ km s^{-1} and a tight correlation between b and N_{HI} parameters which suggests lower temperatures and would imply a further important constraint on the physics of the clouds. More data are necessary to resolve this controversy.

The most recent and accurate esti-

mate of the cloud sizes has been obtained by Smette et al. (1991) from the spectra of a gravitationally lensed high-redshift quasar UM673 ($z_{\text{em}} = 2.7$). They derive lower and upper limits of $12h_{50}^{-1}$ kpc and $160h_{50}^{-1}$ kpc respectively, for the diameter of spherical clouds, or 24 kpc and 320 kpc, for oblate spheroids with an axis ratio < 0.1 .

Under these conditions, gravitational energy is overwhelmed by thermal energy and the clouds could be confined by a hotter, highly ionized and diffuse IGM if non-baryonic dark matter does not

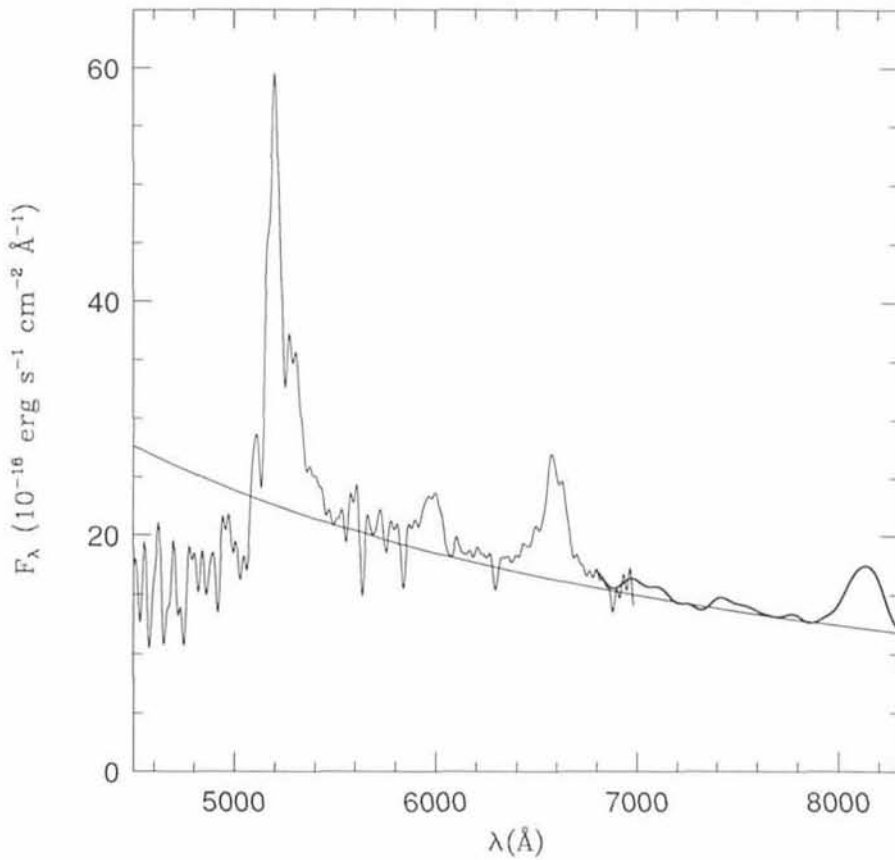


Figure 1: Composite spectrum of Q2126-158. High-resolution data are smoothed to 10 \AA resolution. Thick curve represents the low-resolution data. The fitted continuum is also shown.

quasar absorption spectra particularly suitable to investigate the physical properties of the diffuse and clumpy components of the IGM.

As an example, we present a high resolution spectrum ($R = 22,000$) of the quasar Q2126-158 at $z = 3.27$, extending from 4500 to 7000 \AA , and show how we can extract crucial information like the density of the diffuse neutral hydrogen and the distribution of density and temperature of the Lyman- α clouds.

2. Data Acquisition and Reduction

The quasar Q2126-158 was observed at ESO (La Silla) in August 1991, with the NTT telescope and the EMMI instrument in the echelle mode (see D'Odorico 1990). Two spectra of 7200 s each were obtained on August 6, and one of 9130 s on August 7. The slit was 1.5 arc-seconds wide and the seeing always less or equal to 1 arcsec. Particular attention was paid in order to minimize the effects of the atmospheric dispersion. The absolute flux calibration was carried out by observing the standard star EG274. The data reduction has been carried out using the standard echelle package described in the 91NOV edition of the MIDAS software (Banse et al. 1983). The weighted mean

contribute appreciably to the gravitational potential of the clouds (see however Rees 1986).

The ionization of the IGM can be constrained by the absence of the long looked-for absorption trough shortward of the QSO Lyman- α emission, with the average optical depth $\tau_{\text{GP}} \leq 0.5$, (GP test, see Gunn and Peterson 1965).

Considering that the background ionizing UV flux produced by the quasar population at $z = 2-3$, $J = 10^{-22} \text{ J}_{-22} \text{ ergs cm}^{-2} \text{ s}^{-1} \text{ Hz}^{-1} \text{ sr}^{-1}$ (Madau 1992), keeps both the clouds and IGM ionized, the physical state and evolution of the diffuse IGM can be further constrained under the assumption that clouds are pressure confined (Sargent et al. 1980, Ostriker and Ikeuchi 1983, Steidel and Sargent 1987). Taken together, the above conditions define a region in the density-temperature plane which provides an upper limit to the IGM baryon density Ω_{IGM} which can give information about the efficiency of the galaxy formation processes.

High resolution spectroscopy available with good efficiency over a large spectral range, using the EMMI instrument at the NTT telescope, will allow to collect a homogeneous sample of

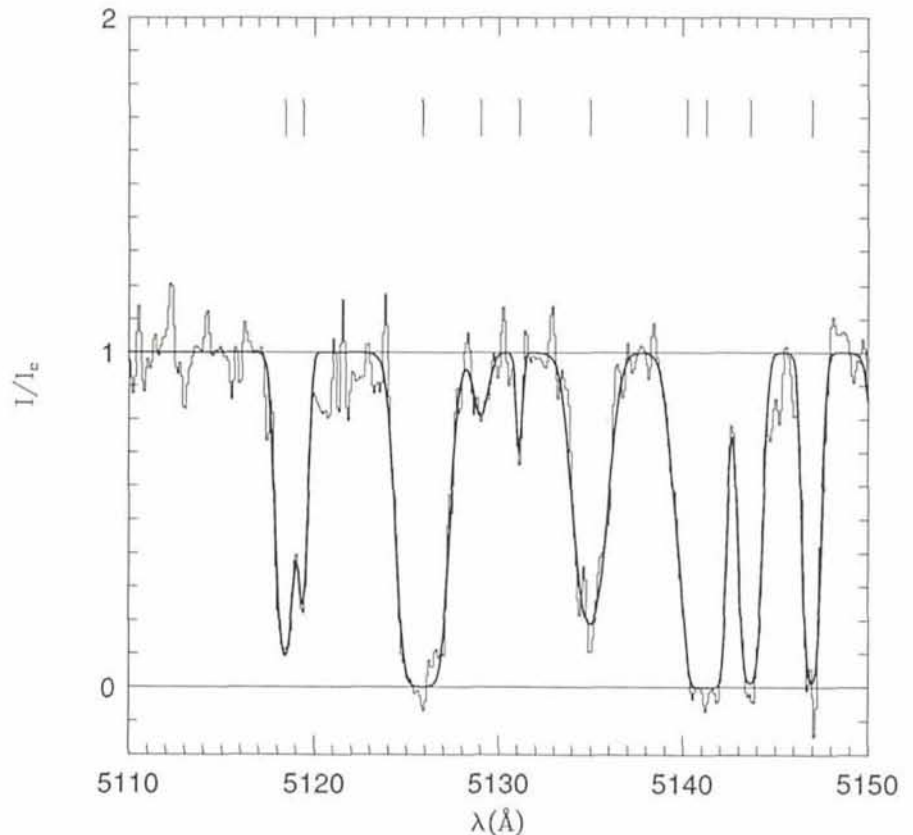


Figure 2: A selected region in the Ly- α forest, with the fitted profiles.

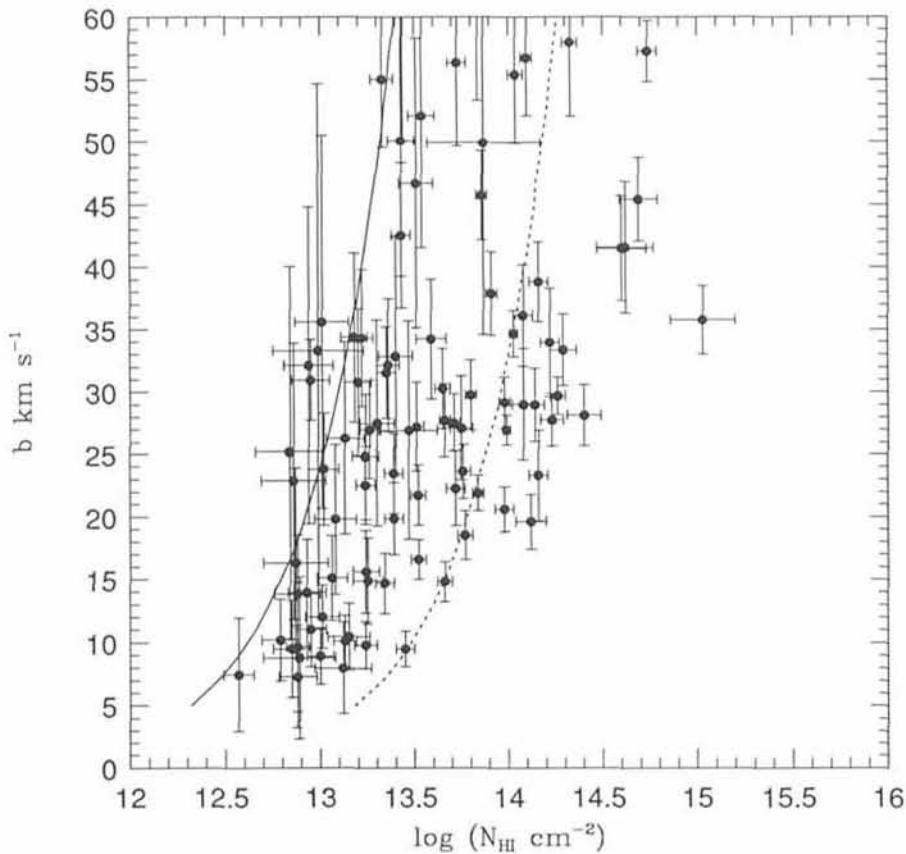


Figure 3: Velocity-dispersion parameter b versus the logarithm of the neutral hydrogen column density $\log N_{\text{HI}}$ of Ly- α lines. The continuous curve represents our selection criterion. The dashed curve corresponds to a central flux of 0.1 where the noise level becomes comparable to the signal and lines start to saturate.

of the spectra has been obtained at the resolution $R = 22,000$ and is shown in Figure 1 smoothed to $\sim 10 \text{ \AA}$ for illustrative purpose. The S/N ratio ranges from 6 to 12 in the Ly- α forest region.

Q2126-158 had previously been observed by us at low resolution ($\sim 25 \text{ \AA}$), using the B & C spectrograph at the 2.2-m ESO/MPI telescope at La Silla on September 3, 1989. Two exposures of 30 min each were taken with a 5 arcsec wide slit in the spectral range 3300-8650 \AA . A standard reduction was carried out with the long-slit package of MIDAS. The absolute flux calibration was obtained observing the standard star LDS 749B.

The two spectra have then been compared, finding that, apart from the difference of a factor 100 in resolution and a renormalization factor close to unity, there was a perfect correspondence within the noise. The red part $\lambda > 7000 \text{ \AA}$ of the low-resolution spectrum has then been appended (after renormalization) to the echelle spectrum as shown in Figure 1.

3. The Quasar Continuum and the Gunn-Peterson Test

The total opacity in the Lyman- α forest is given by the sum of the line

contribution and the GP opacity due to diffuse hydrogen absorption: $\tau = \tau_{\text{GP}} + \tau_{\text{l}}$, and can be measured once the quasar continuum has been established.

From composite quasar spectra and from Figure 1 it can be shown that there are few regions which can be assumed as representative of the true continuum level. The region between Ly α and CIV emissions is affected by the presence of weak emission lines whose broad wings tend to overlap (OI 1302, CII 1335, SiIV 1400) and the region between CIV and CIII] emissions is affected by HeII 1640 and OIII] 1663 and by the blue end of the blended FeII 2000 complex. With this caution the fitted power-law is shown in Figure 1 ($\alpha_{\nu} = -0.62$).

At this point, regions free of strong absorption lines, where the r.m.s. fluctuation about the mean flux becomes consistent with noise statistics, are selected to estimate the GP depression. The power-law continuum estimated longward of Ly α emission is extrapolated in the Lyman- α forest and compared with the local continuum level of the selected regions. We obtain an average opacity at $z = 3$ of $\tau_{\text{GP}} = 0.013 \pm 0.026$. This new value of the hydrogen opacity can be used to constrain density and temperature of the IGM supposed to be ionized by the UV flux of quasars at $z = 3$. For

example, adopting ionization equilibrium with $J_{-22} = 1$ and an IGM temperature of $T_{\text{IGM}} \leq 2 \times 10^4 \text{ K}$ at $z = 3$ we find $\Omega_{\text{IGM}} = 0.006 - 0.013$ for our best fit and 1σ GP estimate respectively (Giallongo, Cristiani and Trèvese 1992).

This is the first direct measure of the GP opacity carried out using high-resolution quasar spectra with good relative flux calibration as can be obtained from the NTT+EMMI echelle-mode configuration.

4. Properties of the Lyman Alpha Absorption Lines

Quasar absorption spectra at a resolution $R > 20,000$ allow a direct determination of the column density and of the doppler parameter b through line profile fitting.

The line detection is performed in the following way. In regions of the Ly α forest with uniform signal-to-noise we construct the histogram of the pixel intensities. In general, because of absorption line contamination in the normalized spectrum, the distribution is not symmetrical in the Ly α forest but is skewed towards lower intensity values. We fit a Gaussian profile to the high intensity side of the histogram starting from the maximum of the intensity distribution: the variance obtained is taken as a conservative estimate of the noise level in the region considered. All the lines whose central relative intensity is less than $(1 - 2\sigma)$ are selected to form a complete sample. It is clear that a threshold of this type corresponds to a well-defined locus in the $b - \log N_{\text{HI}}$ plane (b is in km s^{-1} and N_{HI} in cm^{-2}).

The usual χ^2 fitting procedure is adopted to deblend the line profiles (Carswell et al. 1987, 1991). The number of components is assumed as the minimum which gives a probability of random deviation $P > 0.05$. An example of the resulting profiles is shown in Figure 2. In general this objective procedure is satisfactory though, in some cases, lines with a small number of pixels and poor S/N ratio are classified as single although they clearly appear as double from visual inspection.

After removing metal line systems, which are easily identified through the observation of the CIV doublet seen longward of the QSO Ly α emission, we obtain, in the region from 4750 to 5200 \AA , a complete sample of Ly α lines whose distribution in the $b - \log N_{\text{HI}}$ plane is shown in Figure 3. Two curves of constant central line flux containing most of the sample are also represented. The upper envelope represents our selection criterion: lines with central flux less than the threshold are included in the complete sample. The

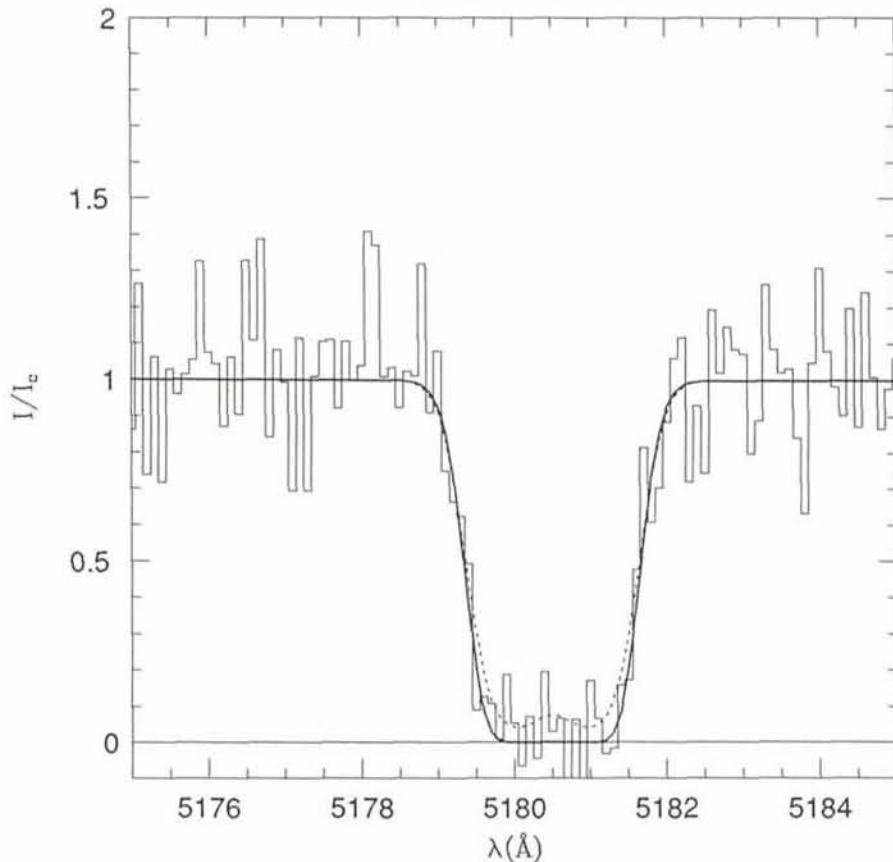


Figure 4: Simulated blend of two lines with $b = 30$, $\log N_{\text{HI}} = 14.1$, separated by 1 \AA , with $S/N = 6$. Dotted curve: profile of the individual components. Continuous curve: single line fitted profile, with $b = 35$ and $\log N_{\text{HI}} = 15.1$.

lower curve corresponds to a central flux of 0.1 where the noise level becomes comparable to the signal and lines start to saturate, in the range of b considered: lines on the right of this curve could be unresolved blends. It is clear that unsaturated lines show a tight correlation which reflects the selection effects (line-selection + non-saturation). However, the saturated lines, which are clearly identified in our spectrum, are

not uniformly distributed in the same range of b occupied by unsaturated lines. In particular, the absence of clearly single lines with $b < 20$ and $\log N_{\text{HI}} > 13.5$ is not due to any bias. Moreover, almost all the saturated features appear as unresolved blends and the reality of lines with $\log N_{\text{HI}} > 14$ in our spectrum is cast in serious doubt. The same could be true for lines with $b > 35$.

According to this interpretation, most

of the lines which appear as saturated could be unresolved blends of unsaturated lines which should occupy the top ($b \geq 30$ and $\log N_{\text{HI}} \leq 14$) of the apparently correlated distribution, as can be seen in Figure 4 where a simulated blend of two lines with the above parameters and $S/N = 6$ has been fitted as a single line of $b = 35$ and $\log N_{\text{HI}} = 15.1$, comparable with the line of highest column density in our sample.

Thus blending plays a crucial role in the interpretation of the observations, as has been shown recently by Trèvese, Giallongo and Camurani (1992). However, increasing the signal-to-noise ratio would raise the upper curve in Figure 3 and move downwards the lower one and allow a better deblending. Thus, recognizing a possible intrinsic correlation between b and N_{HI} in the Lyman- α clouds is within the reach of the present ESO instrumentation.

References

- Banase, K. et al. 1983, "MIDAS" in *Proc. of DECUS*, Zurich, 87.
 Carswell, R.F. et al. 1987, *Ap.J.* **319**, 709.
 Carswell, R.F. et al. 1991, *Ap.J.* **371**, 36.
 D'Odorico, S. 1990, *The Messenger* **61**, 51.
 Giallongo, E., Cristiani, S. and Trèvese D. 1992, *Ap.J.L.* (in press).
 Gunn, J.E. and Peterson, B.A. 1965, *Ap.J.* **142**, 1633.
 Lynds, C.R. 1971, *Ap.J.* **164**, L73.
 Madau, P. 1992, *Ap.J.* **389**, L1.
 Ostriker, J.P. and Ikeuchi, S. 1983, *Ap.J.* **268**, L63.
 Pettini, M. et al. 1990, *M.N.R.A.S.* **246**, 545.
 Rees 1986 *M.N.R.A.S.* **218**, 25P.
 Sargent, W.L.W. et al. 1980, *Ap.J.S.* **42**, 41.
 Smette, A. et al. 1992, *Ap.J.* **389**, 39.
 Steidel, C.C. and Sargent, W.L.W. 1987, *Ap.J.* **318**, L11.
 Trèvese D., Giallongo E., and Camurani L. 1992, *Ap.J.* (in press).

The Galaxy Population in Distant Clusters

A. BUZZONI¹, M. LONGHETTI^{1, 2}, E. MOLINARI¹ and G. CHINCARINI^{1, 2}

¹Osservatorio Astronomico di Brera, Milano, Italy; ²Università degli Studi, Milano, Italy

1. Introduction

Clusters of galaxies are recognized to be the basic building blocks tracing the large-scale structure in the Universe. Thanks to the large number of coeval objects all at the same distance we get more favourable statistics allowing to explore in much better detail the

evolutionary status of the galaxy population.

Moreover, it is relevant to clarify whether or not clusters are dynamically relaxed structures and how environmental conditions constrained galaxy formation among the different morphological types. We know for instance

that ellipticals always reside in high-density regions like the core of the clusters while spirals better trace the low-density peripheral regions (Dressler 1980).

Both the dynamical and photometric questions have much in common as environment conditions might have influ-

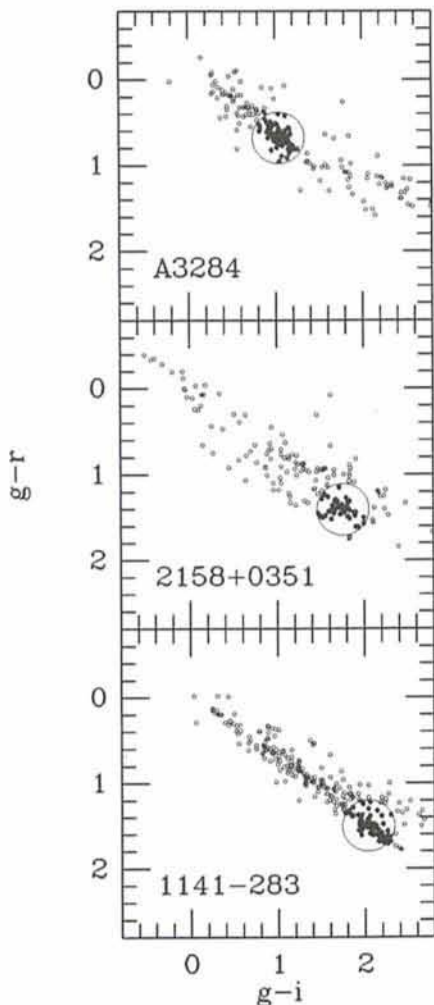


Figure 1: $(g-r)$ vs $(g-i)$ diagrams for the clusters A3284, 2158+0351 and 1141-283. All of the objects with complete photometry are included in the plots. The encircled clump of objects, moving to redder colours with increasing redshift, is due to the cluster elliptical galaxy population. The redshifts of the clusters are respectively 0.15, 0.45 and 0.50.

enced at the beginning the morphological and photometric properties of the galaxies. Therefore, studying cluster galaxies we get both direct clues about their evolutionary status and about that of their parent clusters.

2. The Blue Galaxies' Dilemma

One of the most intriguing and embarrassing problems when dealing with the cluster galaxy population is that an increasing fraction of blue galaxies (i.e. bluer than expected for a population of quiescent early-type galaxies alone) populate clusters at high redshift. This is the so-called "Butcher-Oemler effect".

Since spiral galaxies in the field are known to display similar colours, it has been first questioned that geometrical and projection effects as well as bad field subtraction could induce such a

false correlation (see for example Koo 1988 for an exhaustive discussion). In the last years however a number of observations converged detecting such a component in the population of many clusters at high redshift confirming that despite any possible complication the effect is real (Butcher and Oemler 1984b, Luppino et al. 1991, Molinari et al. 1990, Newberry et al. 1988).

Three main spectral features seem to characterize blue galaxies: (i) Most of them display emission lines (typically [OII], [OIII] and H β) as found for instance in the star forming spiral galaxies (Butcher and Oemler 1984a); (ii) strong Balmer lines in absorption are often detected superposed to a normal E-type continuum (E+A galaxies of Dressler and Gunn 1982, 1983), (iii) when high-resolution imaging is available (Thompson 1988) most blue galaxies seem to display a late-type morphology with signs of possible interaction.

On the basis of our present knowledge it is certainly hard to disentangle the various mechanisms leading to such profound differences in the population of late-type galaxies at early epochs. This is certainly a problem since it has to be established how such late-type galaxies can "vanish" or transform so drastically by the present time.

Alternatively, one should conclude that looking at high redshift in some way we are selecting clusters which are intrinsically different from the local sample. One reason could be that since they are mainly optically selected, the more compact ones are strongly preferred (Cappi et al. 1989). Moreover, clusters with active galaxies could be more prominent. Finally, due to k-correction effects those with a larger fraction of spirals might become more visible with increasing z (Coleman et al. 1980).

That high-redshift clusters might be somewhat different aggregates also stems from an extended analysis by Newberry et al. (1988). In particular, it appears that they display a larger velocity dispersion (typically more than 1000 km/sec) and, statistically, a more compact structure.

3. The Project

In 1986 we started a systematic survey of clusters of galaxies at intermediate and large redshift ($0.15 < z < 0.6$). Previous contributions to this long-term project can be found in Buzzoni et al. (1988), Molinari et al. (1990), Molinari et al. (1992).

To date a homogeneous set of CCD observations in the Gunn g, r, i system has been collected mainly using the 3.6-m ESO telescope at La Silla equipped with EFOSC. About ten clusters

have been observed down to the limiting magnitude $r \sim 24$. Data reduction and systematic photometry in the fields have been performed using MIDAS utilities, and the implemented package INVENTORY (West and Kruszewski 1981). A parallel investigation including multi-object spectroscopy of selected relevant candidates in each field had also been carried out allowing to explore in more detail the absolute spectral energy distribution of the galaxies.

Although of the greatest importance, the spectroscopic approach cannot be widely pursued as it is largely time-consuming. Even fully exploiting the EFOSC MOS mode we need about 4-7 hours integration time to obtain spectra of acceptable signal-to-noise for objects fainter than 20th magnitude. For comparison, good photometry down to magnitude 24 can be achieved in about 1 hour total exposure time. Our analysis rests therefore basically on the multicolour photometry using spectral information as a check of our inferences.

Through comparison with evolutionary population synthesis models (Buzzoni 1988, 1989) we intend to study how consistently photometric properties (i.e. magnitudes and colours) of galaxies in clusters do evolve in a "regu-

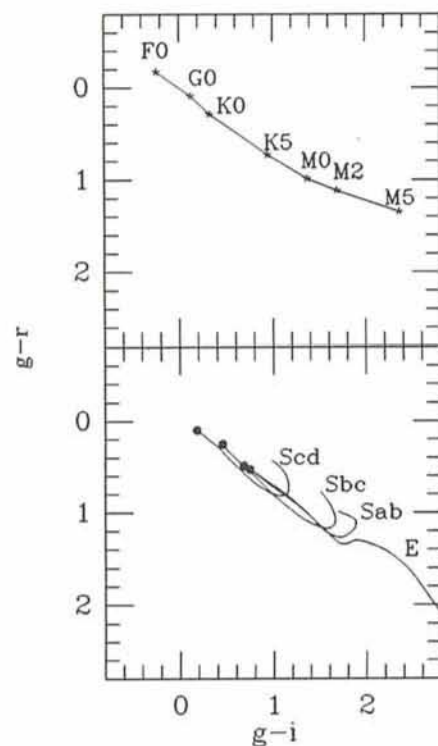


Figure 2: Two-colour diagram for the main-sequence stars (upper panel). In the lower panel the colour excursion for the different galaxy morphological types as a function of redshift (from $z = 0$ to 1 in the sense of increasing $g-i$) are shown with the zero-redshift points marked by filled dots (from Molinari et al. 1990).

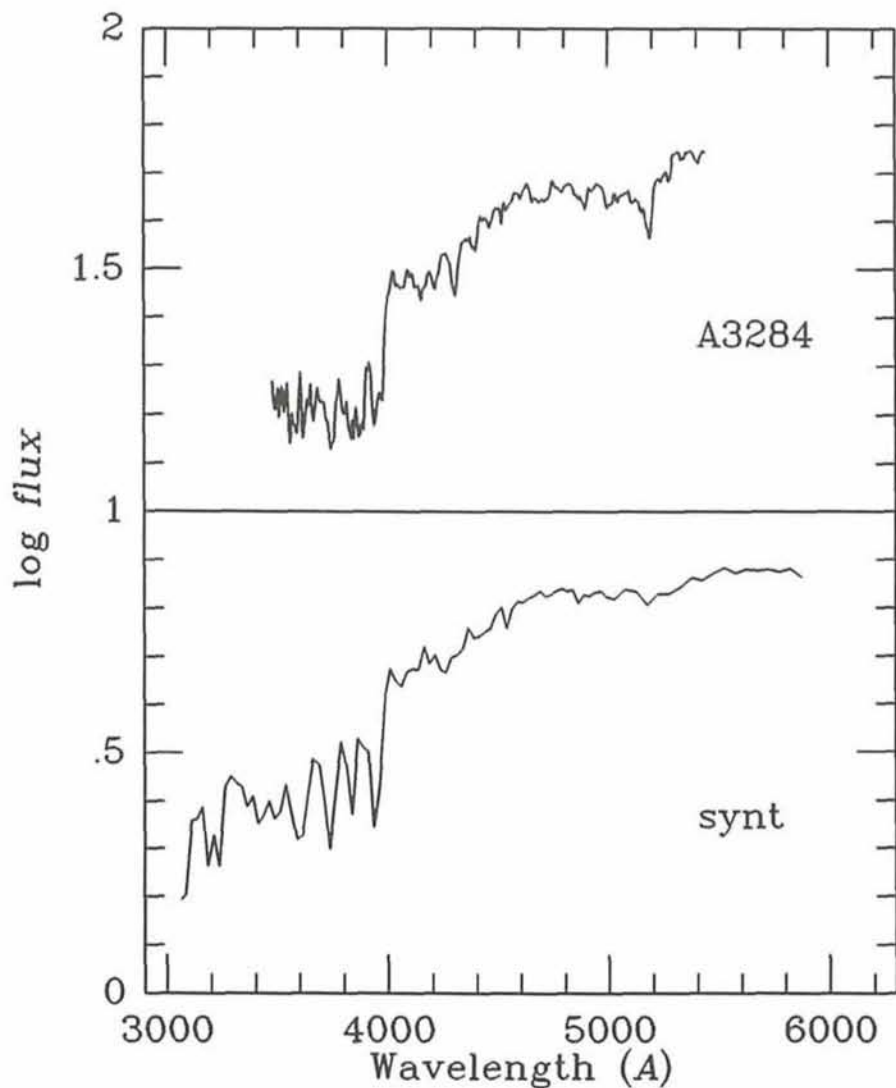


Figure 3: Observed and theoretical spectral distribution of elliptical galaxies. In the upper panel four spectra of red galaxies in the cluster A3284 have been coadded and reduced to restframe (six hours total exposure time with the ESO 3.6-m telescope + EFOSC. Grism B300 with a 230Å/mm dispersion). The lower panel shows for comparison an appropriate synthetic model for a 15 Gyr single burst stellar population (from Buzzoni 1989, his model No. 10 in Table 8).

lar" way following the prescription of stellar evolution. All those which deviate from the expectations will tell us something new, that is about events which have perturbed and/or accelerated the normal course of the evolution. This might be expected especially at high redshift.

4. Galaxy Type and Colour Segregation

A 25 kpc linear size galaxy at redshift z in a $q_0 = 0$ Universe is about $1.8h(1+z)^2/[z(1+z/2)]$ arcsec across (where $H_0 = 100h$ km/sec/Mpc). Its surface brightness dims as $(1+z)^{-4}$ so that this makes very difficult or even impossible to estimate the morphology at high redshift. Beyond $z \sim 0.2$ any direct morphological classification becomes unreliable even in deep CCD frames when taken under typical instrumental and

seeing conditions. That is why we must rely on colours to identify galaxy types.

A two-colour diagram could be used effectively to discriminate between late-type and early-type galaxies in distant clusters. Furthermore, combining it with a colour-magnitude diagram we can also discriminate between foreground and background objects (respectively too bright and too faint to be members of similar apparent colour). On the basis of accurate photometry we showed that redshift of distant clusters (up to $z \sim 0.45$) can be inferred from apparent galactic colours within a 10% accuracy (Molinari et al. 1990).

In Figure 1 we show some relevant $(g-r)/(g-i)$ diagrams for three clusters of our sample with z spanning between 0.15 and 0.50. In each panel the photometry of all objects in the fields is reported. Some striking features are worth of attention. (i) Both field stars and

galaxies spread along a diagonal strip in the diagram; (ii) the density along the strip is not constant and one clearly detects in each panel a clump of objects (encircled in the figure) moving to redder colours with increasing redshift; (iii) a tail of a few faint objects is always present redward the clump. Their apparent magnitude is correlated with colours, the reddest ones being also the faintest.

A full comprehension of the diagrams can be eased by comparing them with the two panels of Figure 2. In the first one we reported the locus expected for Galactic field stars of different spectral type while in the second panel we display the apparent colour excursion of galaxies of different morphological types with increasing redshift. It is now clear that the clump of objects observed in the colour-colour diagrams is originated by early-type galaxies at a redshift pertinent to that of the parent cluster.

Moreover, as a general rule we can note that foreground galaxies always lie blueward of the colour of the main clump due to the fact that E-galaxies are systematically the reddest objects within a given redshift. Accordingly, the faint tail of red objects with $g-i > 2$ is mainly contributed by field galaxies in the background (at $z > 0.5$) belonging to early types (spirals can never reach such colours as displayed in Figure 2). Also a few distant QSOs might be expected to lie in this zone (Irwin et al. 1991).

A complete support of the fact that galaxies in the main clump of the $(g-r)/(g-i)$ diagram can be the true progenitors of present-day ellipticals comes from the analysis of the spectra as shown in Figure 3. Here, an averaged spectrum obtained by summing up four red galaxies in A3284 is compared with a synthetic model of a 15 Gyr burst stellar population taken from Buzzoni (1989, his model No. 10 in Table 8).

5. What Contributes to the Blue Excess?

A more simple approach to the study of the cluster galaxy population rests also on the analysis of the single colour distribution like in Figure 4. In the figure we reported the $g-i$ distribution observed for the clusters A3284. Considering all the objects available (thick line in the figure) one clearly recognizes the major bump due to the early-type component in the cluster population as previously discussed. A second peak appears to bluer colours ($g-i \sim 0.5$) that we interpret as late-type galaxies. This group contains the excess blue galaxies claimed by Butcher and Oemler.

Following the canonical prescriptions (Butcher and Oemler 1984b) we were able to derive the fraction f_b of blue

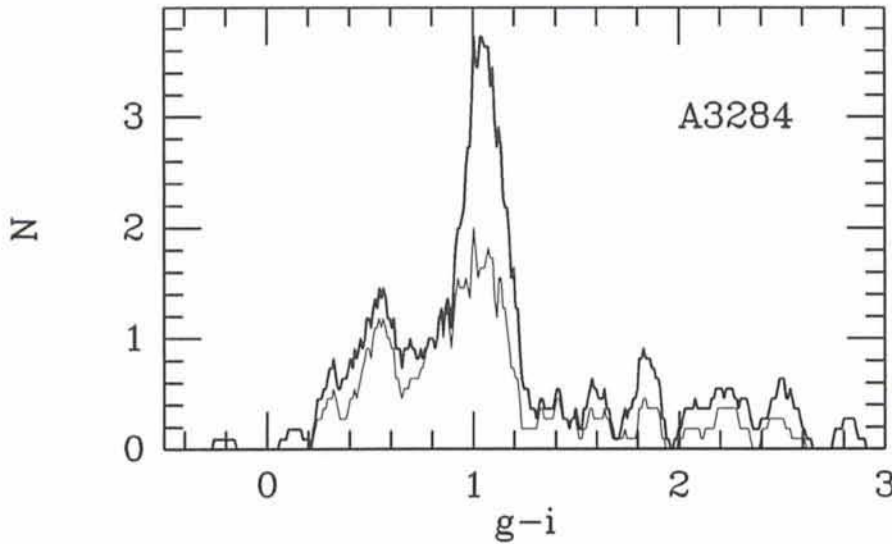


Figure 4: Histogram of the $g-i$ colour distribution in the cluster A3284. The thick line represents the distribution of the whole sample of measured objects, while the thin line accounts for the subsample fainter than $r = 21.5$. The histogram is generated by a moving average with beam 0.3 mag and step 0.01 mag .

galaxies for this cluster and for some others in our sample. The results are summarized in Figure 5 where we compare consistently with the work by Newberry et al. (1988). Our data confirm the Butcher-Oemler effect, with the blue galaxies becoming an increasing fraction of the high- z cluster population.

It is remarkable to note however that both on the basis of our photometric and spectroscopic observations collected to date we do not find any evident sign that the blue excess is due to an extensive presence of active or peculiar galaxies. The radial distribution of the galaxies in the blue bump in fact seems to closely match the trend observed by Whitmore and Gilmore (1991) for normal spirals in a large sample of low-redshift clusters. The question that arises is therefore whether we are observing somehow "active" blue elliptical galaxies or, more likely, a population of spiral-like galaxies.

A striking feature which seems to appear from the observations and could be worth further investigation is that blue galaxies in our sample tend to become relevant at the faint tail of the galaxy luminosity function. This is evident for example in Figure 4 where the thin line shows for A3284 the colour distribution of the objects fainter than $r = 21.5$ ($M_B > -17.5$ assuming $H_0 = 50 \text{ km/sec/Mpc}$).

As this magnitude roughly coincides with the limit where dwarf and non-dwarf galaxies contribute at the same level to the luminosity function (Binggeli et al. 1988) we are not able to univocally identify the real nature of the blue excess. A more complete and deep database will allow us to discriminate

whether or not in the clusters at high redshift the population of dwarfs was more evident, and therefore favours or disfavors the hypothesis of a luminosity-dependent evolution, as the recent results dealing with the dwarf-galaxy nature of the blue excess in the field counts seem to suggest (Cowie et al., 1991).

References

Binggeli, B., Sandage, A. and Tamman, G.A. 1988, *Ann.Rev.Astr.Ap.*, **26**, 509.
 Butcher, H. and Oemler, A. 1984a, *Nature*, **310**, 31.

Butcher, H. and Oemler, A. 1984b, *Ap.J.*, **285**, 426.
 Buzzoni, A. 1988, *Erice Workshop, Towards Understanding Galaxies at Large Redshift*, eds. R.G. Kron and A. Renzini (Dordrecht: Kluwer) p. 61.
 Buzzoni, A. 1989, *Ap.J.Suppl.*, **71**, 817.
 Buzzoni, A. Molinari, E.C., Manousoyannaki, I. and Chincarini, G. 1988, *The Messenger*, **53**, 50.
 Cappi, A., Chincarini, G., Conconi, P. and Vettolani, G. 1989, *Astr.Ap.*, **223**, 1.
 Coleman, G.D., Wu, C. and Weedman, D.W. 1980, *Ap.J.Suppl.*, **43**, 393.
 Cowie, L.L., Songaila, A. and Mu, E.M. 1991, *Nature*, **354**, 460.
 Dressler, A. 1980, *Ap.J.*, **236**, 351.
 Dressler, A. and Gunn, J.E. 1982, *Ap.J.*, **263**, 533.
 Dressler, A. and Gunn, J.E. 1983, *Ap.J.*, **270**, 7.
 Irwin, M.J., McMahon, R.G. and Hazard, C. 1991, *The Space Distribution of Quasars*, ed. D. Crampton, Astr. Soc. of the Pac. Conf. Ser., vol. 21, p. 117.
 Koo, D.C. 1988, *Erice Workshop, Towards Understanding Galaxies at Large Redshift*, eds. R.G. Kron and A. Renzini (Dordrecht: Kluwer) p. 275.
 Luppino, G.A., Cooke, B.A., McHardy, I.M. and Ricker, G.R. 1991, *Astr.J.*, **102**, 1.
 Molinari, E., Buzzoni, A. and Chincarini, G. 1990, *M.N.R.A.S.*, **246**, 576.
 Molinari, E., Pedrana, M.D., Banzi, M., Buzzoni, A. and Chincarini, G. 1992, *Proceedings of the IAU Symp. No. 149 "The Stellar Populations of Galaxies"*, eds. B. Barbuy and A. Renzini (Dordrecht: Kluwer) p. 460.
 Newberry, M.V., Kirshner, R.P. and Boroson, T.A. 1988, *Ap.J.*, **335**, 629.
 Thompson, L.A. 1988, *Ap.J.*, **324**, 112.
 West, R.M. and Kruszewski, A. 1981, *Irish Astr.J.*, **15**, 25.
 Whitmore, B.C. and Gilmore, D.M. 1991, *Ap.J.*, **367**, 64.

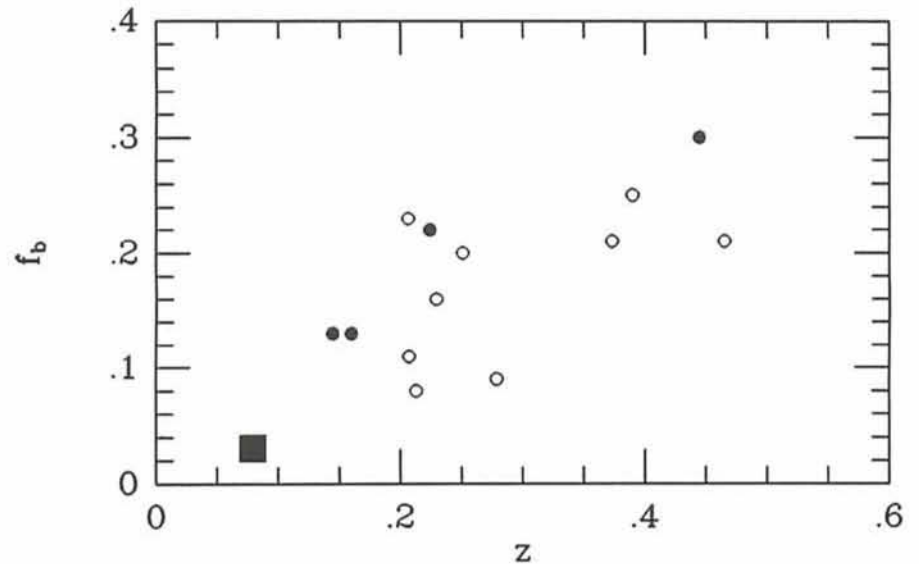


Figure 5: Diagram showing the fraction of blue galaxies f_b . Open dots are taken from Newberry et al. (1988, their Fig. 2). The filled square bottom left is the mean estimate for 8 low-redshift clusters (up to $z = 0.08$) from Butcher and Oemler (1984b). Filled dots are our data and refer to the clusters A3284, A3305, A1942 and 2158+0351 in order of increasing redshift.

Probing Beyond COBE in the Interstellar Medium

E. PALAZZI, M.R. ATTOLINI, N. MANDOLESI, *Istituto T.E.S.R.E., Bologna, Italy*
P. CRANE, *ESO*

Introduction

The COBE satellite, with its instruments, has provided new insights into the origin and evolution of the Universe. The FIRAS (Far Infrared Absolute Spectrophotometer) has supplied the best demonstration that the Cosmic Background Radiation is a blackbody (Mather et al., 1990). The DMR (Differential Microwave Radiometer) has provided what appears to be the first measurement of the structure in the angular distribution of the background radiation (Smoot et al., 1992).

What more is there to do and how can it be done?

Beside what may be done by subsequent satellites, two important measurements can be made using interstellar thermometers. The first is to provide a precise independent check on the absolute calibration of the FIRAS spectrophotometer. The second and most interesting from a cosmological point of view is to demonstrate the homogeneity of the CBR radiation. A third possibility would be to verify the expansion of the Universe via the $(1+z)$ dependence of the temperature of the CBR.

One of the fundamental assumptions in current cosmological models is the homogeneity of the Universe and hence of the CBR radiation. Homogeneity

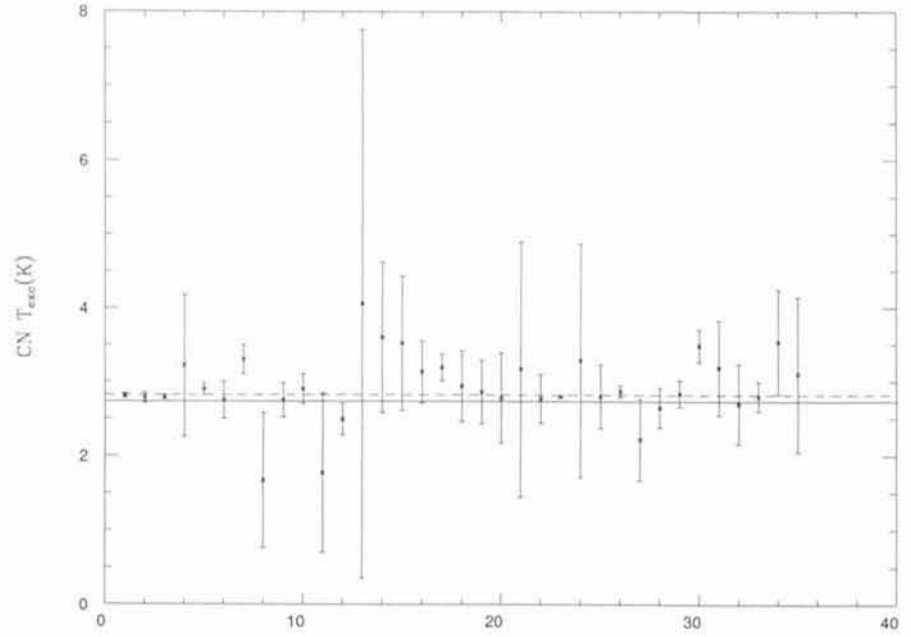


Figure 1: Measured $T_{exc}(CN)$ with the associated 1σ errors vs increasing HD number of the observed stars (Palazzi et al.). The solid line represents the COBE result for T_{CBR} , $T = 2.735 \pm 0.06$ K, the dashed line is the weighted average of the $T_{exc}(CN)$ values, $T = 2.818 \pm 0.018$ K, the dashed line is the weighted average of the $T_{exc}(CN)$ values, $T = 2.818 \pm 0.018$ K.

means that an observer anywhere in the Universe should measure the same global properties. In particular, the temperature of the CBR should be the same.

Soon after the discovery of the CBR, it was recognized that the rotational excitation of interstellar CN could provide one of the best thermometers for determining the T_{CBR} . Subsequently, modern techniques have pushed the method close to the precision of the best radiometers. Although the radiometers are quite precise, they are only able to measure the CBR temperature locally (≈ 1 AU of the Sun) and they depend on sophisticated and complicated methods for calibration.

On the other hand, interstellar CN, which has been seen in several clouds within 1 Kpc, is able to report to us the intensity of the CBR radiation field in its vicinity. In addition, the actual temperature determination relies on a rather direct technique.

CN Measurements of the CBR Homogeneity within 1 Kpc

A recent compilation (Palazzi et al., 1992) of the measurements of CN excitation temperatures for bright stars has not shown any large differences in the T_{CBR} in any direction providing the largest body of data to support the homogeneity of the CBR even if only within about 1 Kpc. However, most of the CN excitation tem-

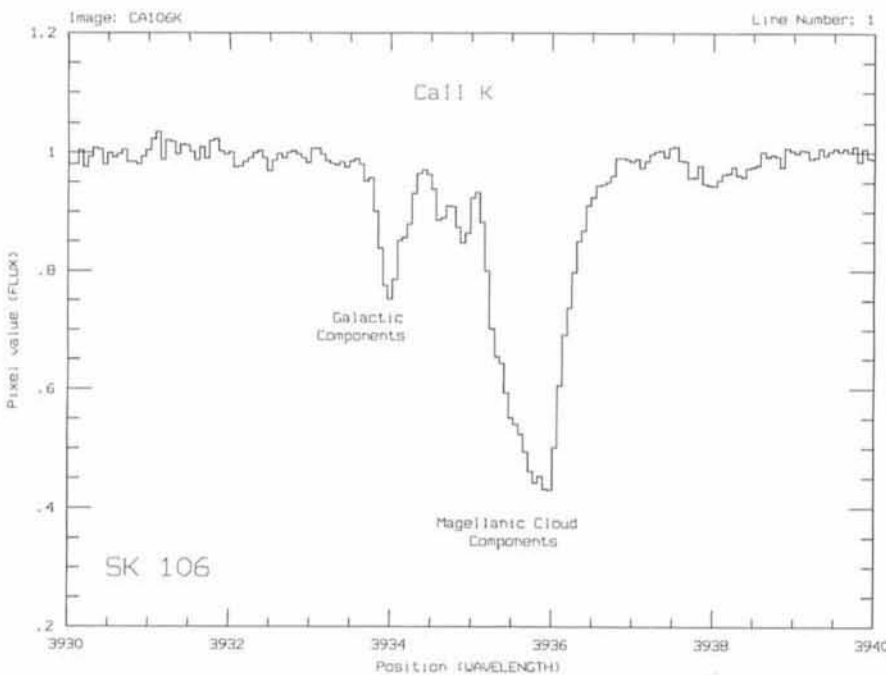


Figure 2: Interstellar Ca II K towards the star SK 106 (SMC). Galactic components and Magellanic Cloud components are well distinguishable.

peratures appear slightly above ($\approx 80 \pm 30$ mK) the COBE measurement of $T_{\text{CBR}} = 2.735$ K (Fig. 1). A possible explanation of this excess would be the presence of local excitation mechanisms (such as collisional excitation). None of the data necessary to quantify these mechanisms are of sufficient quality to provide a clear explanation of the observed difference. Improved observations would be needed to obtain better data on local conditions in molecular clouds and on CN absorption line measurements to show if the excess in the CN excitation temperature is really a result of collisional excitation.

Homogeneity within 50 Kpc

A very real possibility exists to determine T_{CBR} in the Magellanic Clouds if an appropriate sight line with sufficient CN column density can be found. Such a measurement is just within the possibility of the largest telescopes in the southern hemisphere.

We have initiated a programme for observing a sample of lines of sight towards bright and reddened O and B stars in the Magellanic Clouds. The observations were performed in October 1991 at the 3.6-m ESO telescope (La Silla, Chile) using the CASPEC spectrograph with the 31.6 line/mm grating plus the long camera in the wavelength range 3800Å–4500Å.

Preliminary results show that the Ca II H and K interstellar lines (both galactic and Cloud components) are present in all the observed stellar spectra (Fig. 2). Molecular absorption lines of CH and CN are marginally visible (Fig. 3), representing the first detection of the CN species in the Magellanic Clouds interstellar medium. Detection of interstellar CH and CH* has been reported only towards supernova 1987 by Magain and Gillet (1987).

Additional observing time is needed for improving the molecular detection, in particular CN for the measurement of the T_{CBR} at 50 Kpc from us.

Homogeneity on Large Scales

It may be possible to observe the excitation of other molecular rotation or atomic fine structure lines at quite large distances (Bahcall and Wolf, 1968). Indeed a few reports (Meyer et al., 1986; Wampler, 1990) of upper limits to T_{CBR} at redshift around $z = 1.6$ and $z = 2.5$ have been reported for the excitation of CI and CII fine structure lines.

In contrast to the measurements in the Magellanic Clouds the measurements at high redshift introduce a rather large uncertainty in the local condition of the species observed, for example local ex-

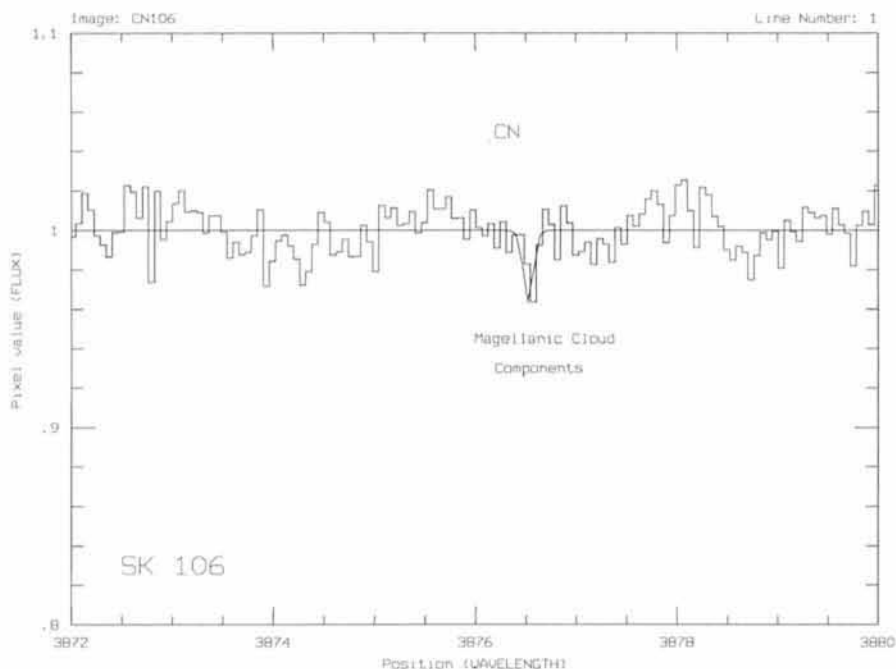


Figure 3: Interstellar CN towards the star SK 106 (SMC). The position of the line coincides with one of the stronger components of the interstellar Ca II K in the Small Magellanic Cloud. The upper limit for the CN column density is $1 \times 10^{13} \text{ cm}^{-2}$.

citation mechanisms such as collisional processes or local UV field are difficult to evaluate. Nevertheless, a determination of $T_{\text{CBR}}(z) < (1+z)[T_{\text{CBR}}(z=0)]$ at any redshift would be very difficult to explain in the context of the standard cosmological scenarios. Though they are affected by large uncertainties, the existent upper limits to $T_{\text{CBR}}(z)$ do not contradict the present theories.

In summary, exciting and important cosmological results are possible from a careful study of the interstellar thermometers available to us.

References

- Bahcall, J.N., and Wolf, R.A., 1968, *Ap.J.*, **152**, 701.
- Magain, P., and Gillet, D., 1987, *Astr.Ap. Lett.*, **184**, L5.
- Mather, J.C., et al., 1990, *Ap.J. Lett.*, **354**, L37.
- Meyer, D.M., Black, J.H., Chaffee, F.H. Jr., Foltz, C.B., and York, D.G., 1986, *Ap.J.*, **308**, L37.
- Palazzi, E., Mandolesi, N., and Crane, P., 1992, *Ap.J.*, Oct. 10, 1992.
- Smoot, G.F., et al., 1992, *Ap.J. Lett.*, **396**, L1.
- Wampler, E.J., 1990, *Ap.J.*, **368**, 40.

New ESO Conference and Workshop Proceedings

The Proceedings of the ESO Workshop on **HIGH-RESOLUTION SPECTROSCOPY WITH THE VLT** have just become available. The 310-page volume, edited by M.-H. Ulrich, is offered at a price of DM 45.-.

The following publications are in press and will become available end of September/beginning of October 1992:

ESO CONFERENCE ON HIGH-RESOLUTION IMAGING BY INTERFEROMETRY II. These Proceedings, edited by J.M. Beckers and F. Merkle, are divided into two volumes (Part I and Part II) and contain more than 140 papers on a total of more than 1320 pages. The price is DM 110.-.

4th ESO/ST-ECF DATA ANALYSIS WORKSHOP. This 188-page volume, edited by P.J. Grosbøl and R.C.E. de Ruijscher, will be available at a price of DM 25.- (all prices include packing and surface mail).

Prepayment is required for all publications. Payments have to be made to the ESO bank account 2102002 with Commerzbank München or by cheque, addressed to the attention of

ESO, Financial Services
Karl-Schwarzschild-Str. 2
D-8046 Garching b. München, Germany

Please do not forget to indicate your complete address and the title of the Proceedings.

IRAC2 at the 2.2-m Telescope

A. MOORWOOD, G. FINGER, P. BIEREICHEL, B. DELABRE, A. VAN DIJSSELDONK,
G. HUSTER, J.-L. LIZON, M. MEYER, ESO, Garching,
H. GEMPERLEIN, A. MONETI, ESO, La Silla

ESO's new infrared camera, IRAC2, is equipped with a Rockwell 256×256 pixel NICMOS3 array for imaging through broad and narrow band filters between 1 and 2.5 μm and a K (2.2 μm) band scanning Fabry Perot. A preview of some of its capabilities was already given in the June 1992 issue of the *Messenger* (68, 42) where we showed a 2.1 μm broad band image of a $z = 0.2$ galaxy cluster and a narrow band [FeII](1.64 μm) mosaic image of the SNR RCW103 obtained during the first test on the 2.2-m telescope in May. In this article we give a description of the instrument and its observing modes together with performance figures derived from the test data and some additional images selected to illustrate some of its possible scientific applications.

1. Description of IRAC2

Figure 1 is a photograph of IRAC2 mounted on the F/35 infrared adapter at the Cassegrain focus of the 2.2-m telescope. The camera itself is housed in a modified Oxford Instruments 4-l liquid helium cryostat which is partially hidden by the attached motor control and detector acquisition electronics. (Although the NICMOS3 array has a long wavelength cut-off at $\sim 2.5 \mu\text{m}$ and requires cooling to only $\sim 60\text{K}$ using pumped liquid nitrogen, a He cryostat was selected in order to keep open the possibility of installing arrays operating out to 5 μm in the same camera in the future.) The black unit sandwiched between the camera and the adapter houses the scanning Fabry Perot etalon(s) and remotely controlled exchange mechanism used to rotate it in front of the entrance window.

Figure 2 shows the layout of the camera optics. The input doublet field lens, which also acts as the cryostat entrance window, provides for a 70-mm diameter (~ 3 arcmin.) field and re-images the telescope pupil at the cold 4.5-mm diameter cold stop just behind a 24-position filter wheel. The field is re-imaged on the detector by one of the five remotely selectable objectives mounted on a wheel. In order to minimize flexure, the camera itself is rigidly attached to the outer vacuum housing via glass thermal isolators and the optics and detector mount are cooled via thermal connections to the inner radiation shield and

inner cryogen tank respectively. Figure 3 is a photograph of the cooled optical assembly showing the filter wheel on the left and, on the right, the objective wheel which is largely hidden by the detector mount.

The NICMOS3 array is a hybrid device consisting of a HgCdTe diode array bonded via indium bumps to a multi-

plexer which is structured in four quadrants having separate output amplifiers. It is controlled and read by a programmable, VME-based, detector controller which has been developed in Garching and contains four A/D converters allowing simultaneous reading of the four quadrants. This system also contains a Motorola 68030 processor which runs



Figure 1: IRAC2 mounted on the F/35 adapter at the 2.2-m telescope.

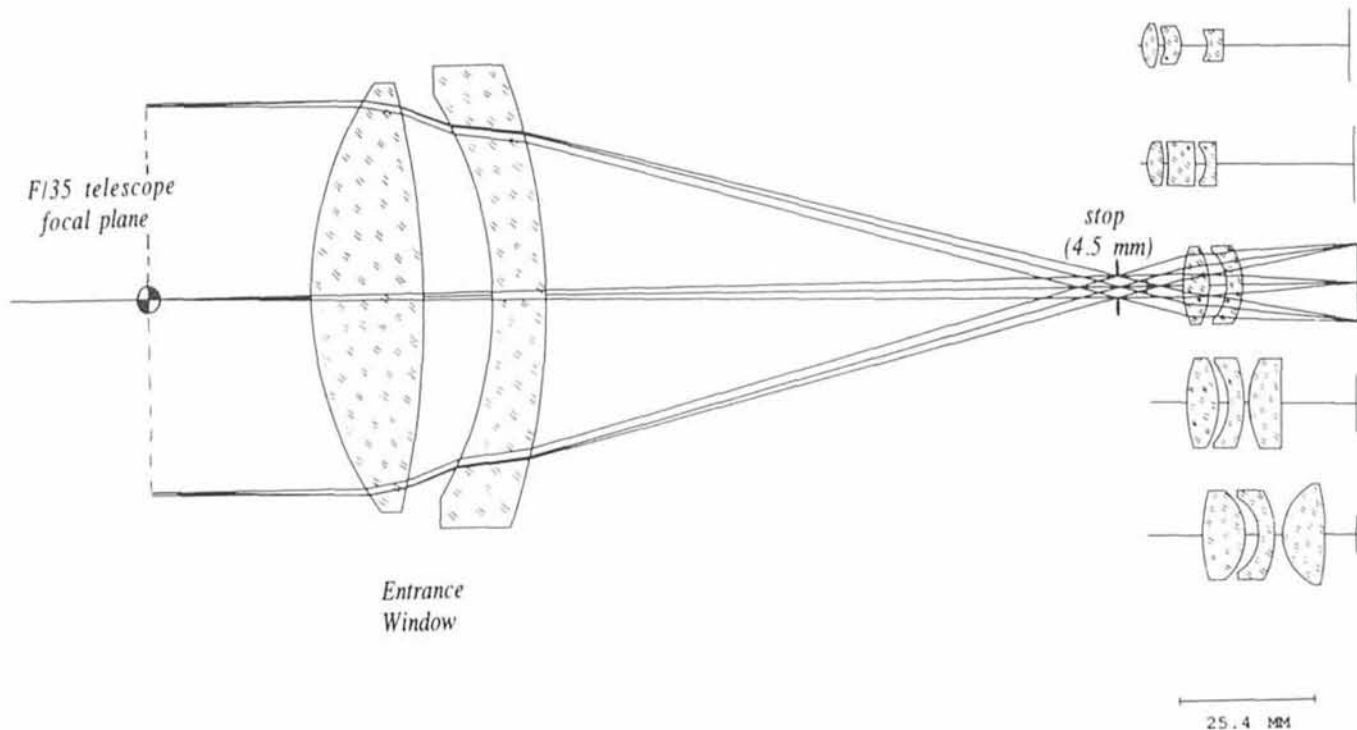


Figure 2: Optical layout of the camera. The input doublet covers a 70-mm (3-arcmin.) diameter field and acts both as the field lens and the cryostat window. A 24 position filter wheel (not shown) is located in front of the cold pupil stop and the five remotely interchangeable objectives mounted on a wheel behind the pupil stop provide for magnifications from ~ 0.14 – $1.1''/\text{pixel}$.

detector pre-processing software under the OS9 operating system. This processor receives command files specifying the required detector set-up from the instrument workstation; transmits real time images to a monitor in the control room and sends images, with or without co-averaging, to the instrument workstation. The real time display is particularly useful during set-up on an object field as pixel values and coordinates can be measured and cut-levels set using only the mouse. The observer can select from a variety of read-out modes including double and triple correlated and multiple nondestructive sampling. A novel variant of the latter mode, tested in May but not yet implemented in a very user friendly way, also achieves partial seeing correction by tracking a reference object in the field and applying a shift and add algorithm to each non-destructively read sub-image before solution of the error equations for the integration ramps. At present, the minimum time required to read out a full 256×256 image is ~ 700 ms. A faster read-out could improve the performance of the real time shift and add mode and could be implemented in the future by installing a faster pre-processor which is now available.

In view of the plan to phase out the HP 1000 series computers on La Silla the user interface runs on a workstation and MIDAS is used on-line for data storage, image display and quick-look anal-

ysis. The arrangement used during the test is shown in Figure 4 but is provisional pending completion of a new standard user interface and VME based motor control system on La Silla. Instrument set-up and control is via typed commands and menu bars on the

HP370 which runs control software written in Basic which was developed originally only for laboratory testing in Garching. This workstation is connected to the instrument via CAMAC for the motor controls, a GPIB bus for the Fabry Perot control and ethernet fibre optics

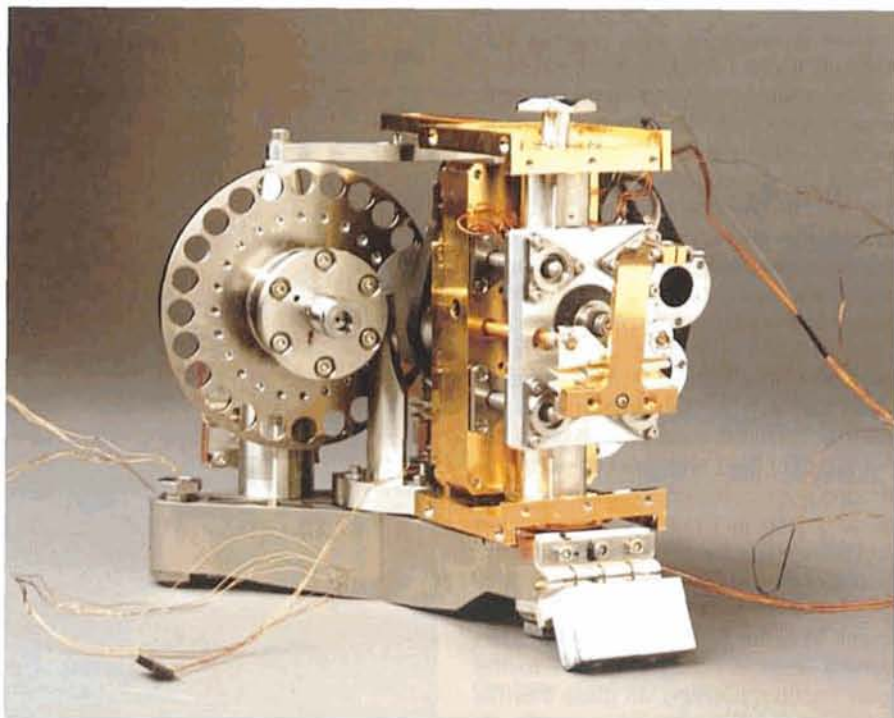


Figure 3: The cryogenic optical assembly showing the filter wheel on the left and the objective wheel on the right which is partially hidden by the detector mount.

links to the detector pre-processor. There is also an RS232 link to the HP1000 telescope computer which is used to step the secondary mirror during focus exposures and to read coordinates which are written in the file headers. The HP730 workstation is used to run two parallel MIDAS sessions. One of these is set in the background mode and is used to display images (with or without background subtraction as requested) and store them in the correct format while the other is available for interactive image analysis using MIDAS. The HP370 should become superfluous once the new user interface is available when both the control software and MIDAS will run on the HP730 with a separate X11 window terminal available for on-line analysis.

2. Observing Modes

IRAC2 provides for imaging at a variety of image scales through broad and narrow band filters between 1 and 2.5 μm and a K(2.2 μm) band scanning Fabry Perot etalon yielding $R \sim 1000$.

The available filters, image scales and corresponding field sizes are summarized in Table 1. The scales A-D are measured values derived from images of astrometric double stars. Although objectives D and E should provide a circular 3' field limited by the entrance window this is slightly vignetted on two sides at present by the dichroic mirror in the F/35 adapter. For broad-band imaging, when background noise dominates, it is recommended in any case to use objective C (0.494"/pix.) in general. This objective has the highest efficiency, yields the maximum square field and provides reasonable sampling under average seeing conditions. Objective B(0.27"/pix.) can be used when better sampling/spatial resolution is more important than field.

The desired observing mode, filter, magnification and detector parameters are set via the workstation user interface. A present, the standard modes are (i) focus (ii) DC observing (staring) and (iii) Fabry Perot scan. Chopping and automatic beamswitching could be implemented but are not considered particularly useful with this array. Real time shift and add is more complicated to set-up and is not yet available as a standard mode.

For focussing on a star the focus mode is used to automatically step the telescope secondary mirror through a specified range of positions and record images which are displayed in a line at the end of the measurement. The best focus can then be determined by measuring the FWHM using MIDAS and the secondary set to that position. Dif-

Table 1: IRAC2 characteristics.

Image Scales and Fields		
Objective	Arcsec/pix	Arcsec
A	0.14	36×36
B	0.27	69×69
C	0.49	125×125
D	0.70	$\Phi = 180$
E	1.1	$\Phi = 180$
Filters		
Name	λ (μm)	$\Delta\lambda$ (μm)
J	1.25	0.3
H	1.65	0.3
K'	2.1	0.34
K	2.2	0.4
NB1 (FeII)	1.262	0.04
NB2 (FeII)	1.645	0.04
NB3 (HeI)	2.058	0.036
NB4	2.105	0.037
NB5 (H ₂)	2.121	0.039
NB6	2.136	0.038
NB7	2.148	0.037
NB8 (Br γ)	2.164	0.037
NB9	2.177	0.038
NB10	2.216	0.075
NB11 (CO)	2.365	0.088
Fabry Perot	$\sim 2-2.5$	$\lambda/\Delta\lambda \sim 1000$

ferential focus changes during the night due to telescope temperature changes can be made using a calibration curve without needing to repeat the star measurements. A focus shift is required when using the Fabry Perot.

The DC mode used for observing requires little explanation. Each image is written into a separate file with its own identifier and a header which contains all the instrument and detector parameters plus the time and telescope coordinates.

In the Fabry Perot mode the required narrow band order isolating filter can be set manually or automatically and both the filter transmission curve and the wavelengths corresponding to the different orders displayed on the screen. A sequence of images can be made by entering a list of the desired

wavelengths which are automatically written in the file headers.

The detector set-up includes selection of the read mode; the on-chip integration time (DIT); the number of integrations (NDIT) to be averaged in the pre-processor before transmission to the workstation and the number of such measurements to be made (cycles) and stored in separate files. If in doubt, the read-mode should be set to double-correlated. Multiple, non-destructive, sampling is needed for the shift and add mode and yields somewhat lower read-noise for long measurements but involves larger time overheads and increases the amplifier glow in the corners of the array. The main considerations in selecting DIT are that it should be short enough to avoid saturation ($K \sim 8$ for DIT = 1s with objective C) but long enough

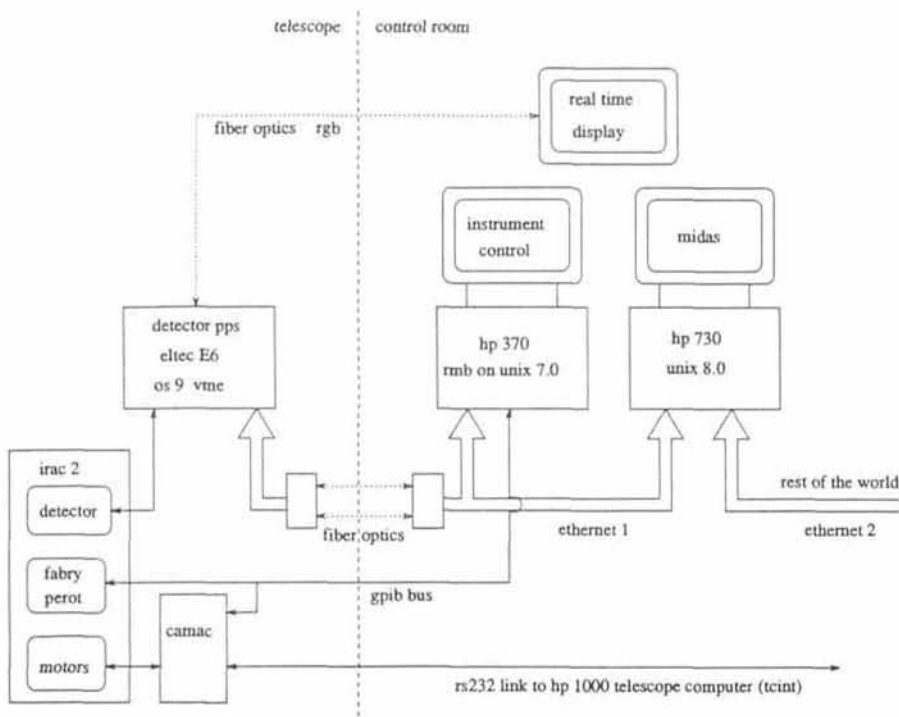


Figure 4: Provisional control set-up for the IRAC2 test in May.

to achieve background limited performance when observing faint sources (typically a few seconds for the broadband filters). Most of the test observations were made using $DIT = 1s$ for standard stars and 10–30s for the science frames. The value of NDIT is a trade-off between the s/n ratio in each stored image and the time between object and sky frames which should not be too long because of sky fluctuations. During the test NDIT was selected typically such that $DIT \times NDIT$ was 2–5 min and $CYCLES = 1$. In order to remove stars and achieve optimal sky subtraction it is, in any case, necessary to have several sky frames on different positions. For the optimal removal of bad pixels it is also desirable to have several object frames on different positions. Particularly for faint sources therefore the best observing procedure is to combine all requirements by making a series of exposures at telescope positions separated by 10–20 arcsec. on the sky. All frames can then be used to derive the mean sky with the stars removed and, after re-registering, be combined into a final object image in which bad pixels have been replaced with good ones from other frames in the stack. This technique was used to produce the galaxy cluster image reproduced in the June 1992 *Messenger*. An alternative, used for several of the test images reproduced here, is to use the same object position but different sky positions or, in the limit, just single object and sky frames. This simplifies the data reduction (particularly the on-line quick look

analysis) but means that only half the total time is spent on the object and bad pixels can only be corrected within the image by median filtering or pixel inter-

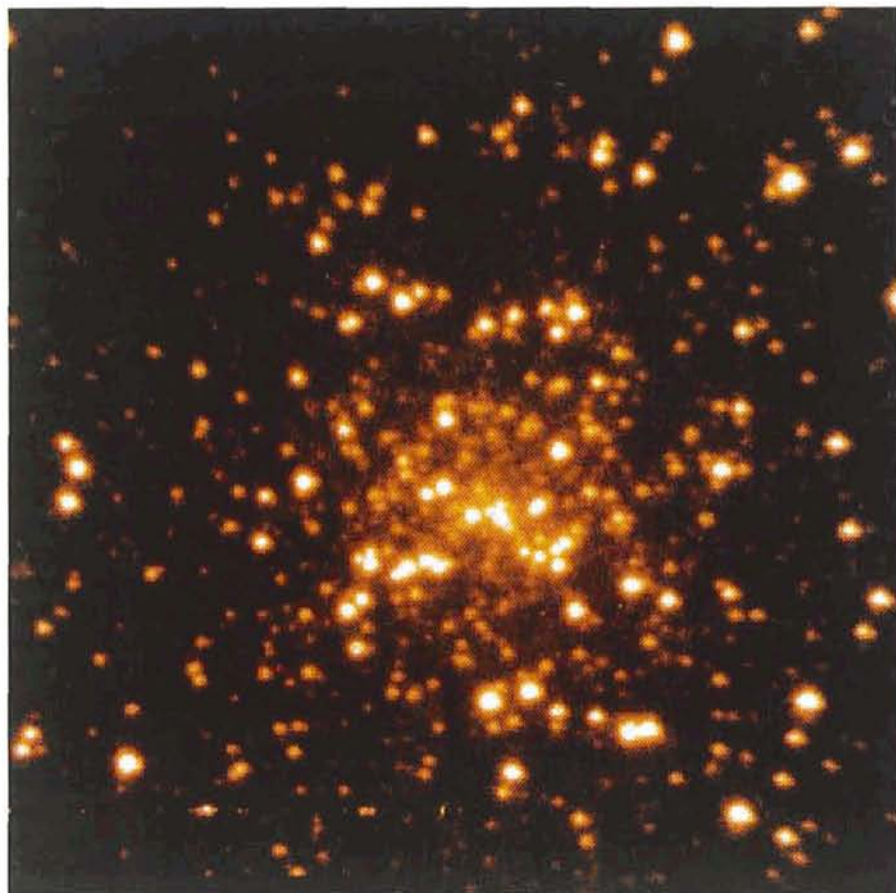


Figure 5: K band image of the core of the globular cluster M15. Integration time was 60s (30×2s) on object and sky and the scale is 0.27"/pixel.

polation/replacement using a bad pixel mask.

3. Performance

Characteristics of the presently installed NICMOS3 array are summarized in Table 2 and the overall broad band system performance as measured on the telescope is given in Table 3.

The magnitude limits obtained in the broad band filters correspond to the background limits expected from the measured counts and for longer measurement times the s/n should improve as $t^{1/2}$. In K' , for example, the limit in 20 min should be 19.6 mag/(arcsec²) while the value derived from the galaxy cluster image shown in the June *Messenger* is 19.8, i.e. actually somewhat better than expected but probably consistent within the uncertainties (e.g. the detector electrons/ADU conversion factor).

Good photometry should be possible with this camera. Zero points determined from standard stars observed over the 7 nights (when the sky was clear) agree to within 1–2% after flat fielding. The flat fields used were obtained by taking difference images of the diffusing screen in the dome with the halogen lamp on and off. This technique

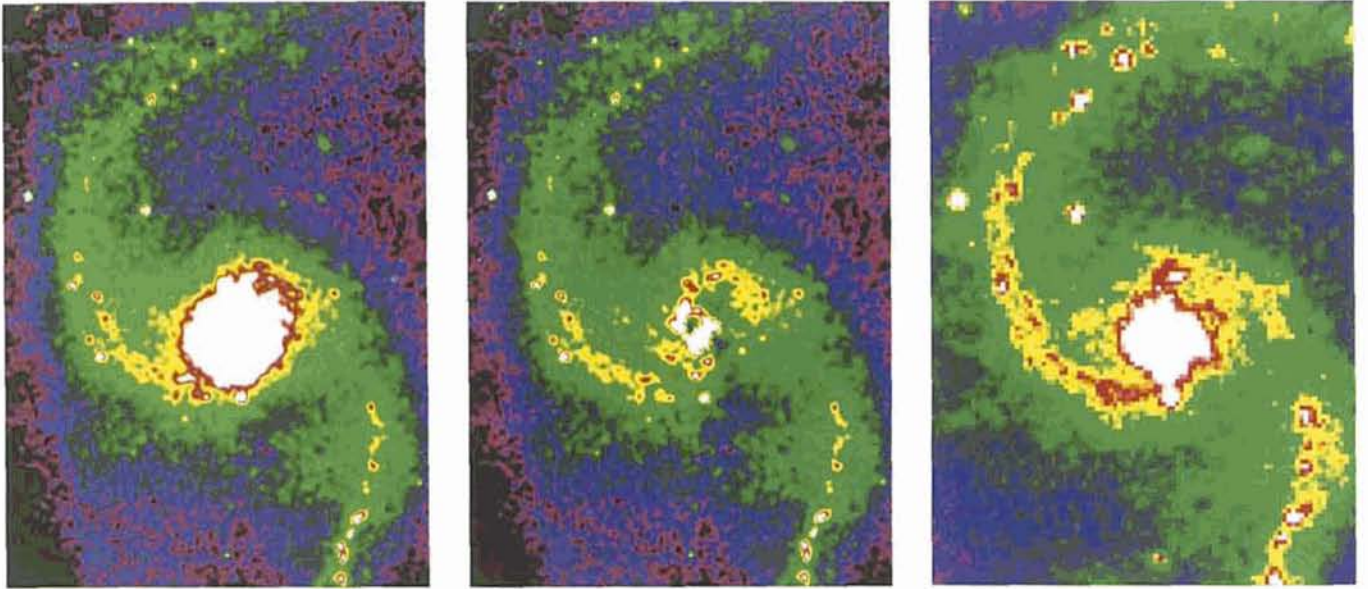


Figure 6: NGC5247. The left panel is a smoothed K' mosaic image; centre panel is the K' image after subtraction of a fit to the inner galaxy disk component and the right panel is an R -band image obtained by scanning the POSS E plate. N is down and E is to the left. The infrared images have been constructed from four 120s (10×12 s) exposures with the $0.49''/\text{pixel}$ objective on each of two overlapping fields on the galaxy and six sky exposures of the same duration offset several arcmin. from the galaxy. Only the frames showing systematic differences less than 1% were used and stars in the sky frames were fitted with gaussians and removed individually before subtraction from the object frames. Smoothing using the MIDAS adaptive filter technique was applied to enhance the visibility of low surface brightness features. Note that a spur off the northern spiral arm is only visible in the POSS R image and not K' suggesting that it is not part of the grand design density wave in the galaxy.

Table 2: NICMOS3 array detector characteristics.

Format (pixels)	256 × 256
Pixel size	40 μm
Cut-off wavelength	2.5 μm
Bad pixels	< 1% ¹
Quantum efficiency	~0.6 (2.2 μm), 0.4 (1.25 μm)
Well capacity	~10 ⁵ e
Dark current	~30e/s ²
Read noise	~30e
1. Including a dead column in one quadrant. 2. Probably dominated by camera thermal background	

Table 3: Overall system performance (objective C).

Band	J	H	K'	K
Overall efficiency ¹	0.15	0.24	0.23	0.24
Background (mag./arcsec) ²	15.2	13.6	12.7	12.3
Mag. Limits /arcsec ² (3 σ in 60s) ³	20.5	19.1	18.3	18.2
Mag. Limits (3 σ in 60s/5" ap.)	18.9	17.5	16.7	16.6
1. Detected photons as a fraction of those incident on the atmosphere taking into account telescope central obscuration and undersizing of the F/35 secondary. 2. Telescope temperature ~ 283K. 3. For 60s object and 60s sky scaled from differences of sky frames with integrations of 20 × 10s.				

has the advantage of cancelling any "dark current" pattern due to radiation seen through the filters and not present with the dark filter. The images reduced so far do appear to be flat within the noise and, at least in the K and K' prime filters, are better than can be obtained using sky flats. This seems to be due to the fact that sky-dark frames contain a faint ring-like structure which disappears in the object-sky images. Its outer diameter just matches the size of the array and is independent of magnification implying that it originates in or close to the detector. As yet, however, no convincing explanation for this effect has been found. The $0.27''/\text{pixel}$ objective also shows an additional ring which appears in both the sky and dome flats and whose origin is equally unclear. These effects are typically a few per cent of the mean background and are not apparent in the reduced images except in one or two cases where the background varied by large amounts during the measurement due to clouds. Although apparently not significantly affecting the overall performance, therefore, this problem still requires further investigation.

Another aspect requiring further study is the stability of the array response. The reproducibility between images and of the zero points derived from standard star observations over seven nights suggests that this is not a problem over most of the array area. Mosaics made

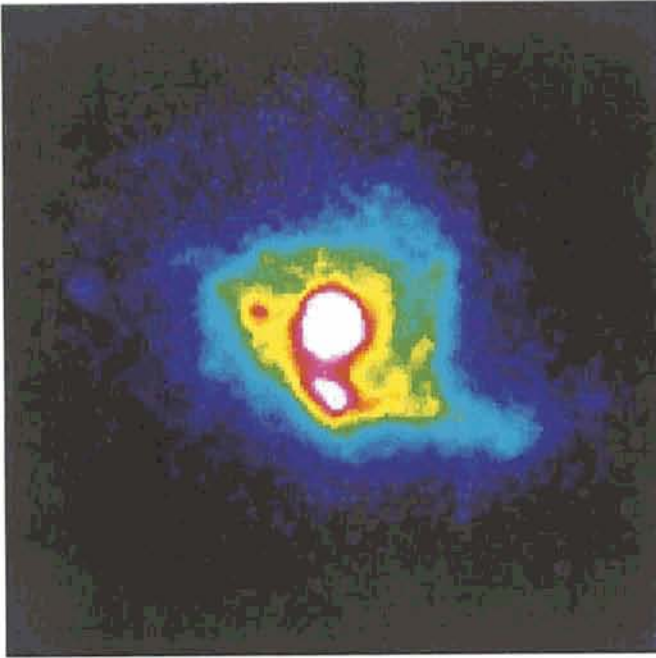


Figure 7: K' image of the merging galaxy system NGC3256. The scale is $0.27''/\text{pixel}$ and the image is the difference of single 120s ($12 \times 10\text{s}$) exposures on the galaxy and sky.

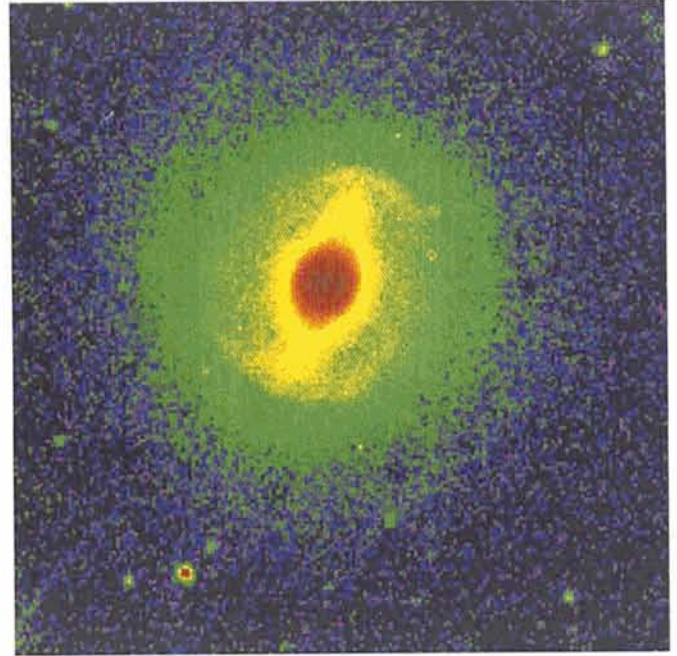


Figure 8: K' image of the Seyfert galaxy NGC3783. Scale is $0.49''/\text{pixel}$ and sky subtraction and bad pixel correction has been made using two sets of four 120s ($12 \times 10\text{s}$) exposures of the galaxy at different positions on the array and eight interleaved sky frames with the same integration time.

from overlapping images (see e.g. the RCW103 image in the June *Messenger*), however, suggest that

some instabilities at the edges could be present. These appear to be variations at the few % level and are confined to a

rather sharply defined strip along one edge. Curiously, however, this effect appears on different, orthogonal, edges in the J and K bands! Pending further investigation we assume these are intrinsic to the array (i.e. as opposed to variations in the background illumination which would be hard to explain).

4. Sample Images

A K' ($2.1 \mu\text{m}$) image of the $z = 0.2$ galaxy cluster A1689 and a narrow-band $[\text{FeII}](1.644 \mu\text{m})$ image of the supernova remnant RCW103 were already included in the June *Messenger* (68, 42) as examples of (i) "deep" imaging by combining exposures made at slightly different telescope positions and (ii) mosaicking of images displaced by almost the full field respectively. Figures 5–11 are some additional images selected to illustrate other possible modes and applications of the camera. As only single-object positions were used for most of these observations the bad pixels have generally been masked and replaced by interpolation in the surrounding area. Unless otherwise stated in the figure caption these images are oriented with N at the top and E to the left.

Conclusions

The overall measured performance of IRAC2 is close to that predicted in advance of the test and, although some aspects still require further investiga-

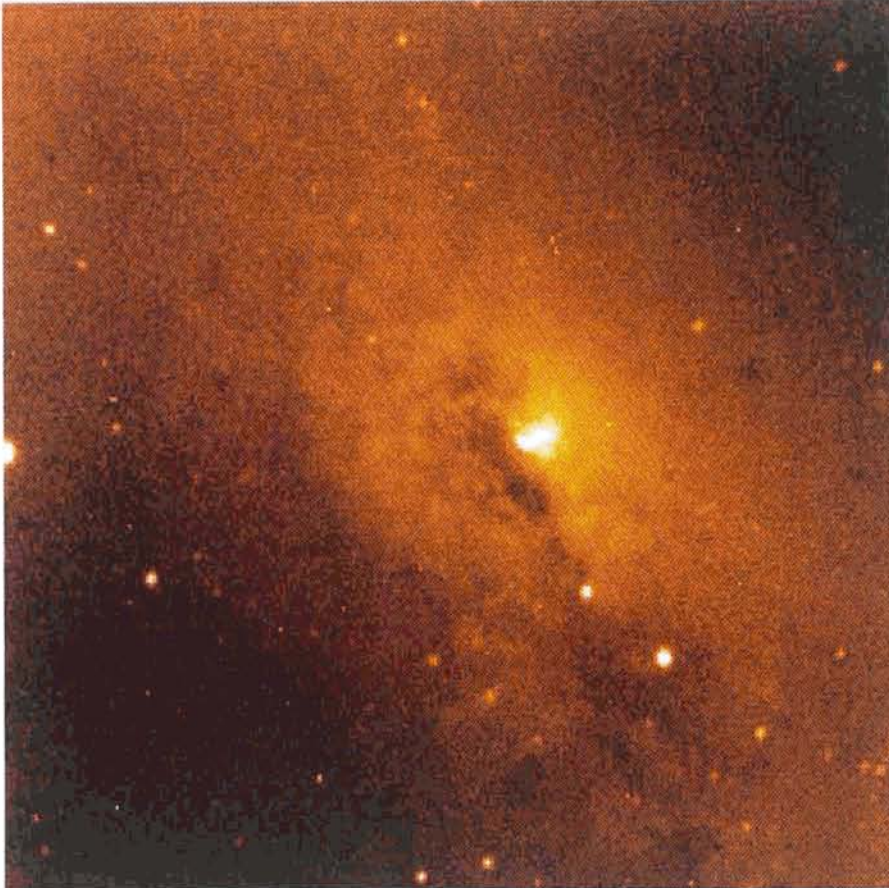


Figure 9: J image of the visually obscured nucleus in the nearly edge on galaxy NGC4945 made from three 120s ($6 \times 20\text{s}$) exposures on the galaxy and two on the sky. Scale is $0.49''/\text{pixel}$.



Figure 10: Narrow-band images of the planetary nebula NGC6302 at $0.27''/\text{pixel}$ in the [SiVI] ($1.96\ \mu\text{m}$) coronal (top), [FeII] ($1.644\ \mu\text{m}$) (middle) and Br $_{\gamma}$ ($2.16\ \mu\text{m}$) (lower) lines. The upper and lower images were obtained with the scanning Fabry Perot and are differences of images measured with the etalon centred on the line wavelength and in the adjacent continuum. The centre image was obtained with the narrow band [Fe II] filter and has been sky subtracted. The exposure time for each frame was 4 min. ($8 \times 30\text{s}$). Note the pronounced, extended, [FeII] filaments which are not present in the other lines.

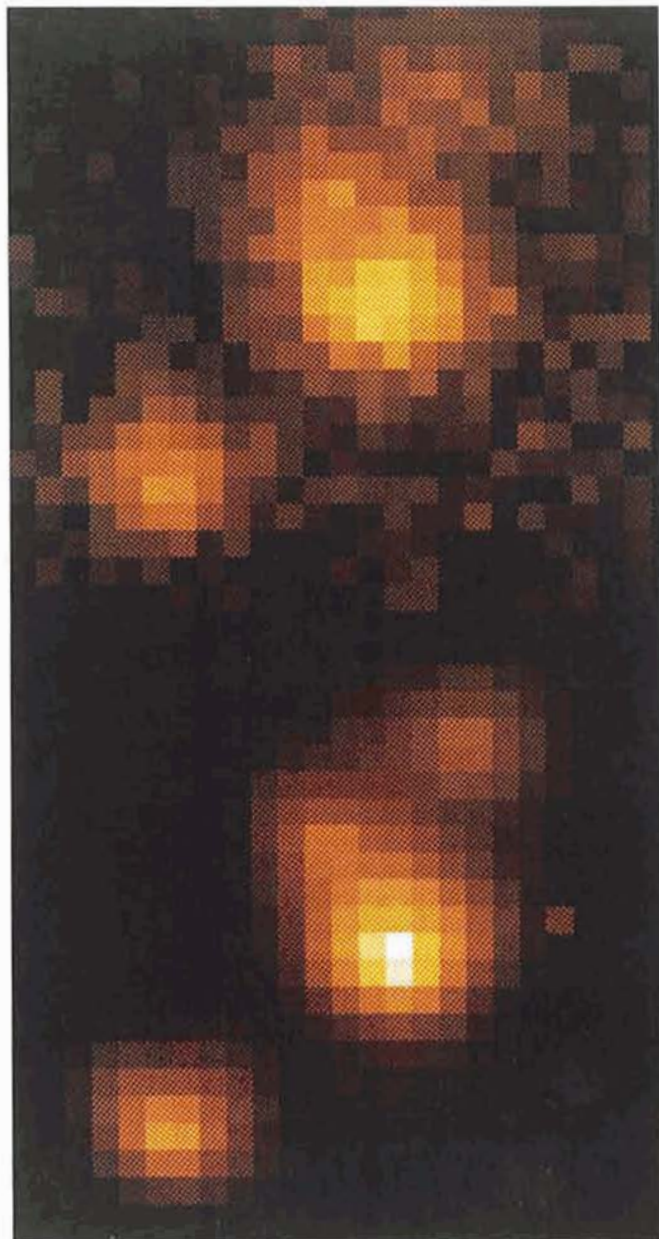


Figure 11: Example of partial seeing correction using the software shift and add feature of the multiple non-destructive read mode. The upper and lower panels show the same small region ($\sim 3.5 \times 3.5''$) of a $36 \times 36''$ K' image of the globular cluster M2 observed at $0.14''/\text{pixel}$ with and without real time application of image shifts. The integration time in both cases was 30s during which time the integration ramp was non-destructively sampled every 700 msec. In the tracked case, each difference pair of non-destructively read images was shifted by an amount corresponding to the movement of the brightest pixel in the reference star image before computing the slopes of the integration ramps.

tion, this camera already offers powerful new infrared observing opportunities on La Silla.

Acknowledgements

We are grateful to Klaus Banse for assistance in setting up the MIDAS sessions at the telescope and to Preben Grosbøl and Reynier Peletier for expert assistance with the reduction and evaluation of the test data.

“Strasbourg-ESO Catalogue of Galactic Planetary Nebulae” Available

The Catalogue which comprises 1820 objects, is divided into Part I and Part II. Part I (195 pages) contains the following subjects: A. Explanation of the Catalogue – B. Tables – C. References of papers containing 20 objects or more – D. Finding Charts, and Part II (747 pages) contains The Catalogue.

Editors are A. Acker, F. Ochsenbein, B. Stenholm, R. Tylenda, J. Marcout and C. Schohn. The price of the Catalogue is DM 135.– (prepayment required). Payments have to be made to the ESO bank account 2102002 with Commerzbank München or by cheque, addressed to the attention of ESO, Financial Services, Karl-Schwarzschild-Str. 2, D-8046 Garching bei München, Germany

A New 2048 × 2048 CCD for the CES Long Camera

L. PASQUINI¹, H. W. DUERBECK^{1,2}, S. DEIRIES¹, S. D'ODORICO¹ and R. REISS¹

¹European Southern Observatory; ²Astronomisches Institut der Universität Münster, Germany

Introduction

The ESO CES spectrograph operates with the 1.4-m CAT telescope or it is fed by a fiber link from the Cassegrain focus of the 3.6-m. The spectrograph has two main configurations: a Short Camera used with the RCA CCD ESO # 9 and the Long Camera used with the same CCD or with a Reticon detector. In July 1992, a large-format CCD, a Ford Aerospace (now Loral) 2048 × 2048 CCD, ESO # 27, with a new ESO VME controller has been mounted and tested at the spectrograph and it is likely to replace the Reticon and CCD # 9 from now on. The characteristics of this device are summarized in Table 1. The main scientific, technical and operational drivers for this change are the following:

(1) The Reticon has so far been kept in operation for two main reasons: the absence of interference fringes which plague the RCA CCD at wavelengths longer than ~6000 Å, thus hampering very high S/N ratios in the observations and its length which, being almost the double of the RCA detector, allows a much broader wavelength coverage per frame. The new FORD CCD, a front-illuminated device, is much more uniform than the RCA CCD and is twice as long, giving the same spectral coverage per frame as the Reticon.

(2) The RCA CCD # 9 presents a rather high Read Out Noise (RON) level (33 e⁻/pixel). When coupled with the Long Camera, the RON becomes the dominant source of noise for many of the applications. The Ford CCD has a RON of less than 10 e⁻/pixel.

(3) By introducing a dedicated CCD detector for the Long Camera and retiring the Reticon, ESO expects to simplify the camera + detector changes at the spectrograph and to improve the reliability and performance of the systems.

The CCD belongs to a batch that ESO has procured from Ford Aerospace in 1991. This particular chip has subsequently been lumigen coated at EEV in order to enhance its blue response. The quantum efficiency curve is shown in Figure 1. The 15-μm pixel size is well matched to the spectral and spatial resolution given by the spectrograph.

Results of the Tests

The test were performed during 5 nights in July 1992.

Table 1. FA 2048, UV-Coated ESO CCD # 27*

Pixel size	15 micron square
Active pixel number	2048 × 2048
QE	16% (350 nm), 34% (550 nm), 38% (750 nm), 18 (850 nm)
Standard oper. temp.	~ 165° K
Standard conv. factor	2.9 e ⁻ /ADU
Read-out noise	6 e ⁻ RMS
Dark current	3 e ⁻ /pixel/hour
Capacity	87000 e ⁻ /pixel (3% deviation from linearity)
CTE	≥ .99997
Bias value	~ 276
Defects	A number of warm and dark columns, but most of them outside the central 500 columns of the CCD
Cosmic ray event rate	1 event/min/cm ²

* Used at the CES with the Long Camera.

The first check was carried out on the spectral resolution. Measurements were performed on spectra from the Th-Ar calibration lamp taken at different wavelengths at a Resolving Power R = 100,000. The results were quite satisfactory: with the exception of the bluest ~150 pixels (see below) the FWHM of the measured lines was uniform within 0.1 pixel over the whole chip length and within 0.04 pixel in the central part. These values are typical for the Long Camera, compatible with the accuracy achievable with the focussing procedure used and prove that deviation from flatness in the CCD surface and the coating do not introduce significant degradation of the expected resolution.

Weather conditions were very poor during the test run, except for one photometric night which was used for absolute efficiency measurements. These were based on the observations of several standard stars (Hamuy et al. 1992). To have a direct comparison, the same central wavelengths as given in the CAT + CES Manual (Lindgren and Gilliotte 1989) were chosen. The result-

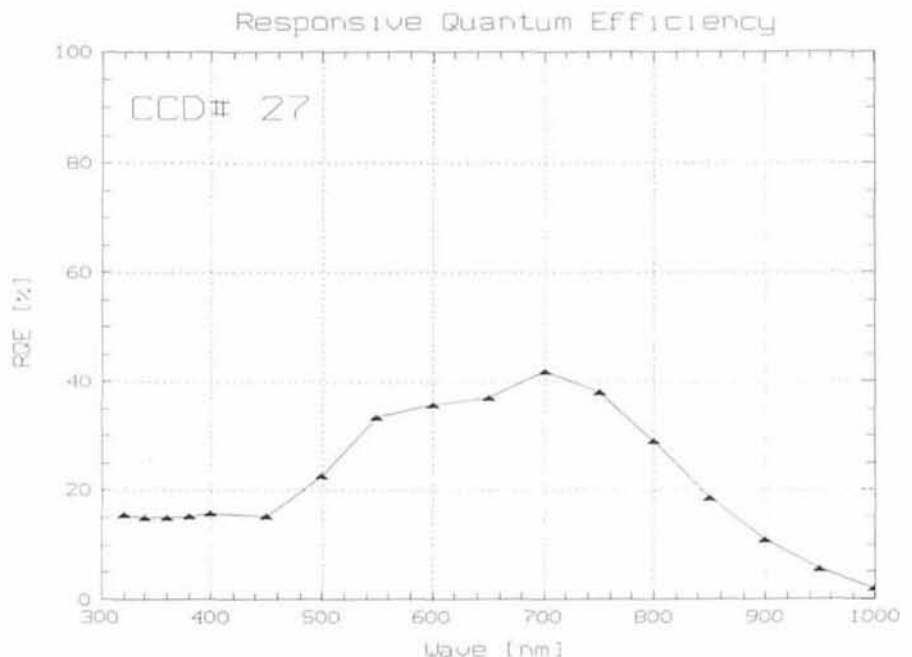


Figure 1: Responsive quantum efficiency of the CCD # 27.

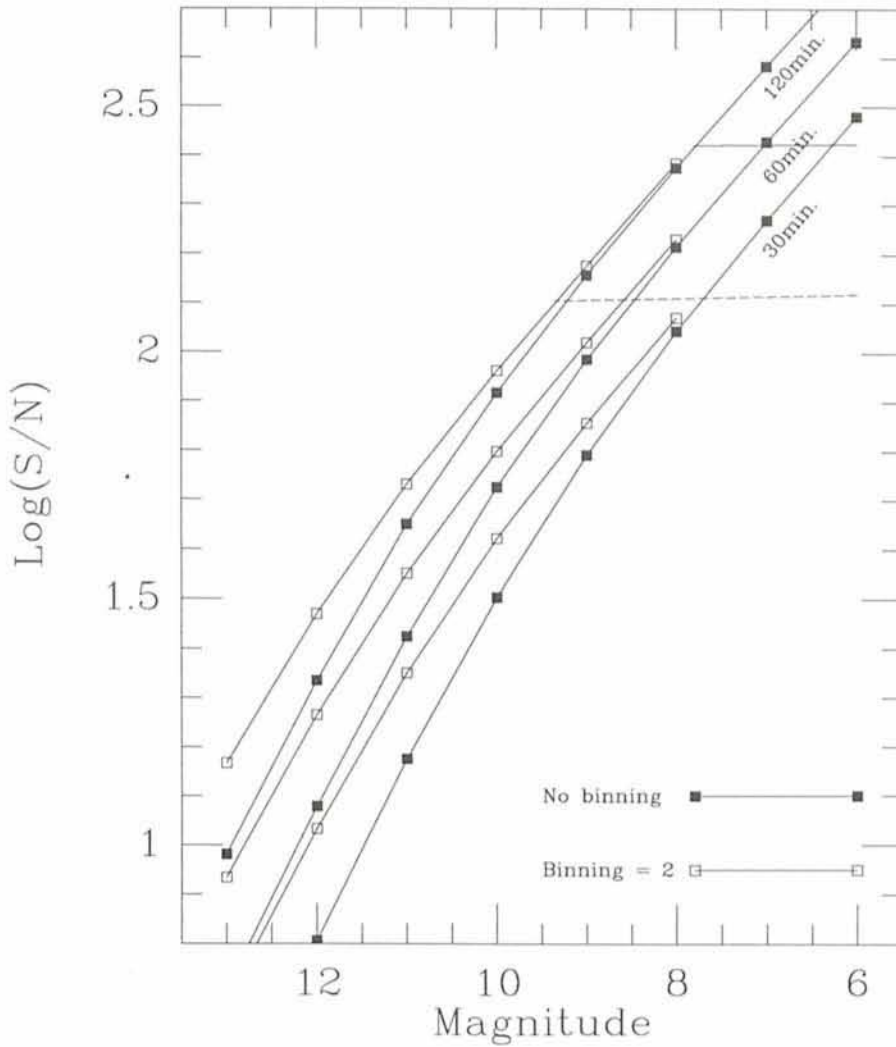


Figure 2: Expected S/N ratios as a function of stellar magnitude and integration times. An efficiency of 4.6 % at 6450 Å is assumed. No slit losses were applied in the computation.

ing efficiencies given in Table 2 are in very good agreement with what is expected from the ratio of the Ford and RCA CCD quantum efficiencies.

The new configuration has a lower overall efficiency but in order to evaluate the instrument performance, all the characteristics of the detector must be taken in account; in particular its RON and Dark Current level. This is particularly important in the CES Long Camera, where the spectrum is spread in the spatial direction over a considerable number of pixels (typically 9). With only 6 e⁻/pix RON (compared with the 33 e⁻/pix of the RCA) the advantage of using the Ford with respect to the RCA CCD becomes prominent, at least for all those observations requiring intermediate to high S/N ratios. Figure 2 shows the expected S/N ratios as a function of integration time and stellar magnitudes. To compute them the same formula used in the CES manual was adopted:

$$S/N = \frac{3600 \times N_0 T^{10^{0.4(m_0 - m_s)}}}{(3600 \times N_0 T^{10^{0.4(m_0 - m_s)}} + (Wb^{-1} N_1)^2 + W^2 TD)^{0.5}}$$

where N_0 is the number of detected e⁻/s/bin for a star of magnitude m_0 , T is the integration time in hours, W is the width of the spectrum in pixels, N_1 is the RON, b the binning factor perpendicular to the dispersion, and D the dark current in e⁻/pix/hour. The points in Figure 2 were computed assuming the Ford characteristics as given in Table 1 and an overall efficiency of 4.6%. Although these numbers must be taken only as indicative (slit losses were not considered), a direct comparison with the performances of the CAT + CES and RCA CCD can be performed. The two almost constant lines in Figure 2 limit the loci of equal performances between the old and new configuration, both for unbinned (continuous line) and binned (dashed line) CCD's. For observations requiring S/N ratios lower than ~260 in unbinned mode and ~130 with a binning of 2, the use of the Ford is more convenient.

Table 2. Efficiency of the CAT + CES + Long Camera + CCD # 27

Wavelength (Å)	Efficiency
5400	3.8%
6450	4.6%
8090	2.2%

We expect that the advantages of using the Ford CCD will be even more conspicuous when the CES is coupled with the 3.6-m telescope fibre link (D'Odorico et al. 1989); in this case in fact the spectrum is spread over a much larger number of pixels (typically 220 with the 11 slice image slicer), therefore the lower RON of the Ford CCD becomes even more important.

The second advantage of this new configuration is the absence of fringes, even at very red wavelengths; in Figure 4, a five-minute normalized spectrum of the standard star HR 718 is shown in the region around 8092 Å. This spectrum has not been flat field corrected and the variations in the continuum are of the order of 0.9% or less.

Last but not least, in evaluating the instrumental performances, we have to consider that almost the double of the spectral coverage is obtained in one frame; this feature is very important not only when the simultaneous observation of several lines is required, but also in those cases where broad lines are observed and a large coverage is essential to determine the continuum level.

As a scientific application, in Figure 3, a 1-hour H α spectrum of the recurrent nova V745 Sco is shown. This object has a visual magnitude of 15.9 and an R magnitude of 13.8, as measured from absolute calibrated EFOSC spectra. The CES spectrum in Figure 3 shows that a S/N of ~ 5 is reached in the continuum close to the H α line.

Considering all the previous points it may therefore be advisable to use the Long Camera and the Ford detector also for observations at red wavelengths and at lower resolution, for which the Short Camera is now used (i.e. R ~ 50000). On-chip binning and the absence of fringes will compensate in many types of observations the lower efficiencies of the Ford CCD and of the Long Camera.

Advice to the Users

Considering the results obtained from this test, ESO will normally offer from now on the Ford CCD on the Long Camera as a standard combination. This implies that the use of both the Reticon

and the RCA # 9 at the same camera will be discontinued and that the RCA CCD will be permanently mounted on the CES Short Camera.

We regard this as an optimum compromise between scientific performances and the severe operational and maintenance constraints of the observatory.

Users must however be cautioned that this new configuration has not yet been extensively debugged. In the next months, their feedback on the astronomical performance and any general comments will be much appreciated.

Some problems have already been identified and are being investigated. Namely:

(1) Some vignetting is present at the blue edge of the spectra and this makes

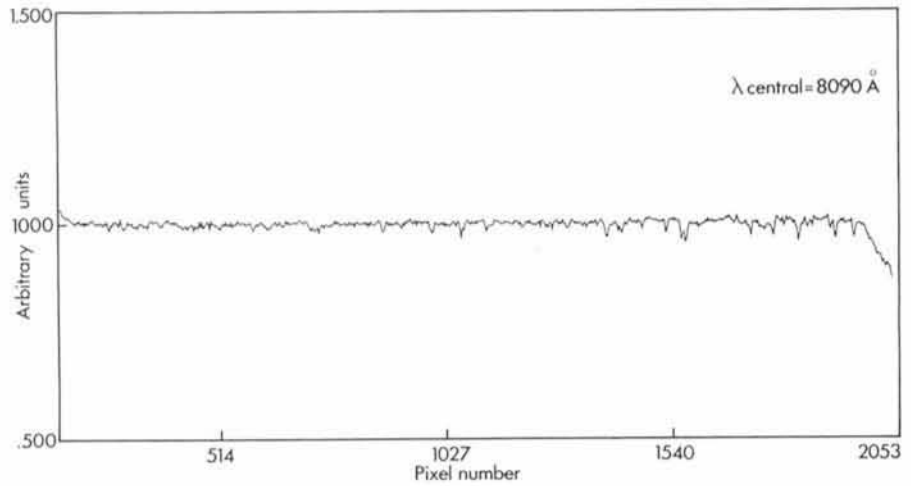


Figure 3: A 5-minute, normalized spectrum of the standard star HR 718 centred at 8090 Å. No flat-field correction has been applied. Note the absence of interference fringes.

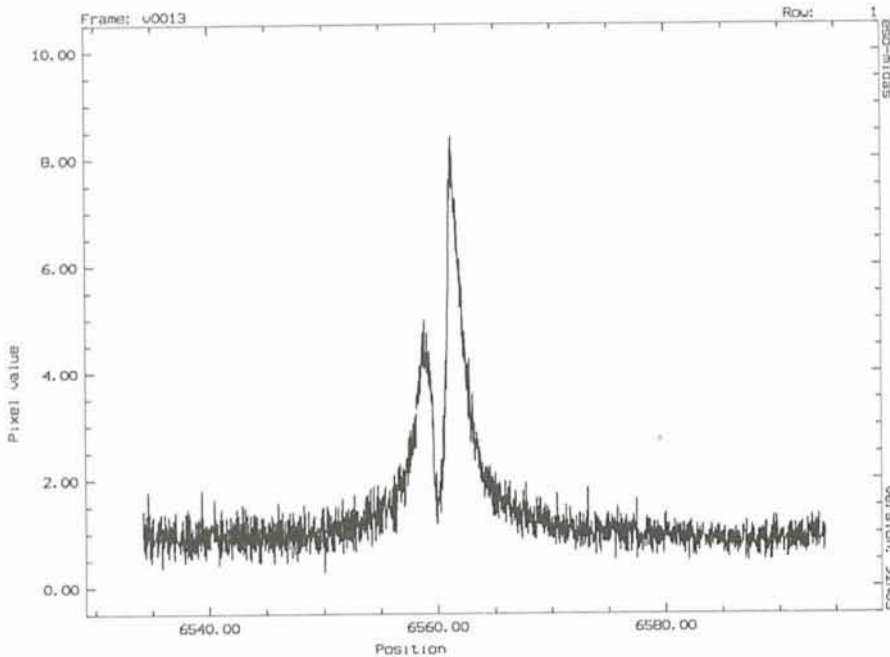


Figure 4: A 1-hour $H\alpha$ spectrum of the recurrent nova V745 Sco. The S/N is ~ 5 in the continuum.

the first ~ 150 rows of little use. Vignetting was present at a lower level in the Reticon spectra: the larger format of the

Ford shows this problem much more clearly.

(2) In order to reach the predicted per-

formance of the new set-up, it is essential to operate the CCD in an optimal way, in particular with regard to the RON and the dark current. During the tests, the level of the dark current was somewhat higher than expected and the on-chip binning introduced variable patterns in the background at a level higher than the measured RON. Both of these problems have already been observed in the past with other CCDs, but they are transient in nature and hence not easily debugged. A careful monitoring of these CCD parameters by the scientific users is recommended and it will be useful to optimize the CCD performance.

Acknowledgements

The mechanics and detector groups at La Silla worked hard and successfully to adapt the new CCD to the Long Camera. H.V. Winkel kindly provided some of the observations.

References

- D'Odorico, S., Avila, G., Molaro, P. 1989: *The Messenger* **58**, 58.
- Hamuy, M., et al. 1992: *A.J.*, in press.
- Lindgren, H., Gilliotte, A. 1989: *The Coudé Echelle Spectrometer - ESO Operating Manual No. 8.*

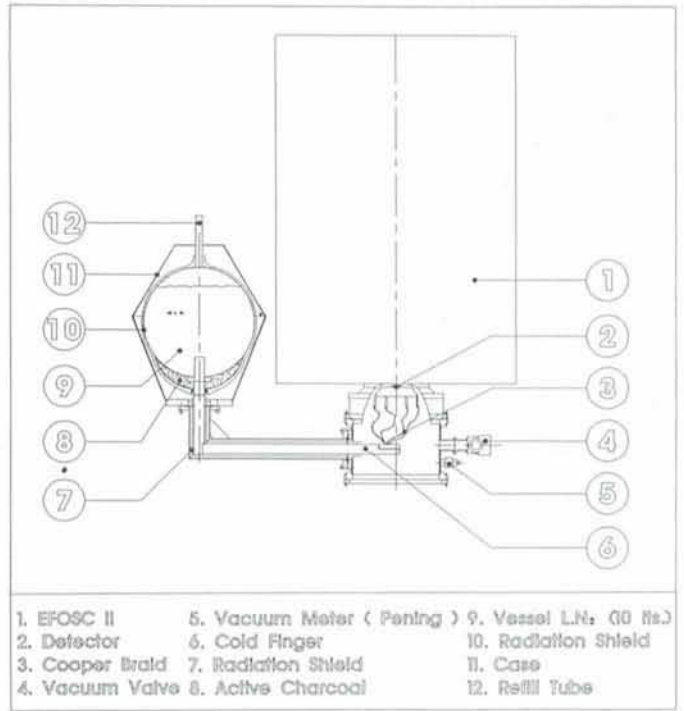
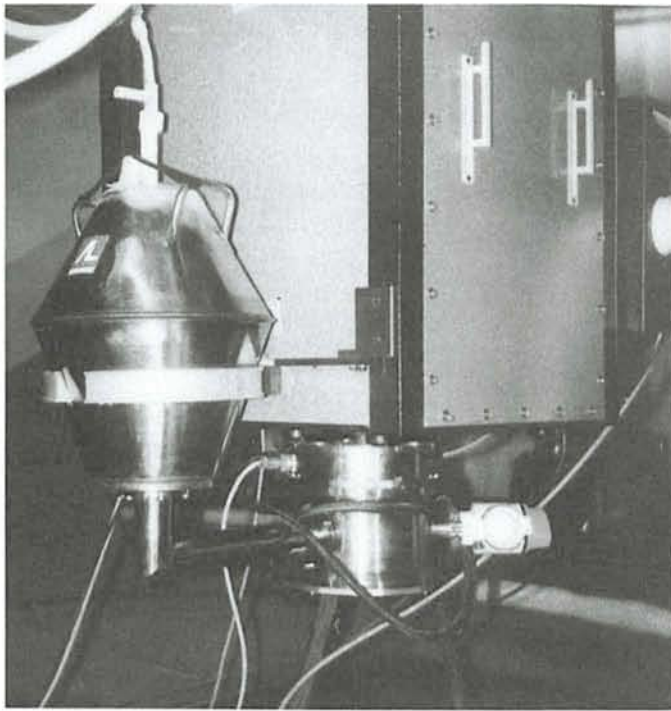
New CCD Cryostat for EFOSC2

At the time of the transfer of EFOSC2 from the NTT to the 2.2-m telescope the instrument set-up had to be revised. The plan was to interface it to the 2.2-m rotator-adaptor (DISCO) in order to pro-

fit from the existing calibration and guiding facilities.

The mounting extension with the large format CCD cryostat at the bottom of the instrument, however, restricted the

declination drive freedom to 63° in the south. The intention was to replace the IR Lab cryostat with a shorter LN_2 container. But the hold time of such a small dewar presented a severe limitation.



Therefore we engaged in the design of a short CCD head connected to an LN₂ storage dewar via a cold finger feed. In the figures the dewar arrangement is sketched. A 70-cm-long copper bar, radiation shielded under vacuum, transfers the LN₂ temperature (77K) from the storage dewar to the detector head. The thermal impedance of the cold finger plus copper braids and thermal connectors was carefully designed in order to reach the detector cold plate with a temperature of 140K. This brings the cooling near the operational temperature range of the CCD and allows to minimize the energy input for the temperature regulation in the detector head.

The results in terms of temperature stability and autonomy are excellent (i.e.: < 0.2° stability and 48 hours hold time at the telescope).

The unit was designed and integrated by Mr. Leonardo González, the La Silla cryogenic technician, while the detector head was machined in the mechanical workshop.

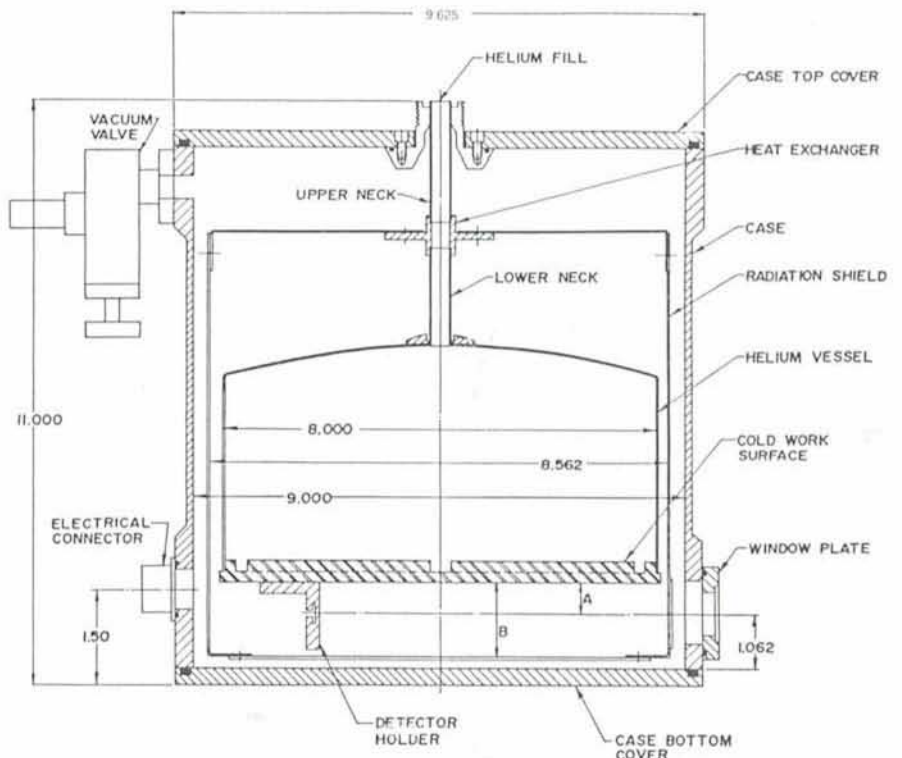
The cryostat was mounted early February this year and free access to the Magellanic Clouds was granted to the

EFOSC2 users at the 2.2-m telescope. Problems? Occasional slippage in the LN₂ refilling schedule brings the system to an unhappy user's scream when the

cooling is stressed through a 3rd night of autonomy!

L. GONZÁLEZ, D. HOFSTADT,
R. TIGHE, ESO-La Silla

DEWAR, MODEL HD-2(8) OUTLINE SKETCH



Characteristics of the EFOSC2 Cryostat

- Vacuum $10^{-5}/10^{-6}$
- Cooling time (starting from ambient T): 6 hours approx.
- LN₂ consumption: 3 lts/day
- Temperature regulation power input: 0.4 Watts

ESO, the European Southern Observatory, was created in 1962 to . . . establish and operate an astronomical observatory in the southern hemisphere, equipped with powerful instruments, with the aim of furthering and organizing collaboration in astronomy . . . It is supported by eight countries: Belgium, Denmark, France, Germany, Italy, the Netherlands, Sweden and Switzerland. It operates the La Silla observatory in the Atacama desert, 600 km north of Santiago de Chile, at 2,400 m altitude, where fourteen optical telescopes with diameters up to 3.6 m and a 15-m submillimetre radio telescope (SEST) are now in operation. The 3.5-m New Technology Telescope (NTT) became operational in 1990, and a giant telescope (VLT=Very Large Telescope), consisting of four 8-m telescopes (equivalent aperture = 16 m) is under construction. It will be erected on Paranal, a 2,600 m high mountain in northern Chile, approximately 130 km south of the city of Antofagasta. Eight hundred scientists make proposals each year for the use of the telescopes at La Silla. The ESO Headquarters are located in Garching, near Munich, Germany. It is the scientific-technical and administrative centre of ESO where technical development programmes are carried out to provide the La Silla observatory with the most advanced instruments. There are also extensive facilities which enable the scientists to analyze their data. In Europe ESO employs about 150 international Staff members, Fellows and Associates; at La Silla about 40 and, in addition, 150 local Staff members.

The ESO MESSENGER is published four times a year: normally in March, June, September and December. ESO also publishes Conference Proceedings, Preprints, Technical Notes and other material connected to its activities. Press Releases inform the media about particular events. For further information, contact the ESO Information Service at the following address:

EUROPEAN
SOUTHERN OBSERVATORY
Karl-Schwarzschild-Str. 2
D-8046 Garching bei München
Germany
Tel. (089) 32006-0
Telex 5-28282-0 eo d
Telefax: (089) 3202362
ips@eso.org (internet)
ESOMC0::IPS (decnet)

The ESO Messenger:
Editor: Richard M. West
Technical editor: Kurt Kjær

Printed by Universitäts-Druckerei
Dr. C. Wolf & Sohn
Heidemannstraße 166
8000 München 45
Germany

ISSN 0722-6691

FELLOWSHIP ON LA SILLA

A post-doctoral fellowship is offered on La Silla starting in the first trimester of 1993. This position is opened to a young astronomer with an interest in observational work. Experience in extragalactic astronomy, and in particular in the field of observational cosmology, will be considered a strong advantage. The ESO fellowships are granted for a period of one year, normally renewed for a second and exceptionally for a third year.

The successful applicant will be required to spend 50% of his/her time doing support activities and 50% of the time on research.

Applicants normally should have a doctorate awarded in recent years. **Applications should be submitted to ESO not later than 31 October 1992.** Applicants will be notified by November 1992. The successful applicant is to start work not later than May 1993. The ESO Fellowship Application Form should be used and be accompanied by a list of publications. In addition, three letters of recommendation should be obtained from persons familiar with the scientific work of the applicant. **These letters should reach ESO not later than 31 October 1992.**

The research interests of the members of the staff in the Astronomy Support Department include low-mass star formation, formation and evolution of massive stars and starbursts, post-AGB stellar evolution and planetary nebulae, supernovae, active nuclei, high redshift galaxies and galaxy clusters. Staff members and senior fellows act as co-supervisors for students of European universities that spend up to 2 years on La Silla working towards a doctoral dissertation.

Enquiries, requests for application forms and applications should be addressed to:

European Southern Observatory
Fellowship Programme
Karl-Schwarzschild-Straße 2
D-8046 Garching b. München, Germany

Contents

A. Balestra et al.: NTT Remote Observing from Italy	1
Tentative Time-table of Council Sessions and Committee Meetings	3
J.M. Beckers: A Fourth VLT Instrument Science Team	5
M. Franchini et al.: "Remote" Science with the NTT from Italy Preliminary Scientific Results	6
M. Ramella and M. Nonino: The Giant Arc in EMSS2137-23	11
H. van der Laan: The Squeeze is on the La Silla Observatory	12
New ESO Scientific Preprints (June - August 1992)	13
E. Oblak et al.: Profile of a Key Programme: CCD and Conventional Photometry of Components of Visual Binaries	14
M. Véron and D. Baade: The 3rd ESO/OHP Summer School: Provençal Summer, Hard Work and Warm Hospitality	17
Visiting Astronomers (October 1, 1992 - April 1, 1993)	19
G. Alcaino and W. Liller: The Instituto Isaac Newton: A Highly Productive ESO-Chile Connection	21
Sporty ESO	25
The ESO Aficionados: The Other Face of La Silla	25
S. D'Odorico: Alive and Kicking into the 90's	27
Chr. de Vegt: Astrometry with ESO Telescopes. A Contribution to the Construction of the New Extragalactic Reference Frame	28
L.D. Schmedel: The ESO Minor Planet Sky	32
L. Wang: A Honeycomb in the Large Magellanic Cloud	34
H. Boehnhardt et al.: Comet P/Grigg-Skjellerup Observations at ESO La Silla During the Giotto Encounter Period	38
R. West et al.: A Minor Planet with a Tail!	40
A. Bianchini et al.: A very Low Resolution Spectrometric Nova Survey	42
Staff Movements	44
A. Vidal-Madjar et al.: Observation of the Central Part of the β Pictoris Disk with an Anti-Blooming CCD	45
G. Soucail: Spectroscopy of Arcs and Arclets in Rich Clusters of Galaxies	48
E. Giallongo et al.: Quasar Absorption Spectra: The Physical State of the Intergalactic Medium at High Redshifts	52
A. Buzzoni et al.: The Galaxy Population in Distant Clusters	55
E. Palazzi et al.: Probing Beyond COBE in the Interstellar Medium	59
New ESO Conference and Workshop Proceedings	60
A. Moorwood et al.: IRAC2 at the 2.2-m Telescope	61
Strasbourg-ESO Catalogue of Galactic Planetary Nebulae Available	67
L. Pasquini et al.: A New 2048 x 2048 CCD for the CES Long Camera	68
L. González et al.: New CCD Cryostat for EFOSC2	70
Fellowship on La Silla	72